UNIVERSITAT POLITÈCNICA DE CATALUNYA BARCELONATECH

Large scale photovoltaic power plants: configuration, integration and control

by

Ana Karina Cabrera Tobar

Universitat Politècnica de Catalunya

Electrical Engineering Department

Doctoral Thesis

Large scale photovoltaic power plants

Configuration, Integration and Control

By

Ana Karina Cabrera Tobar

Barcelona-Spain
March, 2018

Supervisor:

Dr. Oriol Gomis-Bellmunt (Universitat Politècnica de Catalunya)

Co-supervisor:

Dr. Mònica Aragüés-Peñalba (Universitat Politècnica de Catalunya)

Examination Committee:

Dr. Paolo Mattavelli (University of Padova)

Dr. Carlos Coelho Leal Monteiro Moreira (University of Porto)

Dr. Eduardo Prieto-Araujo (Universitat Politècnica de Catalunya)

Universitat Politècnica de Catalunya
Departament d'Enginyeria Elèctrica
Centre d'Innovació Tecnològica en Convertidors Estàtics i Accionaments
Av. Diagonal, 647. Pl. 2
08028 Barcelona

This work was supported by the National Department of Higher Education, Science, Technology and Innovation of Ecuador (SENESCYT).

I have found that the more opposition and the more criticism that one gets
the more one has to perfect one's idea in putting it forward
and half the joy in life consists in the flight
not in the subsequent success.
Barnes Wallis

Acknowledgements

This thesis is fully supported by the National Department of Higher Education, Science, Technology and Innovation of Ecuador (SENESCYT). This scholarship gave me the freedom to develop the thesis under a topic related to the Ecuadorian needs. I am thankful for this type of scholarships as well as with the Government of Ecuador, led by Rafael Correa, which put the education as a priority. I am looking forward to applying my knowledge in different projects related to renewable energies in a country that is a paradise in the middle of the world.

This research project was supervised by Prof. Oriol Gomis Bellmunt from the Department of Electrical Engineering and part of CITCEA-UPC. I want to express my gratefulness to my supervisor who since the beginning offered me an adequate guidance. His patience, humility and bright mind have taught me to be a better person. I hope in the future I could have at least the half of these values. I do believe that I could not have found a better supervisor as him. Nevertheless, this supervision would not have been complete without the work team at CITCEA-UPC. I want to express many thanks to my co-supervisor, Mónica Aragüés that together with Eduard Bullich gave me feedbacks through these years. Besides I also learn from the people who were part of the MEDOW project, it was nice to meet so many people from abroad and with the objective to integrate renewable energies into the electrical system. Also, I want to express my gratitude to the people who are part of CITCEA-UPC , that always have offered me a friendly environment to do my research.

I want to express my gratitude to Prof. Mike Barnes for his kindness and professional supervision during my secondment at the School of Electrical and Electronic Engineering, University of Manchester. Additionally, many thanks to Dr. Joaquín Carrasco from the same university who also guide me during my secondment with another insight from the control perspective. During this period, I met wonderful people in the group who in a small period of time makes me feel at home. Though it was only three months, I feel it that I was there for more time. The technical and the life experience there has been invaluable. I found out that anywhere in the world you can find friends that little by little become your family. Now I can tell, home is where your heart is. I have to express my deepest gratefulness to all the people that have been there to support me in my

up and downs. The people who offered me their friendship being open and honest. It has been a pleasure to meet to all of you and I hope we can see again anywhere in the world. Also, I have to thank my friends from Ecuador that despite the distance they kept supporting me. I am really thankful to all of you. Additionally, I want to express my gratitude to Njord Eggen who has given his time to proofread this thesis.

Finally, I want to express my gratitude to my lovely mother who was there supporting me all this time. The person who I missed the most and thanks to the technology we could contact each day. Now, after all these years, I can come back home. This thesis I dedicate to her and to the memory of my father.

Abstract

This thesis focuses on the operation and control of Large Scale Photovoltaic Power Plants (LS-PVPPs) according to grid code requirements with a special focus on the basic unit: the PV generator. The aim of this thesis is to study to what extent a PV generator can be controlled to comply with the plant operator's requirements considering the capability curves under variable solar irradiance and temperature. In this sense, four challenges were identified: system integration, technical limitations and capability curves, dynamic modelling, and control. These challenges are addressed by a comprehensive literature review, mathematical analysis, and a series of detailed simulations.

A thorough literature review of the current technology and topologies used in LS-PVPPs is performed, concluding that the central topology and radial configuration are the layouts most widely used. Additionally, grid codes presented by Germany, Puerto Rico, South Africa, Romania, and China are deeply analysed. A comparison of these grid codes is developed considering: fault ride through capability, frequency and voltage stability supprt as well as active and reactive power management. In addition a broad discussion about the challenges that the LS-PVPPs have to overcome is presented together with the compliant technology and future trend.

According to this review, one of the challenges to overcome is the understanding of the PV generator's operation in LS-PVPPs. Thus, an analysis of its technical limitations and capability curves is essential in order to improve its control. In this thesis, a mathematical analysis to extract the PV generator's capability curves is developed. These curves are characterized by four main parameters: solar irradiance, ambient temperature, dc voltage and modulation index. These values are dependent on each other in order to obtain the complete curve. In the case where the dc voltage is equal to a single value, the point of operation is limited by the solar irradiance and temperature. However, when the dc voltage varies in a safe range, the PV generator can work in a wider area for the same solar irradiance and temperature. The validation of these curves is tested in steady state under variable solar irradiance, ambient temperature, dc voltage and modulation index. In addition, this thesis analyses how the dynamic response of a PV generator is affected by its capability curves under quick variations of solar irradiance and different temperature values.

Taking into consideration the capability curves and the photovoltaic power plant operation's requirements, the PV generator's control of active and reactive power is addressed. In this thesis, power curtailment and the control of power reserves are addressed under variable

solar irradiance and temperature. Additionally, the control of reactive power is developed by the variation of the dc voltage and the modulation index value according to the instantaneous capability curve under the specific ambient conditions.
The validation of the different studies is developed in DIgSILENT Power Factory. The simulations consider the PV generator performance under variable solar conditions and different references of active and reactive power. The results showed that an adequate control of the active and the reactive power of the PV generator taking into account the capability curves could help to comply with the power plant operator's requirements.

Resumen

Esta tesis se centra en la operación y el control de plantas fotovoltaicas de gran escala de acuerdo con los requisitos del código de red con un enfoque especial en su unidad básica: el generador fotovoltaico. El objetivo de esta tesis es estudiar en qué medida se puede controlar un generador fotovoltaico para cumplir con los requisitos del operador de la planta considerando las curvas de capacidad bajo irradiación solar variable y temperatura. En este sentido, se identificaron cuatro desafos: integración del sistema, limitaciones técnicas y curvas de capacidad, modelado dinámico y control. Estos desafíos se abordan mediante una revisión exhaustiva de la literatura, un análisis matemático y una serie de simulaciones detalladas.

Se realiza una revisión exhaustiva de la literatura de la tecnología actual y las topologías utilizadas en estas plantas fotovoltaicas, concluyendo que la topología central y la configuración radial son los diseos más utilizados. Además, los códigos de red presentados por Alemania, Puerto Rico, Sudáfrica, Rumania y China específicos para plantas fotovoltaicas a gran escala se analizan en profundidad. Se desarrolla una comparación de estos cdigos de red considerando: respuesta a fallas eléctricas, soporte de frecuencia y voltaje, así como control de potencia activa y reactiva. Además, se presenta una amplia discusión sobre los desafíos que las plantas fotovoltaicas deben superar junto con la tecnología compatible y la tendencia futura.

Según el estudio del arte, uno de los desafíos a superar es la comprensión del funcionamiento del generador fotovoltaico en estas plantas a gran escala de potencia. Por lo tanto, un análisis de sus limitaciones técnicas y curvas de capacidad es esencial para mejorar su control. En esta tesis, se desarrolla un análisis matemtico para extraer las curvas de capacidad del generador fotovoltaico. Estas curvas se caracterizan por cuatro parámetros principales: irradiancia solar, temperatura ambiente, voltaje de continua e índice de modulación. Estos valores dependen uno del otro para obtener la curva completa. En el caso donde la tensión de continua es igual a un valor único, el punto de operación está limitado por la radiación solar y la temperatura. Sin embargo, cuando el voltaje de continua varía en un rango seguro, el generador fotovoltaico puede trabajar en un área más amplia para la misma irradiancia solar y temperatura. La validación de estas curvas se prueba en estado estable bajo irradiación solar variable, temperatura ambiente, voltaje de continua e índice de modulacin. Además, esta tesis analiza cómo la respuesta dinámica de un generador fotovoltaico se ve afectada por sus curvas de capacidad bajo variaciones

rápidas de radiación solar y diferentes valores de temperatura.

Teniendo en cuenta las curvas de capacidad y los requisitos de operación de la planta de energía fotovoltaica, se aborda el control del generador fotovoltaico de la potencia activa y reactiva. En esta tesis, la reducción de potencia y el control de las reservas de potencia se abordan bajo una irradiación y temperatura solar variables. Además, el control de la potencia reactiva se desarrolla mediante la variación del voltaje de continua y el valor del índice de modulación de acuerdo con la curva de capacidad instantánea en las condiciones ambientales específicas.

La validación de los diferentes estudios se desarrolla en DIgSILENT Power Factory. Las simulaciones consideran el rendimiento del generador fotovoltaico en condiciones solares variables y diferentes referencias de potencia activa y reactiva. Los resultados mostraron que un control adecuado de la potencia activa y reactiva del generador fotovoltaico teniendo en cuenta las curvas de capacidad podría ayudar a cumplir con los requisitos del operador de la central eléctrica.

Contents

List of Figures

List of Tables

Nomenclature

List of symbols

α_o	first order pole	
A	State matrix	
A_d	diode ideality factor	
B	Input matrix	
C_f	Filter capacitor	[F]
C	Output matrix	
δ	Phase angle between the inverter and the grid voltages	[rad]
D	Feed-forward matrix	
ε_o, ω_o	second order pole	
ε_ω, ω_ω	adaptive gains for the angular speed	
$\tilde{\varepsilon}_\omega$	grid frequency small-signal error	[rad/s]
$\tilde{\varepsilon}_\rho$	Estimated angle small-signal error	[rad]
$\tilde{\varepsilon}_\vartheta$	PLL angle small-signal error	[rad]
$\tilde{\varepsilon}_i$	Current converter small-signal error	[A]
$\tilde{\varepsilon}_{v_g}$	Grid voltage small-signal error	[V]
ε	Observer error	
ε^{pll}	PLL controller sigma error	[Vs]
ε^v	dc voltage controller signal error	[V]
ε_{ac}	error ac voltage	[V]
ε_P	Error signal of active power	[W]
ε_Q	Error signal of reactive power	[W]
$\hat{f}$	estimated frequency	[Hz]
φ	Phase angle between the inverter current and the grid voltage	[rad]
f	ac network frequency	[Hz]
f_{sw}	switching frequency	[Hz]

G	Solar irradiance	$[W/m^2]$
$\mathbf{i_c}$	VSC ac current converter vector	[A]
$\mathbf{i_g}$	Grid current vector	[A]
$\hat{\tilde{i}}_c$	estimated small-signal current converter	[A]
$\tilde{i}_c$	small-signal current converter	[A]
$\hat{i}^c_q$	estimated q axis current converter	[A]
$\hat{\tilde{i}}^c_q$	estimated small-signal q axis current converter	[A]
i_c	current through the dc capacitor	[A]
i_d	diode current	[A]
i^*_d, i^*_q	VSC inner-current controller d-axis reference and q-axis reference	[A]
i_q	current q-axis reference calculated by the reactive power controller	
i_{array}	array current	[A]
$i_{dc_{max}}$	maximum PV array dc current	[A]
$i_{dq^*_{min}}$	minimum VSC inner-current controller in the dq frame	[A]
i^g_{dq}	grid current in the dq frame	[A]
i_d	diode current	[A]
I_{grid}	Grid current	[A]
i_{mpp}	dc current at v_{mpp}	[A]
i_o	saturation current	[A]
i_{ph}	photogenerated current	[A]
i_{pv}	panel current	[V]
i_p	parallel current	[A]
$i_{q_{min}}$,$i_{q_{max}}$	minimum and maximum dq current at the VSC converter	[A]
I_{rated}	Rated current	[A]
i_{sc}	short circuit current	[A]
v_{array}	array voltage	[V]
k^{obs}_i	observer controller integral gain	$[H.rad^5/Vs^3]$
k^{obs}_p	observer controller proportional gain	$[H.rad^4/Vs^2]$
k_i	correction factor for current	$[A \cdot^{\circ} C^{-1}]$
k^{pll}_i	PLL controller integral gain	[rad/Vs]
k^v_i	dc voltage controller integral gain	$[V^2/s]$
k^{pll}_p	PLL controller proportional gain	[rad/Vs]

k_p^v	dc voltage controller proportional gain	$[V^2]$
k_v	correction factor for voltage	$[V \cdot^\circ C^{-1}]$
k_B	Boltzman constant	$[J \cdot^\circ C^{-1}]$
k_d	inner current controller gain for the d-axis	
k_q	inner current controller gain for the q-axis	
L	Luenberger observer matrix	
L_f	phase reactor inductance	[H]
L_g	grid side inductance	[H]
m_{dq}	Modulation index in the rotating frame	
η	Inverter efficiency	
N_s	Number of solar cells connected in series in a PV panel	
N_{par}	PV panels connected in parallel	
N_{par}	number of panels connected in parallel	
N_{PVgen}	Number of PV generators in the LS-PVPP	
N_{ser}	number of panels connected in series	
N_{ser}	PV panels connected in series	
NOCT	Normal Operating Cell Temperature	[°C]
$\tilde{\tilde{\rho}}$	estimated small-signal phase angle	[rad]
$\tilde{\rho}$	small-signal phase angle	[rad]
ΔP	Variation of active power	[W]
ΔP_{tso}	Active power reserve asked by the TSO	[W]
P&O	Perturb and Observe	
P^*	Active power reference	[W]
$P_{ac_{inst}}$	Instantaneous ac active power	[W]
$P_{ac_{mpp}}$	ac active power at v_{mpp}	[W]
P_{ac}	Active power in the ac system	[W]
p_{array}	power array	[W]
P_c	Active power stored in the capacitor	[W]
$P_{dc_{vmax}}$	Active power generated at v_{max}	[W]
$P_{dc_{vmin}}$	Active power generated at v_{min}	[W]
$P_{dc_{vmpp}}$	Active power generated at v_{mpp}	[W]
p_{inst}	Instantaneous active power	[W]
$P_{inv_{in}}$	Active power flowing into the PV inverter	[W]
$P_{max_{array}}$	Maximum possible active power	[W]
$P_{max_{inverter}}$	Nominal active power of the inverter	[W]

P_{max}, P_{min}	Allowable active power in the LS-PVPP	[W]
P_{mpp}	Active power at v_{mpp}	[W]
P_n	Output active power from the PV generator	[W]
P_{PVPP}	Measured active power at the PCC	[W]
P_{pv}	Output power of the PV array	[W]
P_{ref}	Active power reference given to each PV generator	[W]
$P_{reserve}$	Active power reserve	[W]
P_{TSO}	Active power required by the TSO	[W]
Q	Reactive power in the ac system	[VAr]
q	Electrical charge of an electron	[C]
Q^*	Rective power reference	[VAr]
Q_{inst}	Instantaneous reactive power	[VAr]
Q_{min}, Q_{max}	Minimum, maximum reactive power	[VAr]
Q_{mpp}	Reactive power at v_{mpp}	[VAr]
Q_{mpp}	Reactive power at v_{mpp}	[VAr]
Q_n	Output reactive power from the PV generator	[VAr]
Q_{PVPP}	Measured reactive power at the PCC	[VAr]
Q_{ref}	Reactive power reference given to each PV generator	[VAr]
Q_{TSO}	Reactive power required by the TSO	[VAr]
Δ_{ripple}	Current ripple	[A]
R_p	Parallel resistance	[Ω]
R_s	Series resistance	[Ω]
S	VSC apparent power	[VA]
ϑ_{pll}	PLL angle (between the grid and the converter (dq) rotating frames)	[rad]
t	time step	
T_a	ambient temperature	[°C]
T_c	cell temperature	[°C]
T_{min}	Minimum ambient temperature	[ºC]
$\mathbf{u}$	Input vector	
$\mathbf{v_c}$	VSC ac voltage vector	[V]
$\mathbf{v_g}$	Grid voltage vector	[V]
$\mathbf{v_{pcc}}$	Voltage vector at the point of common coupling	[V]

$\tilde{\hat{v}}_g$	estimated small-signal grid voltage	[V]
$\tilde{v}_g$	small-signal grid voltage	[V]
$v_{d^{c*}}$, $v_{q^{c*}}$	VSC steady state voltage in d-axis and q-axis voltage referencenomunitV	
v_{d^g}, v_{q^g}	Grid voltage phasor in the dq rotating frame	[V]
Δv	dc voltage variation at MPPT	[V]
$v_{dc_{meas}}$	dc voltage measured at the bus dc	[V]
v_d, v_q	VSC d-axis voltage, VSC q-axis voltage	[V]
v_d^*, v_q^*	VSC d-axis and VSC q-axis voltage reference	[V]
$V_{a'b'}$	Line to line VSC ac-side voltage	[V]
V_{conv}	Converter voltage line to line	[V]
V_{dc}	VSC direct voltage input	[V]
v_{dc}^*	dc voltage reference	[V]
v_{dq}^c	VSC steady-state voltage in the rotating frame	[V]
V_{grid}	Grid voltage line to line	[V]
v_{min}, v_{max}	maximum, minimum allowable direct voltage	[V]
v_{mpp}	maximum power point voltage	[V]
v_{oc}	Open circuit voltage	[V]
v_{pcc_d}, v_{pcc_q}	ac voltage phasor at the PCC in the dq rotating frame	[V]
v_{pv}	voltage panel	[V]
v_{ref}	voltage reference	[V]
v_t	thermal voltage	[V]
ω_g	Grid frequency	[rad/s]
$\tilde{\hat{\omega}}_g$	estimated small-signal grid frequency	[rad]
$\tilde{\omega}_g$	small-signal grid frequency	[rad/s]
ω_{pll}	PLL frequency	[rad/s]
W_c	VSC dc capacitor stored energy	[J]
W_{dc}^*	square of the VSC direct voltage reference	[V^2]
$\hat{\mathbf{x}}$	Estimated state variable vector	
$\mathbf{x}$	State variable vector	
X	Line reactance	[Ω]
$\hat{\mathbf{y}}$	Estimated output vector	
$\mathbf{y}$	Output vector	

List of Acronyms

ac	Alternating Current
ANRE	National Regulatory Authority for Energy
BDEW	German Association of Energy and Water Industry
CI	Central Inverter
CITCEA	Centre d'Innovaci Tecnolgica en Convertidors Esttics i Accionaments
dc	Direct Current
FACTS	Flexible Alternating Current Transmission System
FERC	Federal Energy Regulatory Commision
FRT	Fault ride through
HV	High Voltage
HVRT	High Voltage Ride Through
IGBT	Isolated Gate Bipolar Transistor
LGIA	Large Gnerator Interconnection Agreement
LS-PVPP	Large Scale Photovoltaic Power Plant
LV	Low Voltage
LVRT	Low Voltage Ride Through
M	Modulation index
MI	Multistring Inverter
MPPT	Maximum Power Point Tracker
NEA	National Energy Administration
NERSA	National Energy Regulator of South Africa
NS	Not Specified
p.u	Per unit
PCC	Point of common coupling
PLL	Phase Locked Loop
PPC	Power Plant Controller
PREPA	Puerto Rico Electric Power Authority
PV	Photovoltaics
QPPT	Reactive power point tracker
RPPT	Reference Power Point Tracker
stc	standard test conditions
SPWM	Sinusoidal Pulse Width Modulation
STATCOM	Static synchronous compensator
SVC	Static Var Compensator
TSO	Transmission SystemOperator
UPC	Universitat Politcnica de Catalunya
VLS-PVPP	Very Large Scale Photovoltaic Power Plant
VSC	Voltage Source Converter

WPP	Wind Power Plants

Part I

Introduction & Literature Review

Chapter 1

Introduction

" There is no substitute for energy. The whole edifice of modern society is built upon it... It is not just another commodity, but the precondition of all commodities, a basic factor equal to air, water and earth " E.F. Schumacher

The aim of this chapter is to explain the motivation behind the thesis together with the general background. It also details the problem and the challenges related to the integration of large scale photovoltaic power plants. Then, the objectives and the research questions are detailed in order to understand the hypothesis constructed at the beginning of the research. Finally, the thesis outline and the approach of each chapter is detailed.

1.1 General Background and Motivation

In 2015, the world population reached 7.3 billion, which implies that the population has grown by 2 billion since 1990. By 2050, the global population is expected to be 2.4 billion more than in 2015. Europe shows a slow rate of population growth in the coming years but this can change due to the high migration rate that it constantly receives. However, this global growth occurs mainly in the least developed areas as Africa and Asia, where the fertility rate remains high (Fig. 1.1) [6].

The impact of population growth is related to resource utilization, transportation, sanity, infrastructure, access to energy and environmental deterioration [7]. So far, not all these issues have been addressed worldwide, as it is the case of energy. In Europe, 10.8 % of the population was not able to keep their home adequately warm due to the increase in energy prices [8]. In the case of developing countries, data reveals more difficulties. There are at least 1.2 billion people who do not have access to electricity [9].

Energy is a critical pillar for the quality of life of any country, as it increases productivity, improves health conditions and promotes economic growth. Despite the importance of this resource, not all the countries have handled it properly. For instance, in low-income countries, traditional biomass for cooking or heating is still being used by a large proportion of the population (2.7 billion). Not having access to modern energy[1] services reduces the possibility that poor countries could develop. Thus, one of the goals of the United Nations is to ensure universal access to modern energy services in a sustainable way by 2030. However, due to the population growth and the large investment that it is necessary to make in order to reach this goal, the size of the remaining task will be huge by 2030 as can be seen in (Fig. 1.1) [11].

The lack of modern energy systems, in developed or developing countries, does not only depend on the demographic growth but also on the availability of the energy source in the area. Oil, coal and natural gas are the dominant sources of energy worldwide (85 %) for different purposes: electricity, industry, buildings, transportation and non-combusted applications. In the case of electricity, the fossil fuel demand from 2005 to 2015 was around 30 % [12].

Nevertheless, the world has entered in a de-carbonization of the energy mix due to some motives: (i) Fossil fuels are a limited source of energy,

[1] Modern energy is a term referred to reliable and affordable energy sources or systems that permit to the population to have basic features as electricity, transportation, and information technology as part of a modern society [10].

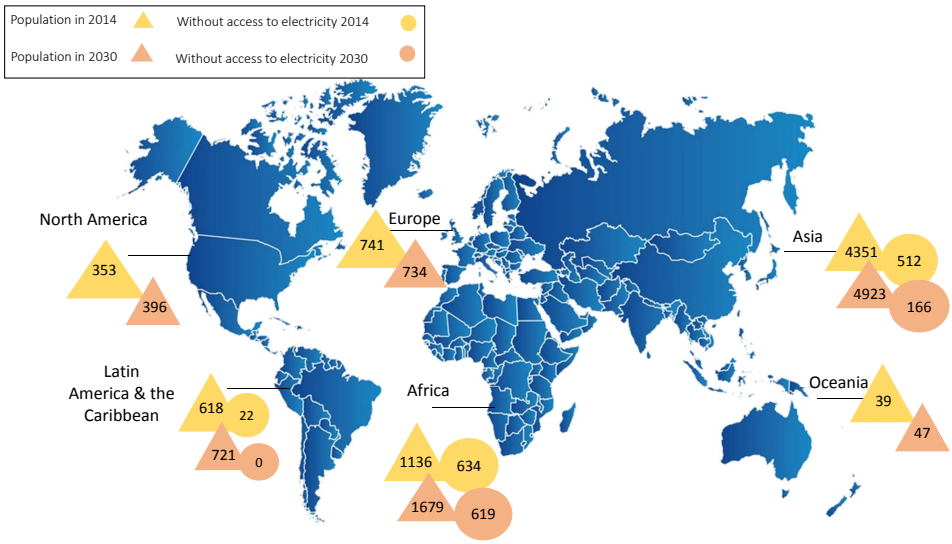

Figure 1.1: Total population in major areas of the world in 2014 and 2030. Total population without access to electricity in 2014 and 2030 [millions].

as it was explained by M. King Hubbert in 1956 [2]; (ii) Burning fossil fuels produce carbon dioxide that increases the greenhouse effect [3]; (iii) The lack of fossil fuels in some countries as a natural source can cause economic and political dependence.

The de-carbonization of the primary energy source and the access to modern energy to the worldwide population can only be guaranteed with the exploitation of renewable energy in a sustainable way. For developing countries, a long-term solution is the development of large scale power plants considering the natural resources available in the country. Thus, the main motivation of this thesis is:

to study an optimal solution to integrate renewable energy into the conventional system through the development of large scale power plants

[2] Hubbert's theory was based on the idea that global oil production will reach a peak in a specific time period and after that, the production will reduce. In 1970 his theory was proven in the case of oil production in the US. [13]

[3] According to 2020 climate and energy package of European Union, the objective is to reduce 20% greenhouse gas emission from 1990 levels until 2020 [14]. In 2015, the total amount of CO_2 was close to 30 billion tones and it is expected to be reduced in the oncoming years[12]

1.2 Problem Definition

The installed capacity of Renewable energy [4] around the world has reached 2 TW [16]. Europe and Eurasia lead the installed capacity of Renewable energy followed by North America and Asia Pacific. Together, they have 90 % of the total installed capacity. On the other hand, Africa, the Middle East, South and Central America have a total installed capacity close to 10 % [12].

Despite the need for developing countries to have access to modern energy, the use of renewable energy, as part of the United Nations objectives, has not been totally exploited. In addition, developing countries are in areas where the access to renewable energy is easier than in developed ones, such as solar energy in the northern part of South America and Africa or hydro-power close to the Amazon region.

There are several problems with renewable energy which are related with the availability of the natural resource– such as dry season for hydro-power, clouds and high temperature for solar energy, wind speed variation for wind energy– that makes difficult its integration with the electrical system. However, depending on the region, the dry season could come together with high solar irradiance and strong wind as it is the case of some countries in South-America (Brazil, Ecuador, Colombia, Venezuela). It means that not only one type of renewable energy should be used in one area, but a mix of them could help to supply power according to the demand.

Despite this issue, the use of renewable energies to supply electricity has grown in the last years, especially wind and photovoltaic power. Wind power plants had the fastest growth during the last years. In fact, the cumulative wind power installation in the European Union at the end of 2016 was 153.7 GW [17], while in Asia, North America, and South America was 184.6 GW [16], 96.94 GW [18] and 13.6 GW [16] respectively. In contrast, photovoltaic (PV) power installations did not have the same growth, due to prices of photovoltaic panels, technology used and social opposition. In fact, the cumulative power installation of photovoltaic for residential and utility purpose connected to the grid at the end of 2016 was 102.3 GW in Europe, 139.47 GW in Asia [16], 36.085 GW in North America[19] and only 1.9 GW in South America [16]. However, due to the reduction of prices for photovoltaic panels and improvement of technology, the to-

[4] Renewable energy is energy generated from natural resources that can be naturally replenished as sunlight, wind, tides, geothermal heat, solar heat [15].

tal installed capacity of photovoltaic power in Europe will reach 156 GW, and 184.9 GW for Asia by 2018 [20]. North America, South America and South Africa show a drastic increment on the development of PV power plants (PVPPs), adding several GWs to the worldwide PV generation. In fact North America has 21.8 GW of PVPPs under development [3].

In the case of photovoltaic power plants, the fluctuation of the solar irradiance during the day, affects the active power, the voltage, and the frequency. Without an adequate control, these power plants cannot provide secure and reliable power to the electrical market as conventional power plants do. Additionally, some transmission system operators to which the LS-PVPP are connected have introduced new requirements established in the corresponding grid code. This leads to the main problem definition:

What is the best way to control and operate large scale photovoltaic power to comply with grid code requirements despite the variation of solar irradiance and temperature ?

1.3 LS-PVPPs challenges

In LS-PVPPs, the challenges arise due to the necessity to integrate them to the electrical system in a smooth way by overcoming the fundamental differences in operation and control with conventional power plants. These challenges can be divided in four areas: System integration, technical limitations, dynamic modelling, and control.

System integration

In conventional power plants, the configuration and the technology used are very well established. The same occurs for wind power plants. For example, the study developed by Mikel de Prada et al. [21], explains the technology used in large scale offshore wind power plants together with the ac collection grid topologies. These basis have helped to study future configuration under the premise of land reduction size, lower cost and power efficiency [22].

In the case of photovoltaic power plants, it is also necessary to establish the basis for grid integration considering: (i) technology used, (ii) PV generator configuration and (iii) ac collection grid topologies. For this, a deep study of the current LS-PVPPs around the world is necessary.

For the system integration, there is the need to analyse the grid codes

that so far have been established for LS-PVPPs. Understanding what the new grid codes are requiring from LS-PVPPs in order to be connected with the bulk system will help to develop better configurations as well as to improve the control.

Technical limitations & Capability curves

The current bulk system has a defined infrastructure to generate, transmit and distribute electricity using conventional generators. In this system, the generation of ac electricity is developed in the premise to inject power according to the demand requirements. For plant operators, however, it is necessary to understand the limitations of the generators used and thus capability curves are considered[5]. Power plant operators can modify the active or reactive power supplied by the generator with the consideration of generator's limitations [24].

Because capability curves are essential for power plant control, they have been also studied for wind technology application. The main focus of these capability curves was the understanding of the wind turbine limitations together with the power electronics drawbacks. These limitations are also related to the wind speed [25]. Many patents have already been developed considering the capability curves for wind technology. The consideration of these technical limitations, in conventional generators and wind technology, has permitted the development of control and the enhancement of the technology.

These capability curves are a key factor for the general control of the power plant. In wind applications, the power converters have a back-to-back configuration with constant DC voltage. Therefore, the PQ capability curve is not dependant on the wind speed. For PV (with single-stage conversion), this is much more complicated, as the DC voltage varies in the time due to the maximum power point tracker (MPPT). Besides, the management of active and reactive power considering solar irradiance, temperature, and electrical characteristics are essential for LS-PVPPs in order to provide ancillary services.

Dynamic Modelling

[5]The capability curves of any generation machinery illustrate the active power vs the reactive power that the machinery can supply or absorb. For these capability curves, the technical limitations as temperature or current are usually considered [23]

The research developed in this field, usually considers the PV array as a constant source of current. Because of the PV panel characteristics, this assumption cannot be used in all type of studies as it could not show the real behaviour of the power plant at variable ambient conditions.

Thus, a modular model of the PV generator should be developed taking into account each of the parts involved: PV array, DC bus, PV inverter, filter, and transformer. The emphasis of this model could be developed according to the variation of electrical characteristics due to the solar irradiance, temperature, capability curves, and power plant operator. Then, the model can be applied in any simulation tool in order to test the behaviour of the power plant under different grid requirements together with the variation of ambient conditions.

Dynamic control

Nowadays, transmission system operators demand that LS-PVPPs behave as similar as possible to conventional power plants. Additionally, these power plants should provide ancillary services – LVRT, frequency and voltage stability support, active and reactive power management– in order to be connected to the electrical system. But the variation of solar irradiance, temperature and grid instability could cause that these power plants cannot fulfil the requirements all the time. This is why a challenge to overcome is the understanding of the dynamic behaviour of these LS-PVPPs under variable ambient conditions when basic PV generators are used [6].

After this is understood, the control of the PV generator can be improved in order to comply with the plant operator requirements. So, the challenge to overcome is to develop the control of the PV generator focusing on different areas:

- *Active power management:* Usually, PV generators only provide active power according to a maximum point of operation at each solar irradiance. Nevertheless, Grid requirements ask plant operators to generate constant active power in a given period of time. This should be accomplished despite the variations of solar irradiance or ambient temperature. Additionally, in the case the active power required by

[6] Basic PV generators is a term used to describe those PV systems commonly used for residential purposes which only provide active power according to the maximum point of operation at each solar irradiance and they are disconnected in case of electrical system failure

the TSO is lower or higher than the current production, ramp rates should be applied. The same ramp rates should be used in the case where the solar irradiance decreases or increases in a small period of time. These considerations open a new paradigm in PV generators' control, that is the reduction of dependence on the maximum power point of operation together with the ambient conditions.

- *Reactive power management:* The basic PV generators, used for residential or commercial purposes that accomplish with the standard IEEE 1547, did not have the feature to supply or absorb reactive power. However, it is now mandatory to absorb or inject reactive power to reduce voltage deviations in power plants connected to low, medium or high voltage [26]. Thus, the LS-PVPP should be able to provide this feature. It has been common practice to install STATCOM or capacitor banks in order to provide a solution. But, the inverter used in PV generators can handle this feature. An appropriate control that takes into account the PV generators' capability curves under different ambient conditions could help to LS-PVPPs accomplish the grid code requirements.

1.4 Objective and Research Questions

Taking into consideration the problem definition stated and the challenges identified in Section , the main objective of this thesis is:

to study to what extent a PV generator can be controlled to comply with the plant operator's requirements considering the capability curves under variable solar irradiance and temperature.[7]

The work conducted on this thesis intend to answer the following research questions:

1. How do temperature and solar irradiance affect the capability curves and the technical limitations of PV generators?

[7] The plant operator's requirements are according to the grid code requirements and the control actions issued by the transmission system operator of the grid to which the LS-PVPP is connected.

2. What is the effect of capability curves in PV generators' dynamic response considering the quick variation of solar irradiance and temperature?

3. How can the active power control of a PV generator be performed for LS-PVPP's application taking into account the capability curves variation with temperature and solar irradiance?

4. How can the control of reactive power be performed to fulfil grid code requirements by considering the capability curves?

The first stage of this thesis focuses on identifying the most used PV generator's configuration and the ac collection grid topologies in LS-PVPPs. From this first stage the PV generator chosen for the current thesis is the one with central configuration that has a single stage of inversion (DC-AC). The main grid codes that establish the general requirements for LS-PVPPs integrated to the electrical system are also identified. Besides. a deep discussion about the challenges that LS-PVPP have to face to comply with the grid code requirements is developed. After this review, the three research questions are addressed in the following stages.

The second stage consists in the analysis of the capability curves of a PV generator in central configuration taking into account the variation of solar irradiance, temperature and electrical characteristics. For this purpose, three main aspects are addressed: (i) the modelling of the main components of the PV generator,(ii) the operational limits analysis of the PV array together with the inverter, and (iii) the capability curve analysis considering variable solar irradiance and temperature. For this analysis, the effect of the ambient conditions, the dc voltage and the modulation index are studied. To validate this study, a PVPP of 1 MW is designed, modelled and simulated in DIgSILENT PowerFactory. Taking into account this analysis, the first research question is fully addressed.

By considering the capability curves, the third phase of the thesis arises. This phase has the objective to understand the dynamic performance of the PV generator under quick changes of solar irradiance. To comply with this objective a modular model of the PV generator is developed in DIgSILENT Power Factory. Besides, the control of the inverter is included together with the corresponding MPPT control. In this stage, the capability curves are included inside the control. These curves change dynamically each time the ambient conditions vary. Thus, the operation point of the PV generator varies according to the dc voltage variation, the solar irradiance and temperature. From this study, the MPPT dynamics, the effect

of temperature and the reactive power limitations in dynamic stage are understood. This stage helps to address the second research question.

Considering the effect that dc voltage and the capability curves have on the performance of the pv generator, an improved control is performed in the final stage of the thesis. The aim of this phase is to propose a control of active and reactive power for a PV generator considering the corresponding capability curves and the grid code requirements. For active power, two main targets are accomplished: (i) Power curtailment, and (ii) Power reserves, by using an adaptation of the Maximum Power Point Tracker (MPPT). For the reactive power control, two considerations are addressed: (i) preference of active over reactive power and (ii) preference of reactive over active power. Then, the control is validated by a simulation of a LS-PVPP modeled in DIgSILENT PowerFactory under different ambient conditions. After this phase, the third and fourth research questions are fully addressed.

1.5 Main Contributions

From the main objective and the research questions listed before, the main contributions of the thesis are:

1. The mathematical analysis of the PV generator's capability curves when a PV inverter of one stage of conversion is chosen. In this analysis, it can be seen that the capability curve is affected by the solar irradiance, temperature, dc voltage and the modulation index.

2. A modular model of the PV generator: PV array, PV inverter, dc bus, ac system. This model permits to do the analysis of the PV generator for different solar irradiance, ambient temperature, dc voltage and modulation index. In this modular model, the control of the PV generator is considered where it can be included the capability curves that varies in each change of solar irradiance, temperature and dc voltage chosen.

3. A simulation platform for the control and operation of the LS-PVPP. This simulation platform is developed in DIgSILENT Power Factory where three stages of control are considered: TSO's active and reactive power requirements, Power Plant control (PPC) and the PV generators control. The platform permits to analyse PV plants' response taking into consideration the effect of solar irradiance and temperature

4. The control of active power by the adequate management of the dc voltage inside the permitted limitations. The control complies with two grid code requirements: (i) Active Power curtailment and (ii) Active Power reserves.

5. The control of reactive power by managing the dc voltage and the modulation index at ambient conditions. To develop this control, the instantaneous capability curves and the P-V curves are used in order to comply with the grid code requirements.

1.6 Outline and Approach

The thesis is divided into four parts: Introduction & Literature review, Technical limitations & capability curves, Dynamic analysis and control, and Conclusions.

Part I. Introduction & Literature Review

The first part of the thesis includes: Chapter 1, Chapter 2 and Chapter 3. The review of the technology used in the current LS-PVPPs is detailed in Chapter 2. Additionally, it also covers the PV generator's configuration together with the ac collection grids that are common for this type of application. After this chapter, the PV generator and the plant configuration are chosen according to the best-established technology so far. Then, the grid codes are compared in Chapter 3. The comparison is developed according to LVRT, frequency and voltage support, active and reactive power regulation. Besides, a critical review of these grid codes is also provided together with a proper analysis on how the control of the PV generators should change.

Part II. Technical Limitations & Capability Curves

In this part, Chapter 4 is included. The detailed model of the PV generator for stability analysis is developed. Additionally, the analysis of the technical limitations, taking into account solar irradiance, temperature and electrical characteristics is presented. Finally, the PV generator's capability curves are presented for different ambient

conditions.

Part III. Dynamic analysis and control

Part III deals with the dynamic analysis and control of the PV generator and it is divided into three chapters. The dynamic model and control of a basic PV generator are detailed in Chapter 5. The dynamic model also considers the inclusion of the capability curves. Additionally, it presents the dynamic response of the PV generator under quick changes of solar irradiance. In Chapter 6, a new control of active and reactive power is presented. Variable solar irradiance, ambient temperature, grid code requirements and the capability curves are considered in the development of this control.

Part IV. Conclusions & Recommendations

The fourth part contains Chapter 7 that provides general conclusions on the present thesis considering the research questions presented before. Additionally, it gives recommendations for future research.

Chapter 2

Topologies of LS-PVPPs

"The phrase "utility-scale solar" is heard so frequently in discussions about renewable that it comes a bit of a shock when one realizes that there is no commonly accepted definition as to what size comprises"
P. Donnely-Shores, 2013

The concern of increasing renewable energy penetration into the grid together with the reduction of prices of photovoltaic solar panels during the last decade have enabled the development of LS-PVPPs connected to the medium and high voltage grid. Photovoltaic generation components, the internal layout, and the ac collection grid are being investigated for ensuring the best design, operation, and control of these power plants. This chapter addresses the review of components as photovoltaic panels, converters, and transformers utilized in LS-PVPPs. In addition, the distribution of these components along this type of power plant and the collection grid topologies are also presented and discussed[1].

[1]This chapter is based on the following publication:
A. Cabrera-Tobar, E. Bullich-Massagué, M. Aragüés-Peñalba, O. Gomis-Bellmunt, "Topologies for large scale photovoltaic power plants", *Renewable and Sustainable Energy Reviews.*, 59 (2016),pp. 309-309.

2.1 Introduction

PV power generation was first introduced to the distribution system, where the power generated was less than 1 MW. These PV systems were installed in houses, neighbourhoods, buildings, and industries, representing a total power installed of 106.2 GW around the world by 2014 (Fig.2.1). During 2014, 19 GW were installed worldwide and it is expected that in 2019, 37 GW will be added to the existing capacity [1], [2].

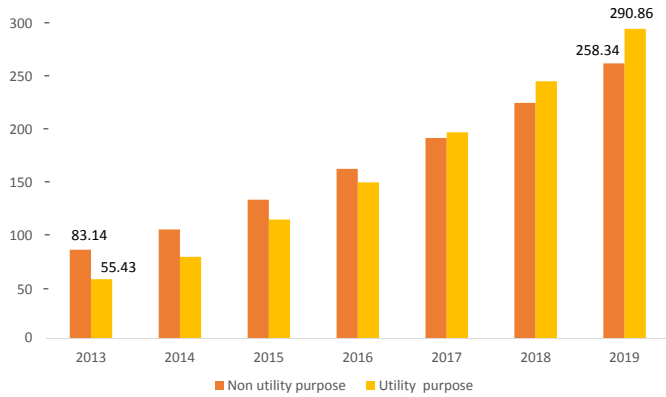

Figure 2.1: Global utility and non utility cumulative power (GW) up to 2019 [1], [2]

The main reason why the consumers were attracted to this type of installation was the economic incentives given by some countries to the citizens for the installation of PV system. These incentives consist especially in the feed-in tariff, that is defined as a payback for the PV system installation. The countries that have succeeded by the adoption of this policy are Germany, Spain, Italy, US, Australia, and Canada [27], [28], [29], [30]. Because of these incentives, Europe leads the residential, commercial and industrial market with a power capacity of around 40 to 50 % of the global market by 2014 [2]. However, due to the reduction of feed-in tariffs in this region, a slower rate of growth in the upcoming years is expected. But the Asian-Pacific countries will lead the residential and commercial market in the future years as the price of the technology decreases[31]. The reduction of prices of PV modules and inverters is not only permitting a higher acceptance of PV systems for the residential, commercial and industrial market, but also the development of PVPPs for utility purpose.

In fact, the price of PV technology for utility is around 1.77 $/Wdc, but for residential is around 3.73 $/Wdc [19]. The feed-in tariff and the reduction of technology prices have permitted the investment in the installation of PVPPs from small ($\leq$ 1 MW), LS-PVPPs ($\geq$ 1 MW) to VLS-PVPPs ($\geq$ 100 MW) [32].

The total global capacity installed for utility purpose around the world was about 76.512 GW by 2014 [1], [2]. This market is expected to grow as it is illustrated in Fig. 2.1. Globally, the PV utility market is expected to grow up 250 GW by 2019 [20]. The leaders of this market are Europe, China, and US that have developed thousands of PVPPs of different capacities. Countries in Latin America, South Africa, and the Middle East are currently developing new LS-PVPPs to VLS-PVPPs that are going to operate in the upcoming years [33]. The map in Fig. 2.2 shows the LS-PVPPs and VLS-PVPPs that had been installed around the world with a power capacity higher than 50 MW, it also illustrates the LS-PVPPs and VLS-PVPPs under development. This map plus the data illustrated in Fig. 2.1 show a clear expansion of the PV utility market.

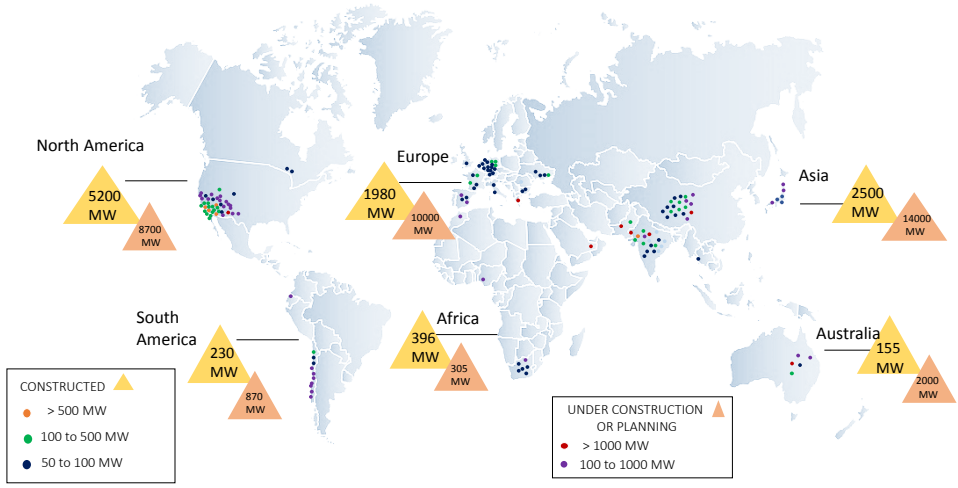

Figure 2.2: Current and future PVPPs around the world with a power capacity larger than 50 MW [3],[4]

Because of this trend, different PV panels, inverters, transformers, protections and storage systems have been developed to improve the overall performance of PVPPs for small, large (LS-PVPPs) and very

large scale (VLS-PVPPs)[2]. Accordingly, this chapter focuses on two main objectives; former, the introduction of the main characteristics of the basic components for LS-PVPPs; and the latter, the definition, and discussion of internal disposition of PV panels, inverters and transformers considering also the ac collection grid topologies for LS-PVPPs.

Numerous publications regarding the review of suitable technology for small PVPPs are found in the literature. The explanation of the components, topology and the control of small PVPPs for houses and buildings are studied in [35, 36, 37, 38]. Meanwhile, [39] and [40] focus on problems related to large scale integration of PV generation into the distribution system as voltage drop and network losses. The topologies used to interconnect PV panels with the inverters, for small PVPPs interconnected to the grid, are studied by [41] and [42]. Besides, Salas, V. et al. [43] study the technology used by inverters in small PV application comparing efficiency, control, cost, weight, and its future trend.

In contrast, there are few publications regarding the review of the electrical layout and the suitable technology for LS-PVPPs and VLS-PVPPs. Stranix et al. [44] and Simburger et al. [45] review the design of LS-PVPPs considering electronic devices, wiring, protections, PV panels, mounting characteristics, installation, maintenance and cost according to the technology used in 1980s. Alternative configurations are studied in [46], comparing technical advantages and disadvantages, but these configurations are only based on central inverters topologies. Ito Masakazu et al. [5] present how different types of PV panels affect to the area occupied by a VLS-PVPP . In [47] and [48], a summary of the problems related to the integration of LS-PVPPs to the grid considering electrical grid codes is described. The control and the implementation of LS-PVPPs are studied on [49, 50, 51] with specific examples. Despite the extensive literature review, there is a lack of information about the internal topology and the ac collection grid for LS-PVPPs. Therefore, the development of this review is critically important in order to describe the components, their internal disposition and the ac collection grid topology used in LS-PVPPs. To accomplish the objectives of this chapter an extensive literature re-

[2]In this thesis I consider small scale if the power rate of the PVPP is in the range of 250 kW to 1 MW, LS-PVPP from 1 MW to 100 MW and according to the International Energy Agency [34], VLS-PVPP has a rated capacity from 100 MW to GW.

view is developed considering publications of the last 30 years presented in journals and magazines. Besides, an extensive review of the technical data of real LS-PVPPs developed around the world is developed to do a deeper analysis of the current trend.

This chapter is structured as follows. Section 2.2 presents a review of the main electrical components used in LS-PVPPs. Section 2.3 is dedicated to the analysis of the internal disposition of the components in a LS-PVPP. Section 2.4 presents the analysis and discussion about the ac collection grid topologies in LS-PVPPs. Finally, the conclusions are presented in Section 2.5.

2.2 Electrical components

The electrical components of LS-PVPPs have three tasks: i) to convert solar energy into electricity, ii) to connect the LS-PVPP to the grid, iii) to assure an adequate performance. The basic components involved in these tasks are: PV panels, PV inverters, and transformers. In this section, a review of these components is developed considering their operating principles, the current technology used, and their future trend.

2.2.1 PV panels

Solar cells are the basis of the PV panel. The function of the solar cells is the conversion of solar energy into electricity [52]. A number of solar cells are connected in series and then encapsulated in an especial frame to construct the PV panel [53].

There are different materials of solar cells affecting to the overall efficiency of the PV panels. The basic types, crystalline (c – Si) and multicrystalline (m – Si) silicon, present efficiency values around 20 % [54]. Other types as the thin film solar cells using amorphous silicon (a – Si) have an efficiency around 6.9 % to 9 % [5, 54] . Thin film solar cells are also using other materials as copper indium diselenide ($CuInSe_2$-CIS), and Cadmiun telluride (CdTe) with efficiencies around 15 % [52] and 12 % [54] respectively. Other materials are in research with the aim to improve efficiency and costs as it is summarized in [55] and [56].

The c – Si and m – Si has dominated the utility market during the last years due to its efficiency, the land used, and its stability during time, reliability and abundant primary resource. The main drawback of this technology is the price due to manufacturing and the quantity of material used [57], [58]. In contrast, thin film solar cells have some benefits as the price, and low-temperature coefficient. But the main drawback for its utilization on LS-PVPPs is the land occupied, lower efficiency, low stability during time [59], [60] and the scarcity of materials [61]

The efficiency of the solar panels affects to the overall dimension of the LS-PVPP, as it is explained in [5]. For the same power, if the efficiency reduces, the area occupied by the LS-PVPP is major. The total cost is also affected not only by the land occupied but also because of installation, transportation, maintenance and mounting characteristics [62]. Fig. 2.3. illustrates the relationship between the efficiency of the different types of solar cells with the size of the PVPP according to the available data in [5] for a LS-PVPP of 100 MW. The Fig. 2.3 shows that the multicristalline silicon solar cells (m – Si) have larger efficiencies (10-12%) than the case of thin film solar cells (7-9%). The area occupied by the silicon solar cells is less than twice the area used in thin film solar cells when amorphous silicon is used. This is also validated by Yimaz at et al. [63] using a small system of 33 kW to compare the performance of (c – Si), (m – Si) and thin film solar cells.

Researchers are still looking forward the improvement of solar cell characteristics by the increment of the efficiency, the decay of prices and the long-term stability [64]. For LS-PVPPs, other solar cell characteristics are also becoming necessaries as sustainability, recycling, and reduction of CO_2 production during its life cycle [65].

2.2.2 PV inverters

The PV inverters are electronic devices that permit the conversion from dc to ac power and are used in different applications. In the case of LS-PVPPs, the PV panels generate dc power, then these panels are connected to a PV inverter to generate ac power [52], permitting its connection to the internal ac grid.

The PV inverter has one or two stages of conversion. In one stage,

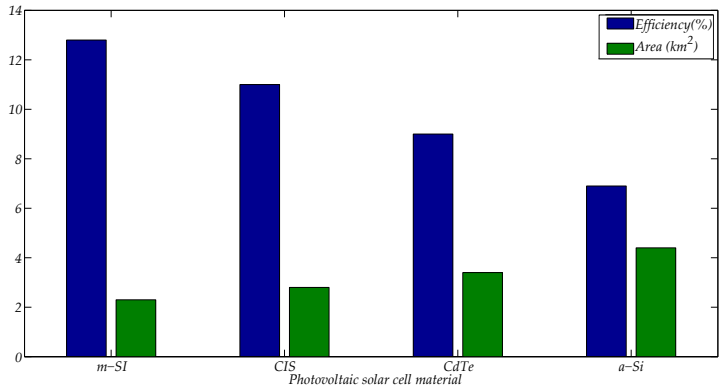

Figure 2.3: Efficiency and Area occupied by PV panels with different types of solar cells for a LS-PVPP of 100 MW [5]

a single inverter (dc-ac) is commonly used, and in two stages an additional dc-dc converter is connected [66, 67]. The use of dc-dc converter in LS-PVPPs is still on research. A review of the state of the art of non-isolated dc-dc converters is studied in [68, 69] and isolated dc-dc converters are analyzed in [70]. In non-isolated converters, the configuration used are boost, buck, buck & boost, Cûk or SEPIC. The leakage current, the voltage stress, and the current ripple are a drawback of non-isolated dc-dc converters. Therefore, the isolated configuration is considered appropriate for LS-PVPPs. The isolation is commonly obtained by a high frequency transformer. The typical configurations are flyback, forward, push-pull, and boost-half-bridge [71]. The switching stress, the cost, and the efficiency are typical issues on these configurations [70].

The choice of the dc-dc converter depends on the dc-ac inverter used at the next stage. The typical inverters used are Neutral Point Clamped (NPC) and Cascade H-Bridge (CHB) [72]. If a dc-dc stage is connected, an isolated converter suites better for CHB as it needs independent dc input for each CHB used [73]. In the case of an NPC, non-isolated converter is connected in a previous stage [74].

In any case, one or two stages of conversion, the PV inverters used in LS-PVPPs must overcome issues related to the technology of the PV panels and electrical requirements. First, PV inverters must have galvanic isolation to overcome any issue related to the leakage current from the PV panels interconnection [70]. Second, due to the non-

linear characteristics of the voltage and current of the PV inverter, a tracker of the maximum power point (MPPT) for any radiation and temperature is needed [75]. Third, the power quality and the operational characteristics of the PV inverters must obey any of the electrical standards applicable to the country.

2.2.3 Transformers

In LS-PVPPs, there are two types of transformers installed (Fig. 2.4). The first one (Tn), steps up the voltage from the PV inverters to the range of 13.8 kV to 46 kV [76]. The second one (T-HV) has two functions: i) to provide galvanic isolation for LS-PVPPs from the electrical grid and ii) to step up the voltage from the LS-PVPP [46]. In the LS-PVPP detailed in [77], forty transformers are used to step up the voltage of the PV inverters from 0.4 kV to 30 kV. In this case, another transformer is used for the complete LS-PVPP to step up the voltage from 30 kV to 110 kV.

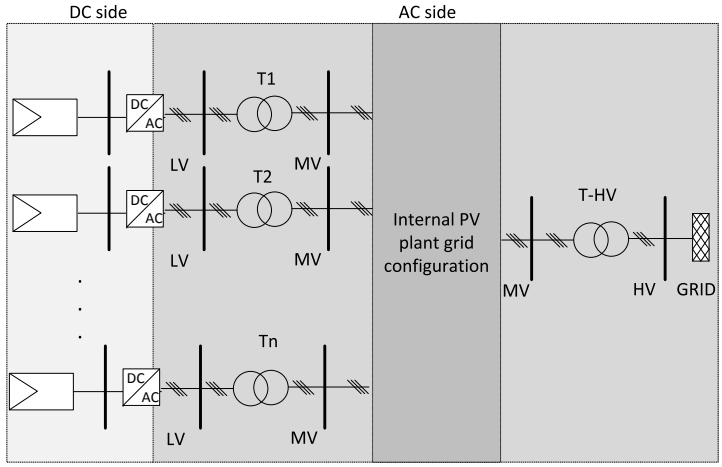

Figure 2.4: Location of the transformers in the LS-PVPP

If the PV inverter has a power rating higher than 500 kW, three winding transformer is commonly used [78]. This transformer has two windings for low voltage (LV), to connect two inverters, and the third one for medium voltage connection (MV) [79, 80]. The existing vector

groups for this transformer are: Dy_ny_n, Dd_nd_n, YNy_ny_n, YNd_nd_n, YNy_nd_n [81]. In the case of PV inverters with a power rating less than 500 kW, transformers of two windings are used [82]. These transformers have two windings, one for low voltage (LV) and other for high voltage (HV). The transformer T-HV has also two windings, one for medium voltage (MV) and the other one for high voltage (HV). The existing vector group for this transformer is Yy.

Any of these transformers (Tn or T-HV) is elected according to the rated power, efficiency, and cost. The transformer could become a bottleneck if the rated power is smaller than the normal operation of the LS-PVPP. If the rated power is too large, there could be some instabilities that cause problems with the overall performance [76, 79]. To overcome this issue, a technique has been designed by A. Testa et al. [83] to choose the transformer according to the power, the efficiency, the cost and the operation of a LS-PVPP.

Currently, researchers are looking for another type of transformers to reduce the area occupied and to improve the reliability of LS-PVPPs. The work developed by B. Hafez et al. propose the use of medium frequency transformers at LS-PVPPs [84]. According to this work, the efficiency of the overall power plant improves by 2 % in comparison with a LS-PVPP developed in Eggebek that uses multistring inverters, but an ac-ac converter is added to the topology.

After the understanding of the definition, function, characteristics and the future trend of the main components in LS-PVPPs, the following section studies the distribution of these components for this type of application.

2.3 Internal PV plant configuration

The connection of PV inverters with PV panels (Fig. 2.5) and transformers (Fig. 2.6) in LS-PVPPs considers three basic topologies: i) central, ii) string, and iii) multistring [41], [42]. There is a fourth basic topology, the ac module integrated, but its application in LS-PVPPs has not been developed yet. The power produced by the different topologies is affected by solar radiation and shading effect, becoming very important the correct choice of the topology according to the power output, location, reliability, cost, and efficiency [35].

In this section, a review of these configurations is developed, describing and analysing their main characteristics, advantages, disadvantages, applications and future trend. To overview a summary of the configurations presented in this section, some tables (see Tables 2.1 to 2.3) and graphics (see Fig. 2.5 to 2.9) are developed according to the data collected from several publications and manufacturers.

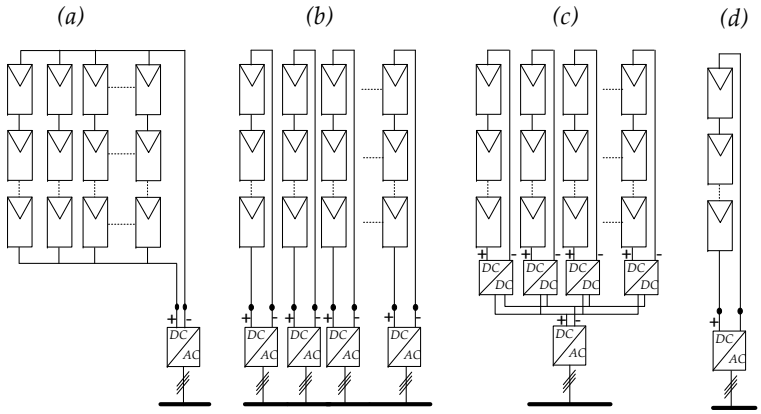

Figure 2.5: PV inverter topologies. (a) Central, (b) String, (c) Multistring, (d) Module integrated

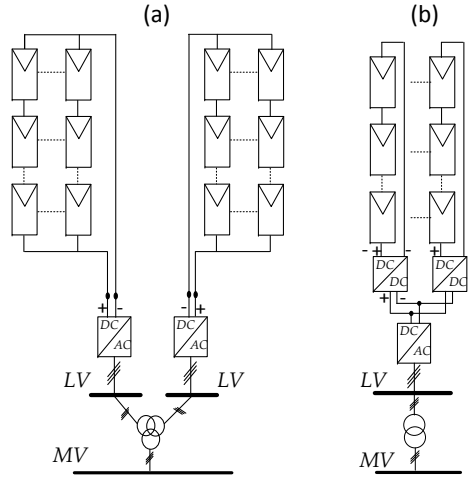

Figure 2.6: Connection of Transformers at Medium Voltage. (a) Central PV inverter with three winding transformer, (b) Multistring PV inverter with two winding transformer.

Table 2.1: Electrical characteristics of PV inverter topologies

Inverter topology	P (kW)	Vin mppt dc (V)	Vout ac(V)	f (Hz)
Central	100-1500	400-1000	270-400	50, 60
String	0.4-5	200-500	110-230	50, 60
Multistring	2-30	200-800	270-400	50, 60
Module Integrated	0.06-0.4	20-100	110-230	50, 60

2.3.1 Description of internal topologies

The interconnection between PV panels and the inverters is illustrated in Fig. 2.5. The central topology (Fig. 2.5(a)) interconnects several thousands of PV panels to one inverter. The disposition of these PV panels is clustered into PV arrays. Each array has hundreds of PV strings connected in parallel, and each string has hundreds of PV panels connected in series. The string topology (Fig. 2.5(b)) connects one PV string with one inverter. The multistring topology (Fig. 2.5(c)) connects one PV string to a dc-dc converter, then 4 or 5 dc-dc converters are connected to one inverter which may or may not be closed to the dc-dc converter. The fourth topology, the ac module integrated (Fig. 2.5(d)) has one inverter per each PV panel. The inverters utilized on these topologies takes the name of the topology used: central, string, multistring and ac module integrated. The electrical characteristics of these inverters are described in Table 2.1.

These topologies are differentiated by four categories: general characteristics, power losses, power quality and cost (Table 2.2[3]). The first category, general characteristics, considers the robustness, reliability, flexibility, and MPPT efficiency [85, 86, 87]. Each topology presents its own general characteristics that depend specially on the power rating, number of PV inverters and number of PV strings. For instance, the central topoleogy has low levels (L) of reliability, flexibility and MPPT efficiency but its robustness is higher than other topologies.

The second category, power losses, considers mismatching, switching, ac and dc losses. Mismatching losses are inevitable in any PV array. These depend on uneven degradation of the PV string, shading, cloud coverage, dust, cooling, MPPT efficiency, among others [88, 89]. In this case, central topology presents higher (H) mismatching losses because several strings are connected to a single inverter.

[3]The following nomenclature is used: H-H: very high, H: High, M: Medium, L: Low, L-L: very low

The switching losses are also a concern that depends on the devices and the control of the PV inverter. The length of the cables in the dc or the ac side influences the cumulative losses of LS-PVPPs. Central inverters have very high (H-H) losses at the dc side as many strings are connected in parallel. In contrast, the ac losses in the central inverter are low (L), as the transformers (Tn) are connected very close to the inverter.

The third category, power quality, is influenced by the dc and ac voltage variations and voltage balance. In the case of central topology, the dc voltage variation is very high (H-H) because many strings are connected in parallel. In this case, the ac voltage variation is low (L) and the voltage balance is high (H) as it has only one inverter. The voltage is unbalanced especially when many inverters are connected in parallel as the case of module integrated. Due to losses, distances and voltage sags, the three phase voltage balance at the point of connection with the transformer (Tn) could be affected. Therefore, when several inverters are connected in parallel, is necessary to develop a master control for a group of PV inverters to reduce the ac voltage variation and to improve the voltage balance.

The fourth category, the cost, involves the installation, maintenance, land cost and length of cables in the dc or the ac side [85, 90, 91]. The comparison of costs for each topology is detailed in Table 2.2, but the land cost is not included as it depends on the location of the LS-PVPP.

Because of comparison analysis, Fig. 2.7 is developed considering each characteristic for every topology presented in Table 2.2. It can be stated that the central topology has the following advantages: robustness, low ac power losses, low ac voltage variation and a reasonable installation and maintenance cost in contrast with the other topologies. The general characteristics of string and multistring topologies [85] are very attractive, but the main drawback is the installation and the maintenance cost as the number of inverter increases. String topology has similar characteristics as the multistring topology, but it is recommended to use it when each PV string has different orientation angle [91, 4]. In real LS-PVPPs, module integrated topology has not been implemented, but it can be concluded that has good characteristics considering flexibility, MPPT efficiency, and reliability. The robustness, power losses, power quality and the general cost are several drawbacks for the module integrated topology.

Table 2.2: Main characteristics of PV inverter topologies

		Central	String	Multistring	Module integrated
General characteristics	Reliability	L	H	M	H-H
	Robustness	H	L	M	L-L
	Flexibility	L	H	M	H-H
	MPPT efficiency	L	H	M	H-H
Power losses	Mismatching	H	L	L	L-L
	Switching	H	L	M	L-L
	ac power losses	L	M	M	H
	dc power losses	H	L	M	L-L
Power quality	ac voltage variation	L	H	M	H-H
	dc voltage variation	H-H	M	H	L-L
	voltage balance	H	M	L	L
Cost	Installation cost	M	H	M	H-H
	dc cables	H	L	M	L-L
	ac cables	H	M	M	H
	Maintenance	L	M	H	H-H

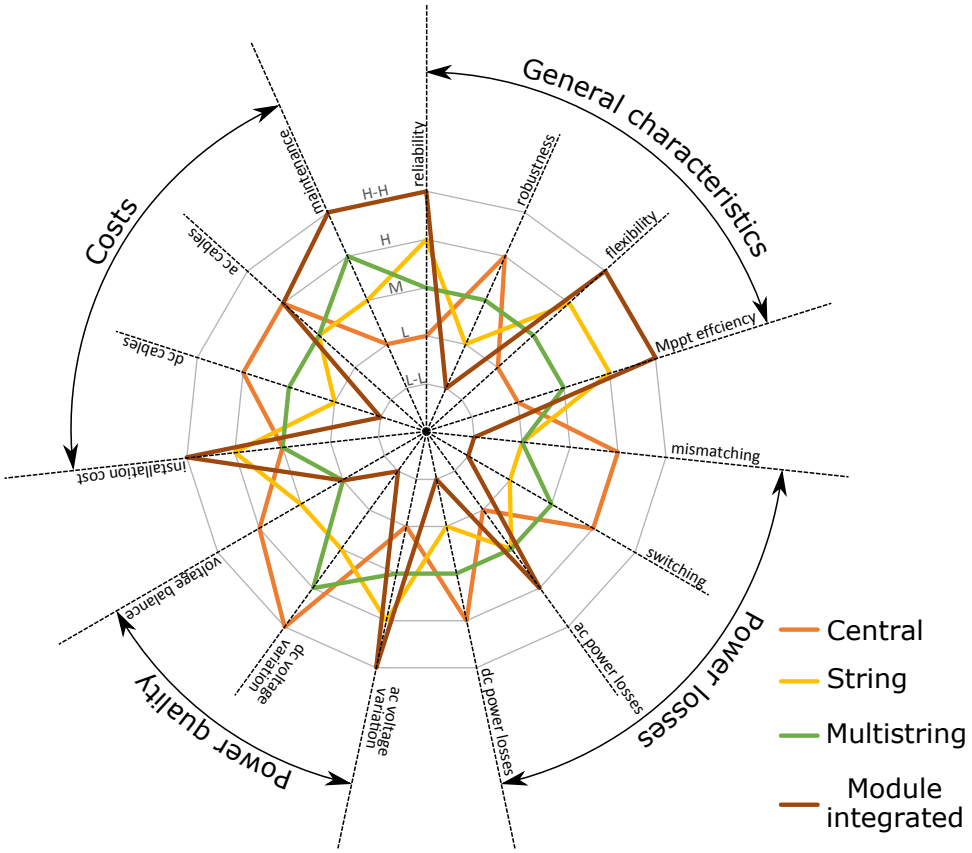

Figure 2.7: Comparison between different PV inverter topologies characteristics for LS-PVPPs

2.3.2 Analysis in real LS-PVPPs

In this subsection, an analysis of real LS-PVPPs is developed to see the applicability of the topologies studied before. A comparison of three different topologies available in the market considering cost, efficiency, and area is illustrated in Fig. 2.8. The topologies compared are central, multistring, and an additional topology called multicentral inverter. This topology encapsulates in one cabinet several central inverters with a power rating less than 100 kW. In the cabinet, there are at least three different PV inverters with the same characteristics. Each of them has its individual MPPT control. The output of each inverter is connected in parallel with the adequate protections to have only one output for the complete cabinet. Fig. 2.8 shows that multicentral inverter has better characteristics on price and efficiency in comparison with central and multistring inverter.

Additionally, Fig. 2.9 compares 22 LS-PVPPs of different power from 6 to 90 MW, where 17 of them have PV inverters connected in central topology. The comparison is made between the area occupied and the number of PV modules in contrast to the capacity rating of the LS-PVPP for central and multistring topology. This graph shows that the central topology is the most used technology due to its feasibility and the small number of inverters used in the power plant. Multistring topology is barely used in LS-PVPPs and the area occupied according to the evaluated data is almost the same as the area used for central topology.

In any of these cases at large scale, string topology has not been used. The work developed by Syafaruddin et al. [92] analyses that an array of PV panels connected to central inverter generates less power than string topology for the same PV array considering non-uniform irradiance condition and a novel MPPT control based on artificial neural network. The study developed by A. Woyte et al. [93] concludes that there is not a considerable difference among central and string inverter with a similar annual yield, thus the performance ratio during the year is similar.

Table 2.3 summarizes the main characteristics of some LS-PVPPs developed by SMA, ABB, SunPower, and Danfoss. This table indicates the area, the number of PV panels, the panel type, the PV inverters

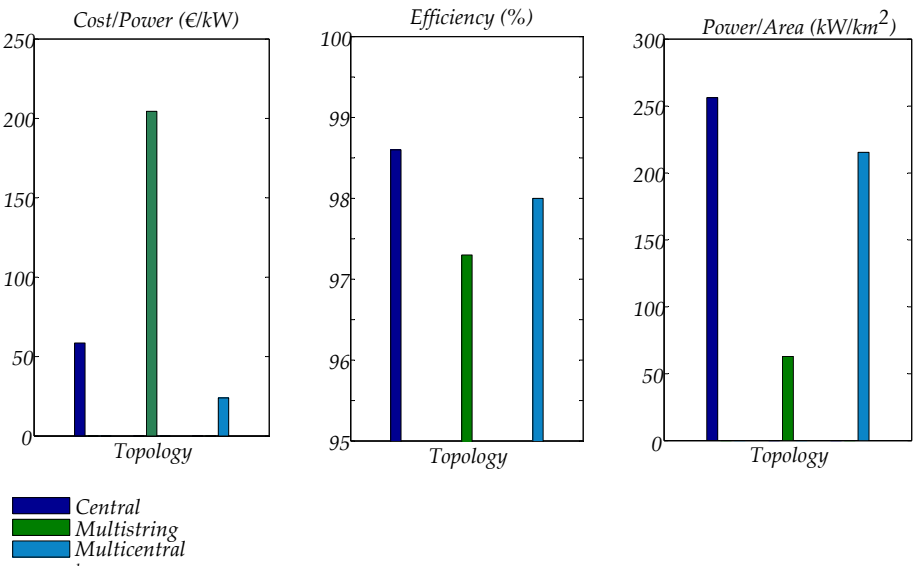

Figure 2.8: Comparison between different PV inverter topologies available in the market for LS-PVPPs

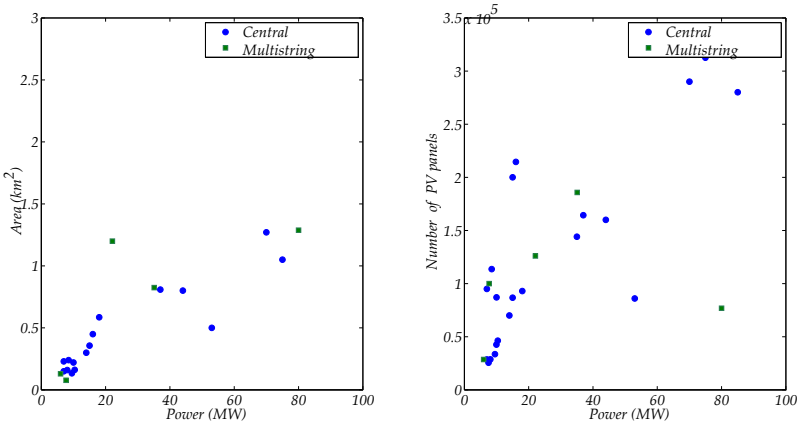

Figure 2.9: Comparison of area and number of PV panels used between different real LS-PVPPs

and the topology[4] used in operating LS-PVPPs. Other components are still necessary for the design, implementation, and operation of

[4]MI=Multistring Inverter, CI=Central Inverter

Table 2.3: Details of some operational LS-PVPPs

Photovoltaic Power Plant	Power (MWp)	Area (km^2)	Panels ($*10^3$)	Panel type	Inverters Number	Topology
Korat I	6.0	0.13	29	m-Si	540	MI
Narbonne	7.0	0.23	95	Thin film	19	CI
Rapale	7.7	0.49	100	Thin film	900	MI
Airport, Athens	8.1	0.16	29	m-Si	12	CI
Saint Amadou	8.5	0.24	113	Thin film	16	CI
Volkswagen Chattanoga	9.5	0.13	33	m-Si	10	CI
Masdar	10	0.22	87	m-Si, Thin film	16	CI
Adelanto	10.4	0.16	46	m-Si	13	CI
Taean	14	0.30	70	m-Si	28	CI
Jacksonville	15	0.40	200	Thin film	20	CI
San Antonio	16.0	0.45	214	Thin film	22	CI
Cotton Center	18.0	0.58	93	m-Si	36	C
Almaraz	22.1	1.2	126	m-Si	6697	MI
Veprek	35.1	0.83	185	c-Si	3069	MI
Long Island	37.0	0.80	164	m-Si	50	CI
Reckahn	37.8	0.98	487	Thin film	43	CI
Ban Pa-In	44.0	0.80	160	m-Si	61	CI
Lieberose	71.0	2.2	900	Thin Film	38	CI
Kalkbult	75.0	1.05	312	m-Si	84	CI
Eggebek	80.0	1.29	76	m-Si	3200	MI
Montalto di Castro	85.0	2.83	280	c-Si	124	CI
Templin	128	2.14	1500	Thin Film	114	CI
California Valley Ranch	250	6.01	749	c-Si	500	CI
Agua Caliente	290	9.71	5200	Thin Film	400	CI

LS-PVPPs, as junction boxes for dc and ac side, sensors [94, 95] and protection devices that are not part of this review.

The data detailed in Table 2.3 shows that the preferred material of PV panel is m-Si and thin film. In LS-PVPPs that uses thin film solar panels occupies twice the area than the PVPPs that uses m-Si. Only, three PVPPs of the table below uses c-Si, and these show less number of PV panels and less area occupied. Furthermore, the number of PV inverters depends on the topology used, a large number of PV inverters is common in multistring topology. For instance, in the cases of Veprek and Long Island solar plant with a corresponding power of 35 MW and 37 MW respectively, have similar area occupied, though the topology is different. The number of PV panels used in the case of Long Island is twenty thousand less than Veprek solar plant, though the power is higher in the first case. The number of multistring inverters, in the case of Veprek, has a total number of 3069 in contrast with 50 inverters used in the case of Long Island. Despite the topology used, the area and the number of PV panels do not seem to have any relation to the topology chosen. However, the area occupied and the number of PV panels has a relation with the type of material used in the PV panel. In Veprek PV plant, c-Si is used, in contrast, m-Si is used in Long Island. In the case that thin film solar cells is chosen for similar power as the Reckahn power

plant, the area occupied increases in 20 % and the number of PV panels is almost three times than the case of Long Island PV plant. However, in both cases the internal configuration chosen is central and the number of inverters is almost similar.

The cost influences in the decision of the topology and the technology used as well as the efficiency required, the performance, the area, the price of land and the location. Despite the importance of the internal distribution of the PV panels, inverters, and transformers, the following section studies the general configuration of the overall plant without considering the PV inverter topology chosen for the PV arrays.

2.4 Collection grid topologies

Collection grid topologies are considered for internal dc or ac power. Very little information has been documented about the ac collection grid topologies for LS-PVPPs and none has been presented for the dc collection grid. This section explains some possible AC collection grid topologies described by some manufacturers as radial, ring, star and their variations considering their advantages and disadvantages. In this explanation, an array of PV panels together with its inverter and transformer is considered as PV generator.

2.4.1 Radial

The radial collection system considers several numbers of PV generators connected to one feeder, developing one string, as shown in Fig. 2.10. The majority of LS-PVPPs uses this topology because it is cheapest and simplest, but its low reliability makes it less attractive. If the first generator connected to the feeder is lost, all the string is lost. One example of this configuration is detailed by Danfoss using one of their Multistring inverters. In this case, a LS-PVPP of 15 MW is proposed. It has two feeders of 7.5 MW, and each of them has 5 transformer stations of 1.5 MW. The low voltage side of the transformer is connected to 88 multistring inverters that are connected in parallel between them [96]. In the case, a PV inverter is lost, the total power production will not be affected significantly, but, if one

transformer station is lost, all the feeders can be lost in the worst case scenario. In this case the power produced will reduce by 50 %.

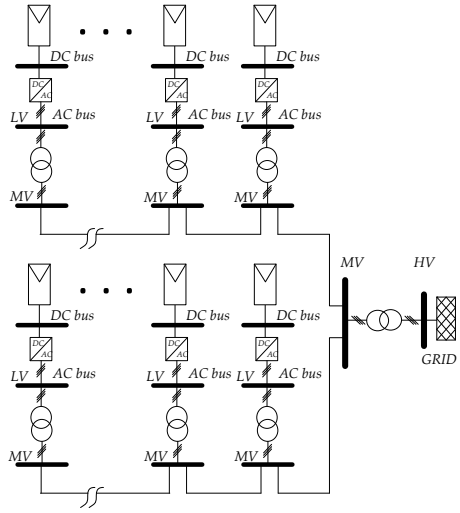

Figure 2.10: Radial collection configuration

2.4.2 Ring

The ring collection topology is the one used to improve the reliability of LS-PVPPs. The connection is based on radial design but it adds another feeder in the other side of the string (Fig. 2.11). If one of the PV generators is lost, then the PV generators connected to the other side of the feeder can still give power to the LS-PVPP. The drawback is the cost and the complexity of the installation. A LS-PVPP of 10 MW proposed by Danfoss uses this configuration considering 15 transformer stations. The low voltage side of these transformers is connected to 42 multistring inverters. In this case, if there is any failure in one of the inverters just a small part of the LS-PVPP is lost (less than 1 %) [97]. In this case, if any transformer station is lost, there is a reduction of power production of 6.3 %.

2.4.3 Star

This collection topology has one PV generator connected to the main collector. Commonly, this collector is in the middle of the LS-PVPP

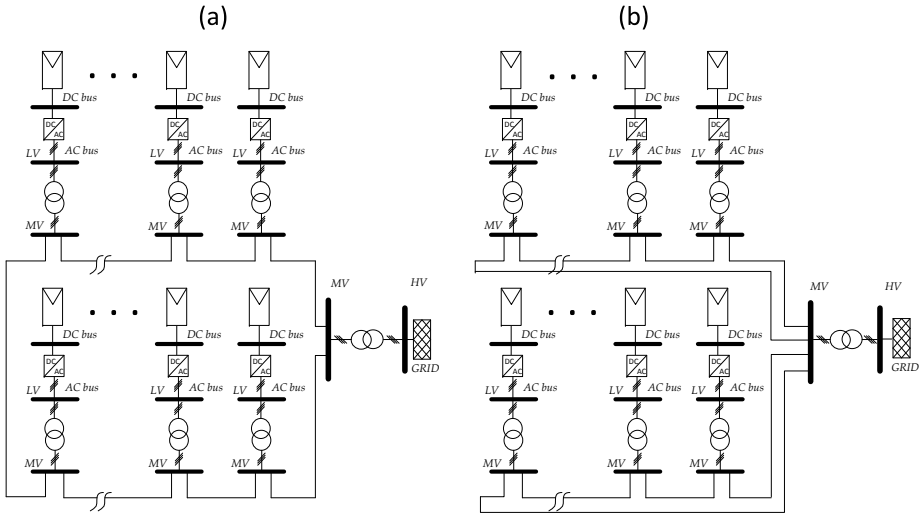

Figure 2.11: Ring collection configuration. (a) case 1 and (b) case 2

to reduce the distances of the cables and to have the same losses between them (Fig.2.12). This solution offers higher reliability than the other cases. On the downside, there is one feeder for each PV generator that increases the total cost. An example of 21 MW LS-PVPP is explained by Abraham Ellis for the integration of Renewable Energy in South Africa [98]. The star configuration proposed considers 8 transformer stations. Each of these transformers is linked to 3 central inverters on the low voltage side. In this case, if a transformer station is lost, 14 % of the power production will be affected. This can be reduced if multistring inverters are used. It will have a power reduction of 4% if any of the central inverters fails.

The ac collection grid topologies presented here have different problems with reliability, cost, and efficiency. These issues can be overcome if there is a complete analysis of these configurations in one case scenario, very few cases have been published making impossible the comparison among them. Finally, the table (Table 2.4) summarizes the technology, the internal topology and the ac collection grid configurations used in LS-PVPPs, considering the above discussion.

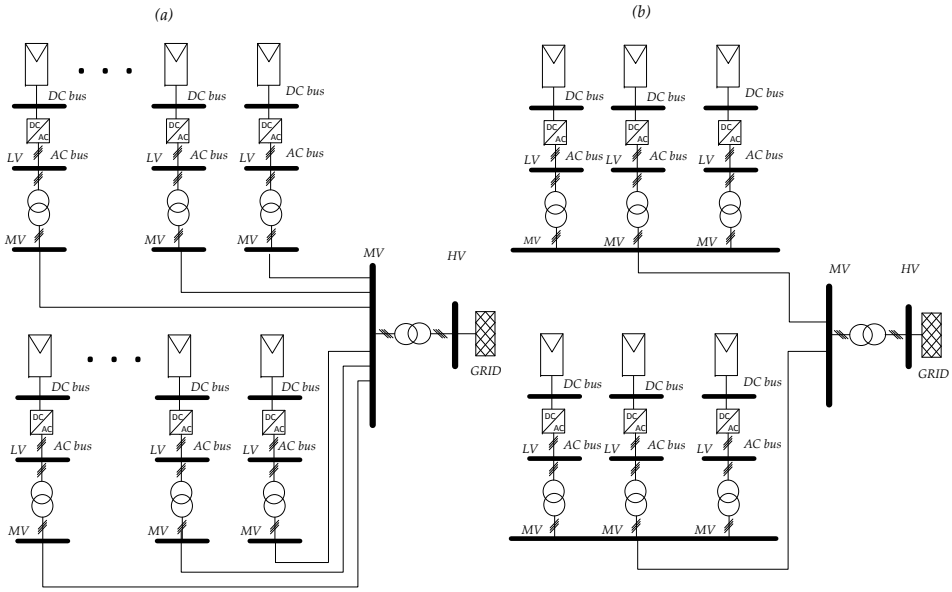

Figure 2.12: Star collection configuration. (a) case 1, (b) case 2

Table 2.4: Summary of basic elements, internal configuration and topologies for LS-PVPPs

	Basic elements			Configuration and topologies	
	PV panels	PV inverters	Transformers	Internal configuration	Collection grid topologies
Technology	m-Si c-Si Thin film solar cells	one stage (dc-ac) two stages (dc-dc-ac) galvanic isolated or non-isolated	Two windings Three windings	Central String Multistring ac module	Radial Ring Star
Most used tecnology	m-Si and Thin film	One stage dc-ac	Three winding	Central	Not enough documented PVPPs
Concerns	Effciency Price Manufacturing stability	Switching losses Effciency Adequate control Compliment of grid codes Galvanic isolation Price	Size Price Power	Power effciency Voltage variation Installation cost Maintenance cost	Reliability Losses Cost

2.5 Conclusions

In this chapter, the main characteristics of the basic components for LS-PVPP have been detailed. In addition, the internal disposition and ac collection grid topologies have been described considering real LS-PVPPs implemented around the world. The tables 2.1 to 2.4 present a general summary of the different topics discussed in this review. It is worth pointing out the right choice of the components af-

fects the area occupied, the efficiency and the reliability of LS-PVPPs. From this review, some conclusions can be argued:

- The material used in the PV panels makes a big difference in the area occupied. Better materials of PV panels makes possible the reduction of the area used by LS-PVPPs. PV panels with higher power and less size must be developed specifically for LS-PVPPs. This will help to reduce the installation costs and the area used. In this sense, silicon solar cells is more suitable for large installations as it has higher efficiency and the land used is less than the case of thin film solar cells. Also, the prices are expected to decay in the future years which will help to the development of LS-PVPPs. However, thin film solar cells technology is still improving and it is expected that more LS-PVPPs will use it, as the price is less than crystaline or multicrystaline solar cells.
- The most widely used PV inverters in LS-PVPPs have one stage of inversion (dc-ac), as it is a known technology and has been deeply applied to the integration of renewable energy into the grid. However, two stages are attractive for the future of LS-PVPPs to improve the control of the PV generator at the dc side which permits to reduce the dc variations. Besides, the addition of galvanic isolation in any of these cases depends broadly on the PV panel type and the electrical characteristics required by the LS-PVPP. Deeper studies are necessary considering real cases scenarios to understand the advantages and disadvantages of the use of converters with one or two stages, galvanic isolated or not.
- The internal topology is critical for the performance of the LS-PVPPs. Central topology has been preferred by the majority of LS-PVPPs developed in the world. This may obey to the simplicity of installation and to the small number of components in the overall power plant. The drawback of the central topology is the mismatching losses caused by the change of radiation reducing the effectiveness of the MPPT control and affecting the output power. Multistring topology has better characteristics of efficiency because it has a dedicated MPPT control per string. The complexity of installation and the large number of inverters installed, make this topology less attractive to investors. The multistring inverter topology has a big potential on LS-PVPPs,

but deeper research on cost, efficiency and behaviour is necessary.

- According to the topology chosen and the rated power of the inverter, the transformer is elected. Two windings transformer was commonly used in PVPPs developed in the 90s due to the power of central inverter. However, the development of central inverters with a higher rating has increased the necessity to have an improved transformer. Today, one of the transformers most used in real LS-PVPPs has three windings that permits to link two central PV inverters with their independent control. But in the case of multistring inverters, two windings transformers is still used. The future trend of the transformers for LS-PVPPs depends especially on how the inverter improves its technology and control. Their size, operation, maintenance, power quality are the current concern in LS-PVPPs and deeply research on new transformer's generation is still emerging.
- A comparison of various conceptual designs for the ac collector system options in terms of losses, reliability, and economics has been presented in this review. In real LS-PVPPs radial configuration is the most used as it has the lowest cable cost. Currently, there is any study comparing the collector system options for this type of application and how the variation of solar radiation and temperature affects the performance of any configuration. In future years the use of radial or ring configuration will be the most used and not so many changes will occur in this area. However, as the PV array supplies dc power, it will be more attractive to have dc collection grid instead of ac. This will depend on how the dc-dc converters and protections will develop in the future years and how the price for dc technology will drop.
- The future of LS-PVPPs depends on the decay of prices, size reduction, efficiency improvement of the different elements used in its development (PV panels, transformers, and inverters). After the prices will be sufficiently reduced, the internal configuration and the collection grid are part of the future concern in LS-PVPPs considering cost, robustness, reliability and flexibility. Together with the concern of the elements and the configuration, the necessity to improve the control and the energy management of LS-PVPPs is increasing.

Chapter 3

Review of advanced grid code requirements

"...But we have learned from experience that we cannot develop one element such as renewable electricity - without considering what happens to the wider network."
Günther Oettinger, European commissioner for energy .

This chapter presents a comparison of the grid codes of Germany, US, Puerto Rico, Romania, China, and South Africa considering: fault ride through capability, frequency and voltage regulation, as well as active and reactive power support. In addition, a broad discussion about the challenges that the large scale photovoltaic power plants have to overcome is presented together with the compliance technology and future trend[1].

[1]This chapter is based on the following publication:
A. Cabrera-Tobar, E. Bullich-Massagué, M. Aragüés-Peñalba, O. Gomis-Bellmunt, "Review of advanced grid requirements for the integration of large scale photovoltaic power plants in the transmission system", *Renewable and Sustainable Energy Reviews.*, 62 (2016),pp. 971-987

3.1 Introduction

A centralized system that performs the functions to supply power to the electrical system and not to a particular customer is known as a power plant. Its main aims are to function independently and to comply with the needs of the electrical system under some regulations [1].

Grid codes and standards define the requirements of these power plants connected to the transmission or distribution grids to enhance its reliability, stability, and security. These grid codes were traditionally developed to permit the interconnection of power plants, based on synchronous generators, with the grid. The use of renewable energy to produce electricity was initially very low in comparison with conventional power plants, but this has changed drastically in the last years. Thus, it is becoming more important to develop grid codes for power plants that use renewable generation as the main source to avoid any problem with the electrical system operation. In this sense, wind power plants have stepped up the path for grid codes development. However, LS-PVPPs and VLS-PVPPs connected to the transmission system, grid codes have recently been developed and further analysis is needed.

In the case of PV inverters connected to the distribution network, the standard IEEE 1547 has been widely used. This standard regulates the interconnection of distributed resources like synchronous machines, induction machines, and power inverters. This standard prevents that the distributed resources participate in ancillary services as frequency and voltage stability support, active and reactive power management [99], [100]. However, due to the growth of PVPPs for utility purpose in the last years, there has been a development of grid codes to permit the integration of PVPPs at the transmission level.

The first grid code specifically for PVPPs interconnected with the Transmission system was developed by Germany in 2008, 4 years after the first grid code developed for WPPs by Denmark [101]. This grid code for PVPPs has been utilized especially by Europe and has become a good example to develop similar regulation around the world. After German's grid code, other countries created their own regulations as South Africa [102], China [103], and Romania [104]. In the case of United States of America (US), there is an electrical

standard for the interconnection of large scale generators (LGIA) to the electrical system, however, each TSO has their own requirements [105]. One of these is the TSO of Puerto Rico that has its own and well-defined grid code for LS-PVPPs [106]. Panama has also developed its grid code, but this is based on the ones named before [107]. Not more grid codes, that consider the integration of LS-PVPPs with the electrical system, are available in other countries. However Mexico, Brazil, Spain and Chile are currently discussing the creation of grid codes for this purpose, as the power generation by PVPPs in these countries is expected to grow.

A short comparison between the grid codes of China, Germany, and US for PVPPs connected to the distribution or to the transmission system, considering also the electrical standards IEEE 1547 and EN 50160 is developed in [108]. As Germany was the first technical grid code launched for PVPPs connected to medium and high voltage transmission network, there are some publications analysing these requirements like [48] and [109]. These focus on the response of the PVPP when there are disturbances. A similar study developed by X. Jiao and Q. Giao considers Chinese grid code [110]. A scope of the challenges for large scale PV integration in the distribution and transmission level is developed by R. Shah et al. [111], comparing some grid code requirements given by Germany and US. The work developed by Manasseh, O and Bass, R [100] compares and analyses the requirements given by some electrical standards for the distribution system as: IEEE 1547, IEEE 519 and IEEE 929. They also analyse the challenges and the trends of the PV systems interconnection with the distribution level. But this work does not consider the grid code requirements for the interconnection of LS-PVPPs with the transmission system. In the case of WPPs a deeper analysis of the most important grid codes is developed by [112], however, a similar study for LS-PVPPs' grid codes is still missing.

Thus, this chapter addresses a comprehensive analysis of the main grid code regulations for LS-PVPPs connected to the transmission system. The grid codes analysed are the ones that up today are accepted by the transmission system operators of Germany, US, Puerto Rico, South Africa, China and Romania which have been used for the current PVPPs installed in those countries. After this comparison, a discussion about the challenges that operators of PVPPs have to face is deeply discussed. Further, the analysis of the compliance

Table 3.1: International grid codes under study

Country Grid Code	Organization	Title	Version
Germany	BDEW	Generating plants connected to the Medium-Voltage network	June, 2008
Romania	ANRE	Technical conditions for connection to public electricity networks for PV power plants.	2013
US	PREPA	Technical Requirements for Interconnecting Wind and Solar Generation	August, 2012
	FERC LGIA	Standard large generator agreement	2006
China	NEA	GB/T 19964. Generating plants connected to the Medium-Voltage network	2012
South Africa	NERSA	Grid connection code for renewable power plants connected to the electricity transmission system or the distribution system in South Africa	November, 2012

technology used and researched so far is analysed and summarised.

3.2 Comparison of grid codes

This section compares the different technical requirements requested by Germany, China, Romania, Puerto Rico, US and South Africa for the interconnection of LS-PVPPs to the transmission system (Table 3.1). The comparison is developed considering four specific categories: a) Fault-ride through requirements, b) voltage and frequency deviation boundaries, c) active power and frequency control and d) voltage and reactive power control.

3.2.1 Fault ride through requirements (FRT)

The type of faults in the grid codes considered by PREPA, NERSA, NEA, and ANRE are symmetrical and asymmetrical where the requirements are the same for both cases. BDEW and FERC LGIA have prepared specific requirements for only symmetrical faults. The basic curve for FRT requirements is illustrated in Fig.3.1. The normal voltage profile at the point of common coupling (PCC) is in area A, where the PVPP works continuously. If the voltage profile at PCC is in Area B, the PVPP has to remain connected for a period of time. In the case that the PVPP's voltage profile is in Area C, it is not mandatory for PVPP to stay connected. ANRE's grid code establishes that the PVPP has to withstand voltage drops up 85% of the nominal voltage for a considerable time of 0.625 s. When a fault occurs, the voltage could drop to 0, and thus the grid codes established by BDEW, PREPA, NEA, NERSA and FERC LGIA stay that the PVPPs have to

withstand voltage drops of 100 %. In this case, the time that the PVPP has to remain connected is 0.15 seconds as it is demanded by BDEW, NEA, NERSA and FERC LGIA. In the case of PREPA's grid code, the time should be 0.6 seconds In this sense, the most restricting FRT requirement is enforced by PREPA under symmetrical and asymmetrical faults where the PVPP has to withstand voltage sags of 100 % during 600 ms. After the fault is cleared, the voltage returns to safety values (V_1) for a given time (t_2). In the case of Germany and China, after 0.15 seconds, the voltage rises up to 30 % and 20 % of the nominal value respectively. The PVPP has to withstand this new condition during 0.5 seconds. After this, the voltage has to trip to V_1 for a recovery time (t_2). In this sense, BDEW requires that PVPPs return as fast as possible to normal operating conditions. The voltage limits and the times are summarized in Table 3.2 and Fig.3.2 illustrates the voltage profile for low voltage requirements in each grid code.

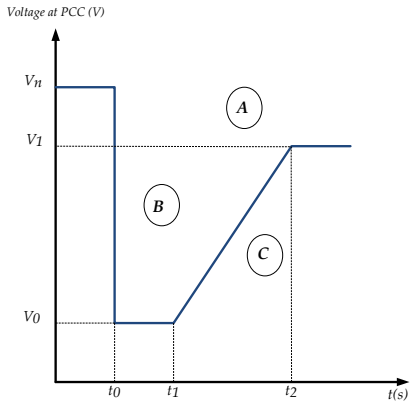

Figure 3.1: General Curve for fault ride through requirements

The PVPP has also to remain connected when over-voltages occur, these are the high voltage ride through requirements (HVRT). These are imposed by PREPA and NERSA for PVPPs (Fig. 3.3) but BDEW, NEA, and ANRE only give the limits of voltage for normal operation and do not clarify any HVRT requirement. FERC LGIA does not clarify this value because it depends on the TSO requirement. Table 3.3 summarizes the requirements given by the grid codes of Germany, Romania, Puerto Rico, China and South Africa. It is evident that Puerto Rico has the most restricting HVRT regulation, that

Table 3.2: FRT requirements in international grid codes

Grid code	During fault		After fault	
	V_0(pu)	t_1 (s)	V_1(pu)	t_2 (pu)
Germany	0	0.15	0.9	1.5
Romania	0.15	0.625	0.9	3
US-Puerto Rico	0	0.600	0.85	3
China	0	0.15	0.9	2
South Africa	0	0.15	0.85	2

Table 3.3: Comparison of HVRT requirements in International grid codes

Grid code	V (pu)	t(s)
Germany	NS	NS
Romania	NS	NS
US-Puerto Rico	1.4 1.3 1.2 1.15	0.15 0.95 1 continuous
China	NS	NS
South Africa	1.2 1.1	0.15 continuous

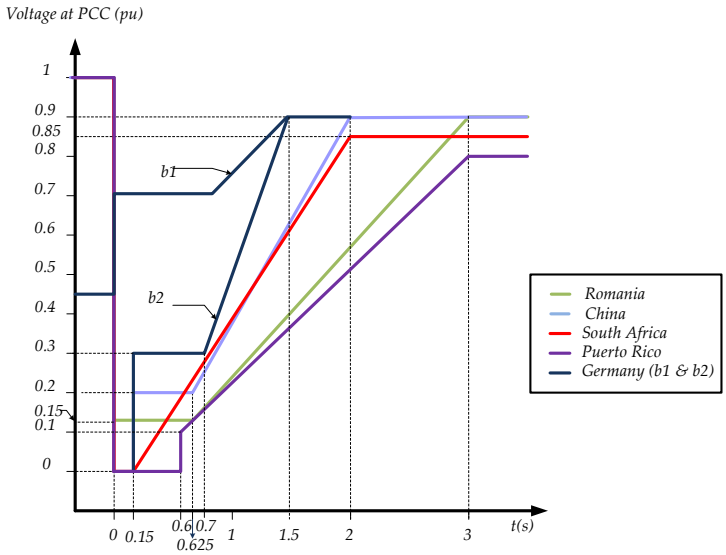

Figure 3.2: Comparison of FRT requirements in International grid codes

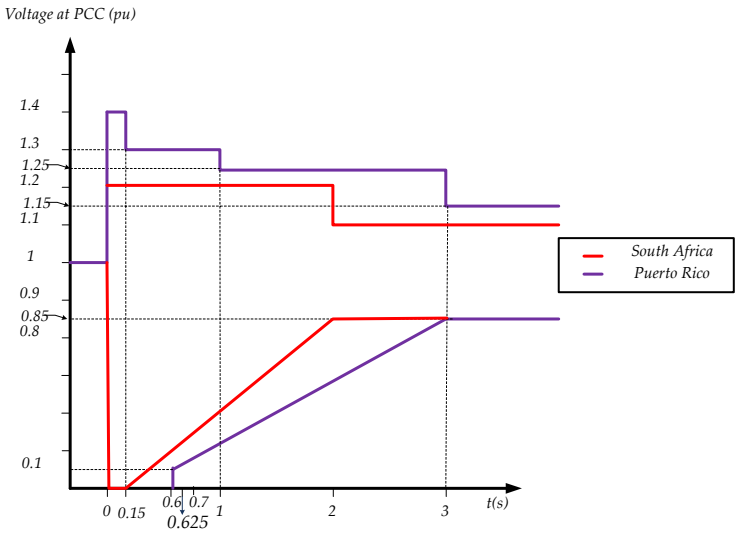

Figure 3.3: Comparison of HVRT requirements in International grid codes

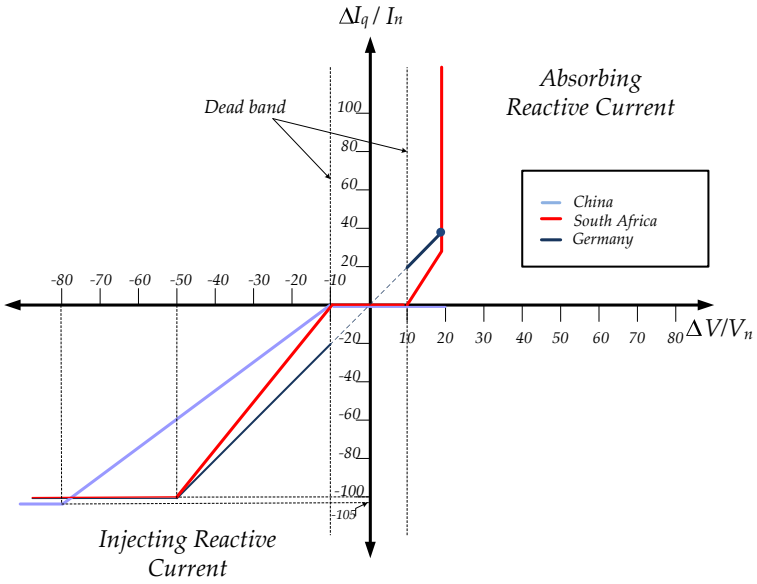

Figure 3.4: Reactive current injection requirement by International Grid codes.

imposes to PVPPs to withstand an over-voltage of 1.4 p.u during 0.15 seconds.

The voltage stability is assisted by the reactive power support. Germany, South Africa, and China have the reactive power requirement illustrated in Fig. 3.4. The grid code of Germany requires a 2% slope of positive reactive current injection for each percent of voltage drop. In the case of a sag value higher than 50 %, the injection of reactive current goes to 100 % or more depending on the converter's current. The grid code given by Puerto Rico requires a variable slope that goes from 0 to 10 %. The dead band without the injection of reactive current is 10 % for Germany, South Africa and China, and 15 % for Puerto Rico.

There is an extra requirement given by NERSA that determines that LS-PVPPs have to supply full reactive current when the voltage goes down to 20 % without limitation of time. China, meanwhile, requires an injection of reactive current response with a 1.5 % slope for voltage variations from 0.2 to 0.9 p.u. The reactive current injection is 105% of the rated current when the voltage sag is higher than 0.8 p.u. Another interesting characteristic in China's grid code is that it does not permit the absorption of reactive current when there is overvoltage and thus the reactive power support is 0 when the voltage is higher than 0.9 p.u. Germany, South Africa, and Puerto Rico permit reactive power absorption when the voltage goes to 120 %. For FERC LGIA and Romania, there is no clarification about the reactive current injected when faults occur [105].

It is important to notice that the most extreme requirements for FRT and HVRT are presented by PREPA's grid code. This is mainly to the weak grid that Puerto Rico has. For this reason, the reactive power support is variable from 0 to 15 %. Regarding the reactive power support, not all the grid codes have the same requirements. It could be interesting to harmonize them in order to develop effective solutions as it is not easy going on task to comply with the injection and absorption of reactive power. In addition, the different grid codes also permit the installation of equipment to overcome this necessity as Static Var Compensators (SVCs), Static synchronous compensators (STATCOMs) and capacitor banks. However, the absorption of reactive power could lead to require more reactive power from the grid which is not a desirable performance.

3.2.2 Voltage and frequency boundaries

The grid codes establish the electrical boundaries under which the PVPPs have to operate continuously. Romania, Germany, South Africa and China have the same voltage range of 90 to 110 % of the nominal voltage. This condition is for any nominal voltage at the PCC according to the Transmission grid code of Romania. In China, however, the variation of 10 % of the nominal voltage is only when the voltage at the PCC is higher than 35 kV. If the voltage is less than 20 kV, the voltage range is between 93 to 107 %. In the US, the boundaries of frequency and voltages depend on the TSO and it is not clarified by FERC LGIA. For instance, Puerto Rico has other boundaries of voltage at the PCC, which are from 85 to 115 % for continuous operation.

The frequency range of normal operation is between 49.5 to 50.2 Hz for China. The PVPP has also to withstand frequencies from 48 to 49.5 Hz during 10 min. If the frequency is less than 48 Hz, the time that can withstand the PVPP connected depends on the PV inverter technology used. In the case that the frequency is higher than 50.2 Hz, the PVPP has to remain connected for 2 minutes, after this, it has to shut down. Germany, Romania, Puerto Rico and China permit the instantaneous disconnection when the upper limit is reached. South Africa's grid code requirements do not permit an instantaneous disconnection, the PVPP has to withstand 4 seconds with an over-frequency higher than 52 Hz. These requirements are summarized on Table 3.4.

It is interesting to point out that the most extreme frequency limits are around -3.5 Hz and +2.5 Hz from the nominal value. Usually, a wider range is accepted by areas that have weak grids or they are isolated as the case of Puerto Rico. The same situation happens with the voltage limits, where Puerto Rico has the widest range. Besides, it is important to notice that Germany has also a wide range of frequency limits for continuous operation as currently this country has a higher amount of renewable energy connected to the grid. The strictest continuous operation frequency limits are demanded by US (59.4 to 60.6 Hz). China has the strictest maximum frequency permitted (50.2 Hz), but the minimum value depends on the inverter performance. This is the only country that considers the technology used in order to set the limitations. Regarding these limitations, the

Table 3.4: Frequency limits in international grid codes

Grid code	Frequency (Hz)	Limits (Hz)	Maximum duration
Germany	50	f > 51.5	Instantaneous trip
		47.5 <f <51.5	Continuous
		f <47.5	Instantaneous trip
Romania	50	f > 52	Instantaneous trip
		47.5 <f <52	Continuous
		f <47.5	Instantaneous trip
US. (Puerto Rico)	60	f >62.5	Instantaneous trip
		61.5 <f <62.5	30 s
		57.5 <f <61.5	Continuous
		56.5 <f <57.5	10 s
		f <56.5	Instantaneous trip
US. (FERC LGIA)	60	f >61.7	Instantaneous trip
		61.6 <f <61.7	30 s
		60.6 <f <61.6	3 minutes
		59.4 <f <60.6	Continuous
		58.4 <f <59.4	3 minutes
		57.8 <f <58.4	30 s
		57.3 <f <57.8	7.5 s
		57 <f <57.3	0.75 s
		f <57	Instantaneous trip
China	50	f >50.2	2 minutes
		49.5 <f <50.2	Continuous
		48 <f <49.5	10 minutes
		f <48	P V inverters characteristics
South Africa	50	f >52	4 s
		51 <f <52	60 s
		49 <f <51	Continuous
		48 <f <49	60 s
		47 <f <48	10 s
		f <47	0.2 s

harmonization of grid codes is almost impossible as it depends on the strength of the grid that is not the same for each country.

3.2.3 Active power and frequency control

The control of the active power in LS-PVPPs should match the variability of solar energy during the day and the grid requirements. According to the grid code of South Africa [102], the control of active power is divided into three main requirements: i) Absolute production, ii) delta production and iii) Power gradient. The first constraint, absolute production, is based on the active power value defined by the TSO that the PVPP has to provide. In the US, the absolute production is known as power curtailment. The second constraint, delta production, determines the active power reserve. This is a percentage of the absolute power that the PVPP could supply in normal conditions. In Puerto Rico, delta production is defined as a power reserve. This reserve helps to have a future control of the PVPP when the frequency or voltage deviation occurs. The third constraint, the power gradient, limits the value at which the power generation has to step up or down the active power with values of MW per minute. In Ro-

mania, Germany, and US, the power gradient is known as a ramp rate limit. The PVPP must comply with any of these requirements despite radiation changes and cloud coverage. These requirements are illustrated in Fig. 3.5.

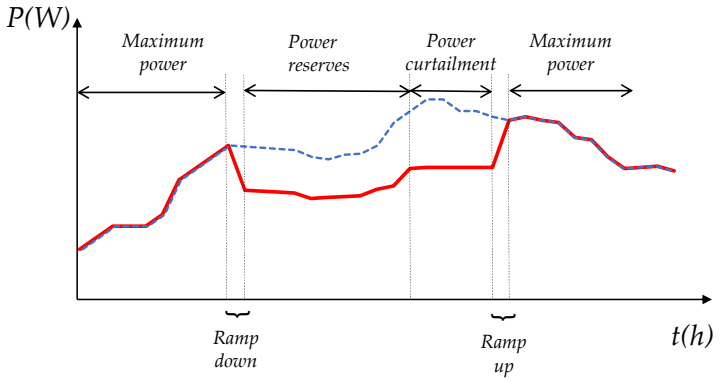

Figure 3.5: Active power control constraints for PVPPs

Table 3.5 summarizes the active power control required by the different international grid codes for PVPPs integration. All of them permit the active power curtailment to a value set by the TSO. The curtailment of active power is developed with a ramp rate limitation which has different values depending on the country. The grid code given by NERSA specifies the need that the PVPP supports the grid with three different active power controls: absolute, delta and gradient constraint to improve the performance of the PVPP connected to the grid. This grid code also specifies the time response for any new set point of active power that is less than 30 seconds.
The frequency control, however, needs the variation of active power during a small period of time. BDEW, NERSA, ANRE, and NEA specify that the PVPP must have primary frequency control to act as a governor. The control requirements for the stabilisation of the frequency vary from one code to another. FERC LGIA does not mandate any active power control, but this decision usually depends on the TSO. In the case of Puerto Rico, the active power control takes action when there is a deviation of more than $\pm$ 0.3 Hz of the nominal frequency. In this situation, the active power has to be at least 10 % of the maximum power capacity for less than 10 minutes. If the deviation is less than $\pm$ 0.3 Hz, the value of the active power can be

Table 3.5: Active power constraints required by international grid codes

Grid code	Curtailment	Reserve	Ramp rate
Germany	X	-	X
Romania	X	-	-
US (Puerto Rico)	X	X	X
China	X	-	X
South Africa	X	X	X

Table 3.6: Ramp rate limits in international grid codes

Grid code	Ramp rate (% Power capacity /min)
Germany	1
Romania	10
US (Puerto Rico)	10
China	X
South Africa	Set by TSO

between 10 to 100 %. China, however, only specifies that in cases of over-frequency (50.2 to 50.5 Hz), the PVPP has to withstand for 2 min and then it can be disconnected. After 50.5 Hz, the disconnection is mandatory.

South Africa, Germany and Romania state clear specifications about the frequency regulation considering the change of active power. Figure 3.6 illustrates the active power response due to variation of frequency outlined by Romania, South Africa and Germany grid codes. In this figure, f_1 to f_4 form a control dead band for the primary frequency control and f_4 to f_6 are set to do critical frequency control. There are two droops or slopes to change from f_1 to f_2 and f_3 to f_5 respectively. These slopes are variable from 0 to 10 %, which is agreed in accordance with the TSO. To provide grid stabilisation, NERSA's grid code requires that the PVPP should be designed with an active power capability that could provide regulation of over and under frequency. This value is called the delta or reserve power which should be at least 3 % of the available power, and it is the new available power in order to provide frequency stabilisation. Romania requires that the available power changes in accordance the frequency variation when there are disturbances. Germanyś grid code states that the primary frequency control is mandatory for PVPPs with a power capacity higher than 100 MW. PVPPs with less capacity can also participate in the primary frequency control only if there is accordance with the TSO. The variation of power when there is over frequency, in the case of Germany, depends on equation (3.1), where P_m is the

Table 3.7: Frequency values for Active Power regulation according to Fig.3.6

Grid code	f_1	f_2	f_3	f_4	f_5	f_6
Germany	49.5	49.5 <f <50	50.05	50.5	51.5	<50.2
Romania	aw-TSO[1]	aw-TSO	aw-TSO	aw-TSO	aw-TSO	aw-TSO
US (Puerto Rico)	aw-TSO	aw-TSO	aw-TSO	aw-TSO	aw-TSO	aw-TSO
China	aw-TSO	aw-TSO	aw-TSO	aw-TSO	aw-TSO	aw-TSO
South Africa	aw-TSO	aw-TSO	aw-TSO	50.5	52	50.2

Table 3.8: Values of P for Active Power regulation according to Fig. 3.6

Grid code	P_1	P_{min}
Germany	-	0.8
Romania	aw-TSO	0
US (Puerto Rico)	NS	NS
China	NS	NS
South Africa	$<0.97*P_{available}$	aw-TSO

instantaneous available power and f_{net} is the network's frequency.

$$\Delta P = 20 \times P_m \times \frac{50.2 - f_{net}}{50.2} \quad \text{at } 50.2 \leq f_{net} \leq 51.5 \tag{3.1}$$

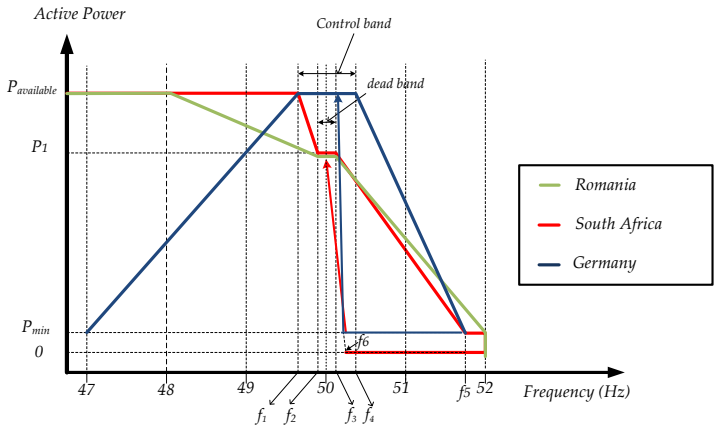

Figure 3.6: Active power control due to frequency regulation requirements by international grid codes.

Comparing the grid codes, the most restricting control is the one required by Romania, where there is under and over-frequency control, but in terms of time response, it is Puerto Rico. It is important to point out that the grid code of South Africa and Puerto Rico demand

[1] aw:agreed with

a power reserve to increase the active power capability to stabilize the grid when the frequency drops its nominal value. It is expected in the coming years, that power reserve will be a requirement for other countries as more and more renewable energy is being introduced.

3.2.4 Voltage and reactive power control

Conventional power plants have to overcome voltage deviations and to provide reactive support to the grid. Commonly, the voltage works in a band of $\pm$ 10 %of the rated voltage. The compliment of this requirement depends on the reactive power support characteristics of the PV inverter and ancillary devices such as STATCOMs or capacitor banks. As PV inverters were initially designed to be installed at the distribution level, they do not usually consider these new characteristics. Some companies like Danfoss, SMA, and ABB have already improved their inverters to permit the control of voltage fluctuations and the reactive power support. To connect LS-PVPPs to the grid, the voltage control has two main challenges: i) the voltage has to be kept inside a dead band regulated by TSO and ii) the LS-PVPP has to comply with the capability curve given by the TSO for the relation between reactive and active power. According to [49] there are several methods for voltage control in LS-PVPPs: voltage regulation, power factor regulation or reactive power control. The voltage regulation controls the value of voltage that is based on a droop function. In this case, the droop is the variation of voltage due to a change of reactive power. The power factor regulation controls the reactive power depending on the value of active power. The last method, reactive power control, manages directly the reactive power at the PCC. The PVPP shall be able to control the reactive power and the voltage with any of these control methods.

Not all the grid codes permit that PVPPs work on one of these three modes. Table 3.9 summarizes the reactive power control requirements given by each grid code. In the case of Puerto Rico, the grid code requires that the control mode should be only the one called: voltage setpoint. The strategy of this control is based on droop control variable from 0 to 10 %. The time response of this control is 1 second for a total reactive power of 95 % . Meanwhile, Germany has a time response of 1 minute and South Africa has a time response of 30 seconds. Considering the time response, the most restricted grid

code is the one of Puerto Rico.

Additionally, to the control method, the fulfilment of a reactive power capability curve in the PCC is also a requirement. US, FERC LGIA have defined a dynamic reactive power range between 0.95 leading and 0.95 lagging, but they do not clarify the requirements for steady state conditions. In Puerto Rico, the reactive power requirements are defined under steady and dynamic operating conditions. In steady state, the PVPP must be able to continuously work with a power factor of 0.85 lagging and 0.85 leading. In dynamic mode, the power factor is between 0.95 lagging and 0.95 leading. It is important to point out that the reactive power requirements defined by NERSA differ depending on the rated power of the LS-PVPP. If the rated power is between 1 to 20 MVA (Category B), the reactive power demanded is 0.228 MVAr. But if the rated power is higher than 20 MVA (Category C), the reactive power demanded is 0.33 MVAr. A comparison of the reactive power requirements is illustrated in Fig.3.7 that includes all the available active and reactive power demanded by the different grid codes together with the power factor limitation.

Regarding the reactive power control, Puerto Rico presents the strictest control. First, the control has to respond as fast as possible to overcome any issue in the grid. Second, as the PQ capability curve at the PCC presents a wide range of reactive power and generally the PV inverters capability is not sufficient, extra equipment is needed. China, Germany, South Africa and Romania present almost the same PQ capability curve with a maximum reactive power requirement of ± 0.33 p.u. Depending on the topology of the LS-PVPP additional equipment may not be needed.

This section has presented a comparison of the most relevant requirements demanded by the grid codes in Germany, China, Romania, US, Puerto Rico and South Africa for the interconnection of LS-PVPP with the transmission system. It can be summarized that Puerto Rico, as it has a weak grid, it has the strictest requirements in FRT, active power and reactive power control. On the other hand, China and the US have the most strict limitations on frequency and voltage boundaries. Considering this comparison of the different grid codes, the following section discusses the challenges that LS-PVPPs have to face in order to be connected to the transmission system.

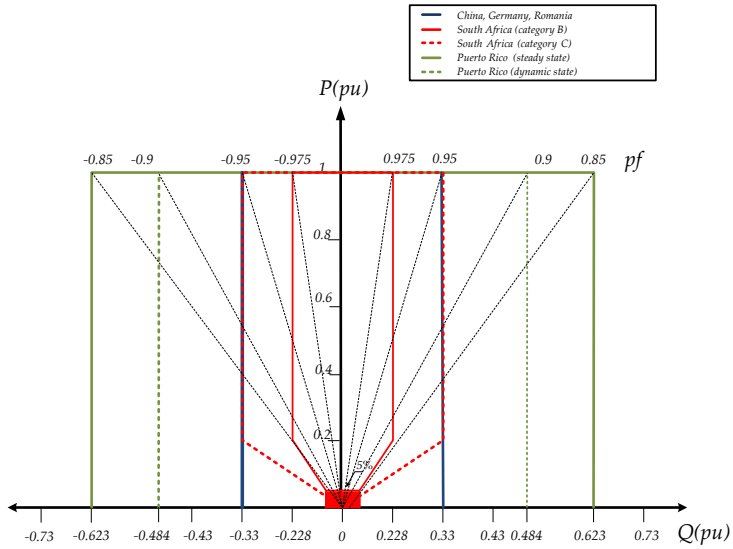

Figure 3.7: Comparison of reactive power requirements imposed by the grid codes of China, Germany, US, Romania and South Africa.

3.3 Challenges for grid integration of LS-PVPPs

A PVPP should comply with the minimum requirements given by the grid codes of the different countries. Because of these grid codes, there are many challenges that the PV generators, the LS-PVPPs, and the electrical network have to face in the upcoming years. This section studies the challenges that the current technology has to face to comply with the grid code requirements.

3.3.1 Voltage variation

As PV systems were first developed for residential, commercial and industrial applications, there are several studies about the voltage instability caused by a high penetration of these PV systems at the distribution level. According to IEEE 1547 these PV systems interconnected with the grid should not perform any voltage regulation at the PCC. The studies developed for this type of application have been conducted in order to understand the problems caused by a high PV penetration that has not considered any control to support

Table 3.9: Voltage and reactive control required by international grid codes.

Country	Control mode	Set point	Power factor ranges
Germany	Voltage control Power factor control Reactive power control	cos φ (fixed) cos φ (P) Q(fixed) Q(V)	0.95 leading 0.95 lagging
US (Puerto Rico)	Voltage control	V	0.85 lagging (stable operation) 0.85 leading or 0.95 leading (dynamic operation) 0.95 lagging
Romania	Voltage control Power factor control	cos φ	NS
China	Reactive power control	Q(V)	0.95 leading, 0.95 lagging
South Africa	Voltage control Power factor control Reactive power control	cos φ (P) Q(V)	0.975 leading (category B) 0.975 lagging (category B) and 0.95 leading (category C) 0.95 lagging (category C)

the voltage at the point of interconnection. Yan, R and et al [113] focus on the investigation of cloud coverage impact on the PV systems interconnected in an IEEE 13 bus system. This study concludes that the cloud transient affects the voltage at the distribution level as tap changers of transformers does not act as quickly as possible to maintain the voltage level. Similar conclusions were obtained in [114]. Besides cloud coverage, the distance of the feeder is also an important factor to consider. This is studied in [115] where a 8 MW PVPP connected to the distribution system at different distances is analysed. It shows that the voltage at the feeder is affected depending on the location of the PVPP which also affects the entire performance of the distribution system. Thus, the optimal placement of the PVPPs at the distribution level is considered vital to reducing power losses and voltage instability [116].

In the case of LS-PVPPs developed for utility purpose, its effect on voltage stability has not been broadly studied. Omran, W and et al [117] have studied the impact on the voltage profile affected by the installation of PVPPs at different sites of the grid. The results show that the voltage at the feeder presents a parabolic trend when the output power of the PVPP increases (0.2 to 10 MW). The maximum point of this voltage profile will depend on the total impedance of the PVPP and the transmission line. A similar studied is performed in [118]. These studies consider that PVPPs supplies the maximum power possible, but the output power variation during the day is

not considered. There are no deep studies about the effect of cloud coverage along the park and how it affects the LS-PVPP performance. In the case of WPPs the studies focus on how the variability of wind speed can affect the voltage stability.

Today, the challenge is to understand how the LS-PVPP affects the voltage profile at the PCC due to cloud coverage, radiation, and temperature. Thus, studies considering the variability of the source should be developed. The size and internal topology should also be part of the analysis. For this reason, the creation of accurate models of LS-PVPPs to simulate static and dynamic performance are also part of the challenge. Understanding the voltage profile at the PCC, different solutions and control algorithms can be conceived.

3.3.2 Frequency stability

In the current electrical system, the frequency is related to the rotating speed of the conventional synchronous generators. The control of these generators depends on the balance between the load and the power generated by the management of the acceleration or deceleration of each electrical machine to reduce or to increase the frequency [119]. The inertial response of the generator plays an important role in the electrical system in the frequency control. The kinetic energy is released to the electrical system limiting the initial rate of frequency decline in the case a demand-generation power imbalance occurs [120], [121], [122], [123].

In the case of LS-PVPPs, the technology used: PV array and inverter makes a big difference with the conventional power plants. The lack of rotating machine together with the power variability during the day can bring several problems to the electrical system in terms of frequency stability [124], [125]. The study developed by [126] details the case of the Australia network considering the integration of wind and solar power. It concludes that low inertia and PV variation causes problems in the frequency regulation of the electrical system. This study considers small PV systems interconnected at the distribution network with a total capacity of 500 MW. The work developed by Abdlrahem, A and et al [127] explains how the frequency of the electrical system is affected by four LS-PVPPs of 50 MW each one. Besides, four synchronous generators of 700 MW each are considered for the study. This study contemplates the increment and

decrement of radiation on each PVPP. The analysis is conducted to see how these changes affect the electrical system. The conclusion, in that case, is that PV penetration does not affect drastically the frequency stability, but this study is not considering any reduction of conventional generation. On the other hand, a statistical evaluation of the electrical system with high PV penetration shows that this increment of PV power in the electrical system affects the frequency stability [128].

Deeper studies of this phenomena are still missing. Up today LS-PVPPs have been installed around the world, so it could be beneficial to understand how its lack of inertia impacts the current grid. The study developed by [125] is a good start to understand the lack of inertia in the electrical system. The big challenge for LS-PVPP is to provide a solution to overcome the lack of inertia for primary and secondary frequency control. Besides, if LS-PVPPs work at maximum power point they do not have a power reserve to control the decrement of frequency.

But the challenge is not only for LS-PVPP it is also for the current conventional power generation. The transition from conventional to renewable power generation requires that synchronous generators adapt their power output to accommodate the variable power of these new power plants in order to maintain the stability of the electrical network.

3.3.3 Active power regulation

The operating power point of the current PV inverters is at the maximum active power that varies according to the irradiance. To fulfil this point, different algorithms have been developed as the perturb and observe, incremental conductance, ripple correlation, particle swarm optimization, fuzzy logic control, differential evolution and others as they are explained in [129], [130], [131]. The main drawbacks of these algorithms are the time of response, the number of sensors used and the delay to notice that the radiation has changed.

Using this control, the LS-PVPP will be always working at maximum power in each solar radiation. Due to cloud transition, the electrical system could experiment large and quick fluctuations of active power. This behaviour affects the grid power balance, trigger-

ing to emergency situations. Besides economic dispatch will be also affected [132]. A study analysing the impact of the PV systems installed at the distribution network on active power dispatch during the day is explained in [133], where the PV production shows ramp rates higher than 2.5 MW/min due to solar radiation variation.

Thus, grid codes require at least two types of active power control: power curtailment and ramp rate control. In addition, Puerto Rico and South Africa demand power reserve. Considering these requirements, the MPPT tracker would suffer some modifications. It is no longer necessary to be working at maximum power point all day, but it will be necessary to track the power required by the TSO. The maximum operation point should be less than the power capacity of the LS-PVPP or storage equipment should be installed. However, the main concern is the power curtailment with a ramp rate control. The reduction of power at a constant ramp rate could not be easy to approach with the current technology and control used in the PVPP. The intermittent and non-uniform cloud coverage along the LS-PVPP are also big challenges to overcome. The understanding of these challenges comes together with a deep analysis of the problems caused by LS-PVPP integration, but these studies are still missing in this area of concern.

3.3.4 Reactive power regulation

The current technology of PV inverters used at the distribution level does not have a PQ control as IEEE 1547 does not require it although the inverter can perform it. However, due to the increased development of LS-PVPPs and the grid code requirements, the PV inverters have to control not only the active power but also the reactive power [134], [135]. The MPPT control used in normal PV operation does not permit to have a complete control of the PQ capability during the day and limits the system performance. PV inverter developers do not reflect the limitation of dc voltage, solar radiation, and temperature in their capability curve.

Today, the challenge is to understand the limitations of these inverters considering the variation of solar radiation, temperature and dc voltage. In the case of WPPs deep studies about the reactive power capability have been performed. For instance, the reactive power capability curve of a doubly fed induction generator has been studied

in [136] which relates the reactive power capability of the inverter plus the capability of the generator. In the case that the wind farm does not have enough reactive power to comply with the grid requirements, other equipment is installed as STATCOMs, SVCs or capacitor banks. A comprehensive and extended comparison of these technologies used in WPPs is developed by A. Pathak et al. [137]. Thus, similar studies could help in the development of solutions to approach the grid code requirements.

In this section, the challenges that technology developers, researchers, industry and plant operators have to overcome for the correct performance of the LS-PVPPs have been analysed. This discussion was conducted by the investigation of high PV penetration impact on the electrical system on voltage stability, reactive and active power regulation. Taking into consideration these challenges the next section will discuss the current technology used to comply with grid codes' requirements.

3.4 Compliance technology

Nowadays, grid codes and TSOs are demanding that PVPPs behave as similar as possible to conventional power plants. Thus, the PVPPs should manage the active power, support the frequency of the grid, support reactive power, voltage sags and voltage deviations. Through the last years, two solutions have been developed: (i) the addition of equipment as energy storage, diesel generators, SVCs, STATCOMs, capacitor banks and (ii) the development of a smart control for the LS-PVPP. Figure 3.8 illustrates a scheme of a LS-PVPP that includes the additional equipment and the new control duties of all the equipment involved in the power plant. On the one hand, it considers the active power control including power curtailment, ramp rate, power reserves and frequency deviations. On the other hand, it is considered the reactive power control to support voltage deviation, to inject or absorb reactive power to the grid. In this figure, it is also shown the possibility to use other equipment in order to comply the requirements asked by the TSO for active or reactive power control. This section explains each of these components and control improvements for the fulfilment of the grid code requirements.

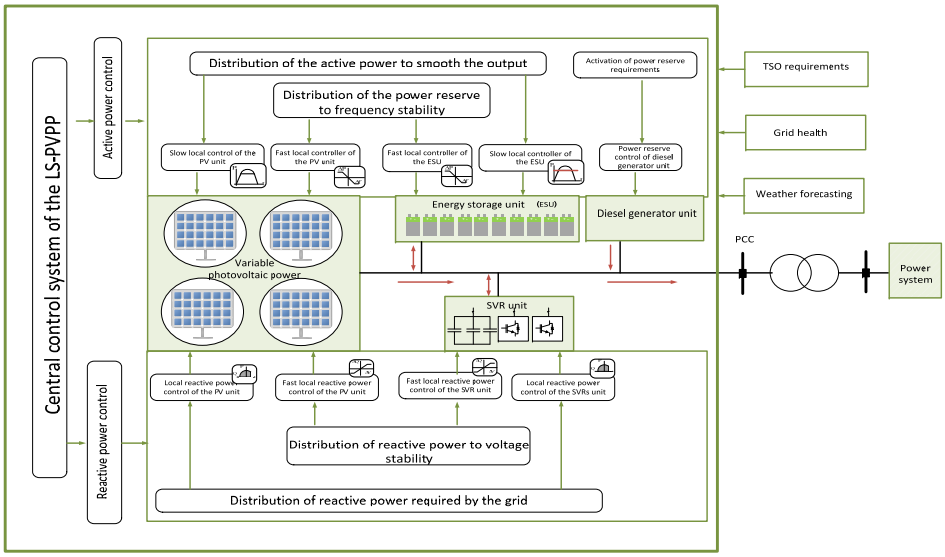

Figure 3.8: Control tasks and additional equipment in LS-PVPP

3.4.1 Fault ride through capability

In normal conditions, the inverters operate satisfactorily, as the ones used in wind farms [138], but they have to overcome different issues during faults. The inverters installed in PVPPs have three main reasons to disconnect from the grid: overcurrent due to low voltage, excessive dc voltage and loss of synchronization [48].

During a disturbance, for instance a short circuit, the voltage at the output of the inverter decreases and current rises. The inverter is still giving active power to the grid despite there is a fault condition. The input power from the PV array is constant at the maximum point of power depending on the irradiation and temperature [139]. The inverter tries to balance the input and output power rising the current and the DC voltage. As a result, the PV inverter is disconnected. This behaviour obeys to the natural response of the PV array connected to the inverter because of the use of the MPPT control. In this case, the MPPT is causing problems to the stability of the plant. Some studies have been developed to enhance this control and to improve the FRT response. In references [140] and [141] explain an enhanced MPPT control as a new strategy of the PV inverter to over-

come faults. The voltage elected should be higher than the voltage of the MPP to reduce as fast as possible the output power.

To overcome the fault conditions, reactive power should be supplied by the PV inverter. The requirement when the voltage drops below 50 %, is to have an injection of reactive current of at least 100 %. Thus, the PV inverter has to be oversized in the range of 1.1 to 1.2 to comply with this requirement. In the case of wind farms, a study has been developed using a converter 40% oversized. This study shows that the larger capacity of the converter, the reactive current support is increased [142]. In [109] a LS-PVPP of 10 MVA is studied under different fault conditions with and without reactive power injection. The results show that the LS-PVPP can provide support of reactive current when faults occur in case of symmetrical faults. In asymmetrical faults, the inverter triggers due to system protection. The work assayed by Marinopoulos et al. [48] compares the different grid code requirements concerning the reactive current injection when a fault occurs. The control of FRT is performed locally at the inverter control due to the time requirement. The PVPP is modelled in DIgSILENT Power Factory® and several voltage sags are tested. The results show that during a fault, large amount of active power is lost and the reactive current injection allows a better performance of the PVPP at the PCC.

The fulfilment of FRT requirements depends on the control used in the PV inverter and the capability of the inverters. But a deeper study that analyses the performance of the LS-PVPP during fault conditions considering MPPT control and the variation of the PV power during the day is still necessary.

3.4.2 Reactive power control

PV inverters can control the reactive power but this feature has not been possible to use at the distribution level as IEEE 1547 required. Today, the PV inverters used for LS-PVPP have already enabled this characteristic. Lin Zhou and Yan Chao [143] study the reactive power control strategy for PVPPs, where the proposed control is to change reactive and active power in an independent way to permit the stability of the voltage at the PCC. Youngsan Bae et al. [144] assay the enhancement of the reactive power control of inverters to improve the power quality and to comply with German grid code. In this

case, the control mode can be either by the setting of power factor or reactive power. Another study is developed by Minambres et al. [145] which regulates the voltage at the PCC when the mode chosen is power factor control. However, none variation of radiation or temperature are considered in the simulation, only disturbances from the grid. Meanwhile, the study developed by Tu Van Dao et al. [146] focuses on reactive power control to enhance the response of voltage of the PVPP despite the solar generation fluctuation during the day. The results show that the PVPP takes responsibility for their own disturbances improving the voltage stability at the PCC. Similar research is developed by Xiao et al. [147]. The online supervisory voltage control proposed to allocate the reactive power and to track online the voltage stability considers the variation of radiation during the day. The transient response in a weak network is improved with this type of control. Studies that consider different PV penetration levels are conducted by [148] where the voltage is controlled using the PQ capability of the PV inverters. The voltage stability improves significantly, but as the inverter can absorb reactive power, the grid starts to supply the reactive power needed by the PVPP. This practice makes that the electrical system will be less efficient.

As the PV inverters can be used as STATCOM devices, some studies are focusing on how the LS-PVPP can help to overcome reactive power change overnight period. Varma et al. have extensively studied the utilization of PV inverters as STATCOM during the night period [149] when they are connected to the distribution system. The results show that small PVPPs connected to the distribution system help to stabilize the grid and to increase the power generation for other power plants as wind farms. A similar approach has been developed in [150] in which the LS-PVPP is used especially as FACTS to compensate the voltage between two feeders. In this case, the LS-PVPP is interconnected between two feeders and the control developed manages the reactive and active power together. With this control, the voltage has a better profile at the point of interconnection. In these studies, the network improves its power quality and the voltage compensation especially at night periods.

In the case that the reactive power of LS-PVPP is not enough, additional reactive power compensation is needed to support the reactive power required by the grid like STATCOMs and capacitor banks. The inclusion of additional equipment is accepted by grid codes to

comply with the requirements, however, there is no reported study to view the advantages and disadvantages of these types of equipment in LS-PVPPs. Different LS-PVPP designers as SMA and GPTech have already added STATCOMs or capacitor banks in their installations in order to comply with grid code requirements. The power plant control manages the reactive power from the PV inverters and the additional equipment as it is explained in [151]. The optimal control of these equipments should be developed as it will manage the reactive power for grid requirements and for the health of the system.

3.4.3 Active Power control

The controllability of active power during the day independently the external condition is an important issue in LS-PVPPs. Grid codes require that LS-PVPPs provide active power curtailment, under and over frequency control, overvoltage and undervoltage control, ramp rate control, power reserve, reducing in some way the problematic of the lack of inertia that the LS-PVPP has. For this purpose, the addition of equipment and the control improvement are a common practice nowadays. This section summarizes these solutions for active power and frequency control.

To comply the grid codes, LS-PVPPs are adding energy storage units (ESU) and/or diesel generators. The ESU helps to smooth the active power despite the variable conditions along the LS-PVPP. Thus, the ramp rate and the power curtailment required by the grid codes can be managed by an adequate control of the ESU. It also can work as a power reserve depending on the system design, but the cost of the ESU could be a drawback. On the other hand, a group of diesel generators is commonly used for power reserve, power curtailment, and frequency regulation. Depending on the application one or two of these solutions are installed. For instance, the LS-PVPPs developed in Puerto Rico by GPTech [152] have a system with a storage unit and a diesel generator in order to comply with the strict grid code requirements. Another example is the LS-PVPP of 5 MW constructed in Cobija, Bolivia developed by SMA. This LS-PVPP is not connected to the utility system but it has to provide service to a growing community that currently is consuming 37 GWh/year. In this application, the main objective is to determine the maximum permissible

PV power to reduce the fuel consumption and to provide electrical stability.

In the energy storage unit, batteries are commonly used together with an inverter and an energy management system (EMS). The types of batteries used in LS-PVPP are molten salt, lithium-ion (Li-ion), lead acid and flow batteries. Lead acid batteries are commonly used in small PVPPs for their low cost. But its short lifetime has not made it suitable for large scale applications. Flow batteries are an emerging technology with higher lifetime, but its low energy density has not already attracted to LS-PVPP developers. Today, molten salt and lithium-ion batteries are being used in current LS-PVPP due to its high efficiency and energy density. However, the lifetime of molten salt batteries is relatively lower than Li-ion [153], [154].

Despite the technology used, a main concern is to manage the energy stored together with the PV output power. The industry and researchers are coming toward different EMS solutions to comply with grid code requirements. A control is proposed in [155] that uses energy storage to mitigate the PV power fluctuation due to cloud coverage. The control approach is based on the coordinated response between the PV inverter and the energy storage using the inverse characteristics of the PV array output. The results show that the active power is smoothed during and after a severe cloud transient, however, the simulation is not developed for LS-PVPP. Instead, it is used for PV systems along the distribution grid located in different geographical areas. The use of vanadium redox batteries (VRB) in LS-PVPP is studied in [156]. This study shows that the implementation and the control of the battery has smoothed the output power of the LS-PVPP when cloud coverage occur. This storage unit can supply 5 minutes of constant power. A ramp rate control based on life cycle technology for real LS-PVPPs installed in the US is researched in [157]. In this study not only batteries are considered, also flywheels and ultracapacitors. With an appropriate weather forecasting and storage sizing, the results show that 99 % of the violations of ramp rate have been prevented.

Other researchers are trying to develop energy storage units with another type of technology as fuel cells, flywheels, and ultracapacitors. The addition of fuel cells is studied by Monai, T and et al [158]. It helps to have uninterrupted power supply and to enhance the performance of the PV unit. N. Kakimoto et al. [159] study the

inclusion of ultracapacitors for ramp rate control. The inclusion of this device helps to smooth the active power control when there are quick variations of solar radiation, showing a good response. The use of flywheels is also attracting to LS-PVPP developers, but further research is necessary. This technology helps to have an inertia reservoir of the LS-PVPP in the case a failure is produced in the electrical system [153].

As it was mentioned before, diesel generators are also part of the LS-PVPP. The addition of diesel generator is a common practice for LS-PVPPs located in rural areas. Usually, the control developed for these hybrid PVPPs has the main objective to minimize fuel consumption and to maximize the PV output power of the plant. As the output of the diesel generator should remain constant, the use of it is especially for power reserve. As the PV output power cannot be smoothed by the use of this generator, the addition of energy storage could be necessary. Besides, it helps in the reduction of start/stop cycles of the generator [160]. A deep review of the system control for LS-PVPPs with diesel generator in rural areas or weak grids is studied in [161]. This review summarizes the most used techniques for the control of these systems. The addition of a diesel generator is also used for active power curtailment according to the studies developed by Tonkoski et al. [162]. The results show that the PVPP has a good performance when there are frequency deviations and overvoltages. Datta, M and et al [163] discuss a new control approach for the use of diesel generator in LS-PVPP. In this work, a fuzzy control for frequency stability and for MPP tracker is developed. The control alternates between these two modes depending on grid conditions. The performance of the grid improves with the solution proposed. However, it does not consider the fulfilment of the grid code requirements.

Besides the addition of the equipment, the modification of the MPPT is also necessary to control the active power according to the grid code requirements. Craciun et al. [164] develop a new control method of the PV unit for power ramp limitation and frequency support without the use of any additional equipment. The control is based on changing the voltage to a value higher than the one for the MPP, to support as quickly as possible frequency variations. The results show a good response in the frequency response and the ramp rate control when the PVPP is in an IEEE 12 bus. Xin, Huanhai et al.

propose a frequency regulation of small PVPPs connected in the distribution network, to provide primary and secondary frequency regulation to the power system. In the case of LS-PVPPs, Rahmann and et al have studied a control to mitigate the fluctuation of cloud coverage [165] without using energy storage and to reduce the frequency variations. This control is based on the deloaded operation concept of the PV array, that is the operating point when the PV array is shaded. However, for this control, it is necessary to have sensors and microinverters connected to a small number of PV panels. According to the measurements, the MPPT will track the optimal operating point in deload operation when the shading occurs. The results show that the LS-PVPP reduces 15 % the ramp rate response when there is no control. The drawback is the number of sensors and microinverters necessary to install in the LS-PVPP.

In addition to the modification of the MPPT control, the development of different control modes for active power management has also been researched. For instance, Yang, Yongheng and et al [166] propose a new control method of a single phase PV system in order to have two modes of control during the day: i) MPPT control when power is less than the limit set by the TSO and (ii) a constant power generation when the PV power is higher. Another interesting research is developed by Huanhai et al. [167]. It discusses two other modes of active power regulation. One mode is a frequency droop control that helps the PV unit to work as a virtual governor. The second mode is the emergency control that is enabled when there are changes in frequency caused by the variation of meteorological conditions or loss of load.

The improvement of the technology and control of PVPPs is still emerging, but it will grow fast as in the case of the technology utilized in wind farms. The enhancement of PVPPs response concerning fault ride through capability, frequency and active power support, voltage and reactive power control will make easier the integration of LS-PVPPs as part of the generation system. Today, there is the necessity to understand the economic impact of the additional equipment to comply with the grid code requirements. Besides, the adaptation of the control is an important issue nowadays to improve the LS-PVPP performance.

3.5 Global harmonization and future trend of the grid code regulations

Taking into account the increase of PV generation, the grid code requirements are being updated demanding a larger contribution in grid support. China, Germany, and US, which are leading the utility market, together with Romania and South Africa have adapted their grid codes as they expect that more LS-PVPPs will be installed in their grids. These grid codes demand that LS-PVPPs provide ancillary services as FRT, active and reactive power control, voltage and frequency support in order to have a similar performance as conventional power plants.

The grid codes analysed present some similarities, but also important differences as the requirements are adapted to the electrical characteristics of each grid. In the case of FRT, the time that LS-PVPPs have to withstand the fault is different in each grid code. For instance, Germany imposes that LS-PVPPs remain connected for 0.15 s while the disturbance occurs, but Puerto Rico states that the necessary time should be about 0.625 s. In voltage and frequency boundaries, there are no similarities between the grid codes as these values are strongly dependent on the grid characteristics. In the active power control, power curtailment and ramp rate are required by each grid code except Romania that does not specify any ramp rate requirement. The power reserve is only required by the grid code of South Africa and Puerto Rico. Regarding the reactive power support, every grid code permits that the LS-PVPPs support voltage disturbances by supplying reactive power. The PQ capability, that the LS-PVPP should have, presents similarities between the grid codes of China, US, and South Africa, but Puerto Rico demands a wider capability. It can be stated that Puerto Rico presents the most strict requirements as the grid is isolated and any power plant installed should perform a strict voltage and frequency regulation, active and reactive power control and also withstand any system disturbance.

Due to these differences, there is the necessity to harmonize these grid codes in a more consistent manner. These would help PV inverters' manufacturers to develop universal solutions that could comply with the main grid code requirements. In this trend, the European Commission has developed a common grid code regulation that applies for the integration of renewable energy: wind and PV

power plants [168]. Currently, this grid code, specifies the general requirements as FRT, voltage and frequency deviation boundaries, frequency control and voltage and reactive power control. In addition, this grid code gives the freedom to each TSO to set the specific values for each requirement. However, for a correct harmonization of grid codes, the following issues should be considered:

- The frequency and the voltages ranges depend on the stability of the grid. There are weak grids as the case of Puerto Rico and South Africa, where there is continuous variation of voltages and frequencies, where the PVPP has to support the grid and withstand onerous conditions. Therefore, the harmonization of the grid codes considering frequencies and voltage ranges is not an easy task because of the dependence of the electrical system.
- The reactive current support for under or over voltages is necessary to harmonize in order to improve the characteristics of the PV inverters. Until now the PV inverters developed do not give reactive power support to work on disturbances as IEEE 1547 demands. Therefore, the installation of STATCOM, FACTS, and capacitor banks has been necessary to overcome any issue during disturbances. However, PV inverters should help to work during harsh conditions as their characteristics could permit it. Therefore, a harmonization of these requirements could help developers to improve the control of the PV inverters in order that these can provide reactive power without the need for extra equipment.
- The frequency control for under and over frequency for each grid code presents different requirements, response curves, and specific constraints. The differences among them do not help to have a universal solution. For instance, ENTSO-E mentions two operation modes for power plants with a power capacity higher than 50 MW: limited frequency sensitive mode and the frequency sensitive mode [122]. However, the grid codes presented by Germany, Romania, Puerto Rico do not have these definitions but they do have the same approach for under and over frequency control. Future grid codes should consider the harmonization of these requirements considering terminology, time response, and similar droop characteristics for under or over frequency control.

- It is necessary as well, that grid codes consider the natural constraints of the LS-PVPP during day and night. Some of the ancillary services cannot be performed without solar irradiance as active power will not be generated. Therefore, it is necessary that grid codes clarify when the LS-PVPP should enter to support the grid. Though it can be a disadvantage to not produce active power during the night, the LS-PVPP can be used as STATCOM for voltage deviation support at these hours. If the grid codes do not show flexibility on this issue, it will discourage the installation of these power plants around the world as the cost of installation will increase.
- As more renewable energy is integrated to the grid through power converters as is the case of WPPs and PVPPs, the natural inertia of the grid to overcome frequency deviation will be affected. Therefore, future grid codes will ask for inertia emulation to these technologies. Spain and Ireland are already requiring that WPPs to have this characteristic [112]. In the case of PVPPs, the inertia emulation is still not required but it is expected to be a requirement in the future together with damp power oscillations, spinning reserve and blackstart.
- Due to the increase of renewable energy systems interconnected not only to the transmission system but also at the distribution level, new grid codes are being developed. For instance, Germany has introduced the grid code VDE-4105 since 2012. This specifies the technical minimum requirements for the connection of distribution generators to or parallel the distribution network [169]. These requirements are similar to the ones asked to LS-PVPPs interconnected to the transmission system as frequency and voltage support. Therefore, it is expected that more grid codes ask ancillary services not only to LS-PVPPs but also to PV systems interconnected at the distribution level.

The harmonization of grid codes will become a higher priority whenever more renewable energy will be integrated into the electrical system. Grid codes should be aware of these conditions and therefore could be necessary to demand another type of technology to be integrated into the grid as flywheels or energy storage power plants. The experience joined between research and industry will help to developed enhanced grid codes for the integration of LS-PVPPs as well as other types of power plants.

3.6 Conclusions

The challenges that LS-PVPPs have to overcome to be connected to the grid have been reviewed together with a comparison and analysis of the different requirements imposed by the grid codes of Germany, US, Puerto Rico, Romania, South Africa and China. The requirements of fault ride through capability, frequency and active power control, voltage and reactive power support have been compared. The technology and the control techniques developed to comply with the grid code requirements have also been detailed and discussed. From this review, the following conclusions are drawn:

- The integration of LS-PVPPs in the electrical system is becoming more challenging as more requirements are necessary to be fulfilled. The variability of the solar radiation and cloud coverage cause problems of instability in the PCC regarding the voltage and the frequency response. This intermittent energy source makes difficult the control of the LS-PVPP for power curtailment, ramp rate, and power reserve. Another big challenge is the lack of inertia, as LS-PVPPs do not have rotational machinery as conventional power plants that affects the grid stability. Up today, all the grid codes discussed require that LS-PVPPs perform primary or secondary frequency control. As more conventional power plants are displaced from the grid, the control of frequency by LS-PVPPs could be challenging. Thus, dealing with the lack of inertia and the intermittency of the solar power are two of the main challenges to overcome nowadays.
- The industry and researchers have already developed solutions to permit LS-PVPPs to follow the grid codes imposed by each country. One solution is the addition of extra equipment to help to control active and reactive power. STATCOMs and capacitor banks have been installed for reactive power support at the PCC. Energy storage units and diesel generators have also been installed in some LS-PVPPs to comply with power curtailment, power reserve, and ramp rate requirements. In addition, other solutions as the use of flywheels and ultracapacitors should be studied further for this type of application. On the other hand, the improvement of the PV unit control together with the control of the entire LS-PVPP are also part of the solution. The MPPT control that has been widely used in small PV systems

is suffering some changes as it may not be needed to get all the time the maximum power. However, deeper research considering the improvement of control and coordination of all the equipment is still necessary together with an analysis of the investment and operational costs.

Taking into account this review, one of the challenges to overcome is to understand the capability curves of the PV generator for future grid code compliance. This is studied in the following chapter.

Part II

Technical Limitations and Capability curves

Chapter 4

Capability curve analysis of PV generators for LS-PVPPs

"My house is solar powered. I tell Republicans, you can hate the subsides-I hate the subsides, too - but you cannot hate solar panels. These are rocks that make electricity, so they are incapable of receiving your hate"
Thomas Massie

The present chapter assesses the study of the PV generator capability curves for their use in LS-PVPPs. For this purpose, the chapter focuses on three main aspects: (i) the modelling of the PV generator's main components, (ii) the operational limits analysis of the PV array together with the inverter, and (iii) the capability curve analysis considering variable solar irradiance and temperature. To validate this study a PVPP of 1MW is designed, modelled and simulated in DIgSILENT PowerFactory ®. The results for each case scenario shows that the capability curve and the limitations are directly affected by: the solar irradiance, temperature, dc voltage, and the modulation index[1].

[1]This chapter is based on the following publications:
A. Cabrera-Tobar, E. Bullich-Massagué, M. Aragüés-Peñalba, O. Gomis-Bellmunt, "Capability curve analysis of photovoltaic generation systems", *Solar Energy*, 140 (2016),pp. 255-264.
A. Cabrera-Tobar, E. Bullich-Massagué, M. Aragüés-Peñalba, O. Gomis-Bellmunt, "Reactive power capability analysis of a photovoltaic generator for large scale power plants", *5th IET International Conference on REnewable Power Generation (RPG)*, London, United Kingdom, 21-23 Sept. 2016, pp. 1-6.

4.1 Introduction

PV inverters have been progressively introduced to provide ancillary services in LS-PVPPs as the grid codes demand. However, there is still no deep study on the inverter limitations considering the power production, the solar irradiance, ambient temperature, DC voltage and pulse modulation. Alonso Albarracin [170] studies the photovoltaic reactive power limits of inverters used by small PV system. In this study, the converter has two stages: a dc-dc converter and then a dc-ac converter. The analysis is developed with this type of unit for a single PV panel where the dc-dc converter has the task of stepping up the voltage and to work at the maximum power point. Because it is a small system, the variation of the dc voltage is not considered. It also does not consider the pulse modulation factor. Another study was developed by F.Delfino et al. [171], that obtains the capability curve for a PV generator (PV panel and inverter). The analysis considers the variation of the modulation index but assumes that the dc voltage is constant. In both studies, the implication of solar irradiance or temperature has not been considered in the control or in the analysis. Besides, the voltage considered in both studies is equal to the value that permits the PV generator to operate at maximum power point (MPP).

Accordingly, the aim of the current chapter is the analysis of the PV inverter capability curves taking into account the solar irradiance, the ambient temperature, the dc voltage variation and the inverter operation. For this purpose, this chapter is structured as follows: Section 4.2 explains the mathematical model of the PV generator. Section 4.3 presents the mathematical analysis and the capability curves of the PV generator. Section 4.4 presents the influence of ambient conditions and the inverter operation on the capability curves. The validation of the mathematical analysis is developed in Section 4.5. Finally, the conclusions are drawn in Section 4.6.

4.2 PV generator model

In Chapter 2, the possible configurations of PV generators for LS-PVPPs were studied and it was concluded that central configuration is the most used configuration. Thus, in the present thesis, this con-

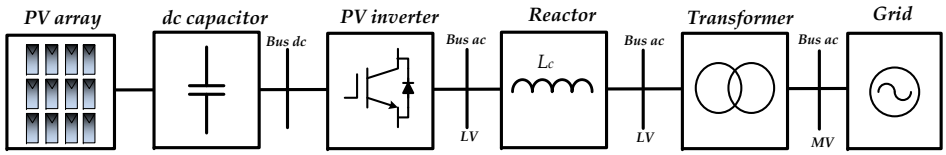

Figure 4.1: Components of a PV generator interconnected with the grid

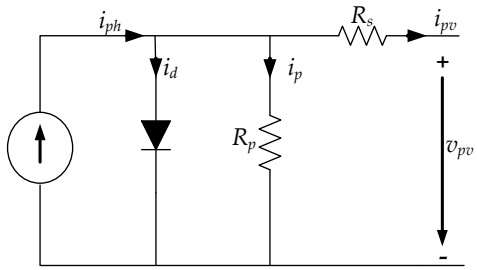

Figure 4.2: Simplified model of the PV cell

figuration is the one under analysis. The main components of this configuration are illustrated in Fig. 4.1. In this section, the model of each component is detailed.

4.2.1 PV array model

The PV array is modelled as a source of current connected to a capacitor, where its current and voltage depends on the solar irradiance and temperature. The PV array is an assembly of many PV panels connected in series to increase the voltage and in parallel to increase the current. The PV panel is an arrangement of PV cells, where the circuit illustrated in Fig.4.2 corresponds to its model [53]. In this model the losses are taking into account by the addition of a series and parallel resistance (R_s and R_p). The output current (i_{pv}) of the PV cell is expressed as Eq. 4.1, which depends on the photogenerated current (i_{ph}), the diode current (i_d) and the parallel current (i_p). The photogenerated current depends on the solar irradiance level Eq.4.6. The diode current is the current that flows through the anti-parallel diode, which depends on the saturation current i_o 4.2. And the parallel current corresponds to the current that flows through the resistance R_p 4.3 where v_{pv} is the panel voltage.

$$i_{pv} = i_{ph} - i_d - i_p \tag{4.1}$$

$$i_d = i_o \times e^{\frac{v_d}{v_t}} \tag{4.2}$$

$$i_p = \frac{v_{pv} - i_{pv} \cdot R_s}{R_p} \tag{4.3}$$

To calculate the output characteristics of the PV panel is necessary to consider the open circuit voltage (v_{oc}) , short circuit current (i_{sc}) at standard test conditions (stc) that are usually available on PV panels data sheets. These conditions corresponds to a solar irradiance of 1000 W/m^2, temperature of 25 °C and atmospheric density of 1.5. At standard conditions, the basic variables to use for further calculations are the thermal voltage (v_t), the saturation current ($i_{o_{stc}}$) and the photogenerated current ($i_{ph_{stc}}$). The thermal voltage (Eq. 4.4) depends on Boltzmann constant (k_B), the number of solar cells interconnected in series in the PV panel (N_s), the temperature at standard conditions ($T_{c_{stc}}$), the diode ideality factor A, the electron charge (q). For standard conditions, the saturation current is calculated in Eq. (4.5) shows. The photogenerated current reference is calculated in Eq. (4.6).

$$v_{t_{stc}} = k_B \cdot A.N_s \cdot \frac{T_{c_{stc}}}{q} \tag{4.4}$$

$$i_{o_{stc}} = (i_{sc_{stc}} - \frac{v_{oc_{stc}}}{R_p}) \cdot e^{\frac{v_{oc_{stc}}}{v_{t_{stc}}}} \tag{4.5}$$

$$i_{ph_{stc}} = i_{o_{stc}} \cdot e^{\frac{v_{oc_{stc}}}{R_p}} + \frac{v_{oc_{stc}}}{R_p} \tag{4.6}$$

However, for other solar irradiance (G) and ambient temperature (T_a), the values of voltages and current changes but they still depend on the variables at standard conditions. Besides, the cell temperature (T_c) is variable during the day depending on the ambient conditions. The basic formula to calculate the PV panel temperature is in eq. 4.7 which depends on the normal operating cell temperature (NOCT).

$$T_c = T_a + G \times \frac{NOCT - 20}{800} \tag{4.7}$$

The new photogenerated current (i_{ph}) and the new short circuit current i_{sc} varies according to the solar irradiance value and temperature Eq. (4.8) and Eq. (4.10). The current variation because of temperature has a correction factor: k_i. This value is commonly very low and thus the final equation considered in the present work will only depend on the radiation value eq. (4.9). The short circuit current has a similar equation and approximation.

$$i_{ph} = i_{ph_{stc}} \cdot \frac{G}{G_{stc}} + k_i \cdot (T_c - T_{stc}) \tag{4.8}$$

$$i_{ph} \approx i_{ph_{stc}} \cdot \frac{G}{G_{stc}} \tag{4.9}$$

$$i_{sc} \approx i_{sc_{stc}} \cdot \frac{G}{G_{stc}} \tag{4.10}$$

The previous equations are valid only if the solar irradiance is higher than 200 W/m^2. For lower irradiance, the equations are expressed in (4.11) and (4.12) as it is explained in [172].

$$i_{ph} \approx i_{ph_{stc}} \cdot 0.008. \frac{G^2}{G_{stc}} \tag{4.11}$$

$$i_{sc} \approx i_{sc_{stc}} \cdot 0.008. \frac{G^2}{G_{stc}} \tag{4.12}$$

Besides the variation of current depending on ambient conditions, new values of voltages are necessary to calculate. The new thermal voltage (v_t) for other ambient condition is calculated in Eq. (4.13). Then, the open circuit voltage for new ambient conditions (v_{oc}) is calculated in Eq. 4.14, which depends on the cell temperature and a temperature correction factor: k_v [2].

$$v_t = v_{t_{stc}} * \frac{T_c}{T_{stc}} \tag{4.13}$$

$$v_{oc} = v_{oc_{stc}} + k_v \times (T_c - 25) \tag{4.14}$$

Taking into account the previous equations, the diode and the saturation current can be calculated (Eq. 4.16 and (4.15))

[2] In this model, the temperature correction factors for current and voltage (k_i and k_v) should be given by the PV solar cell's manufacturer.

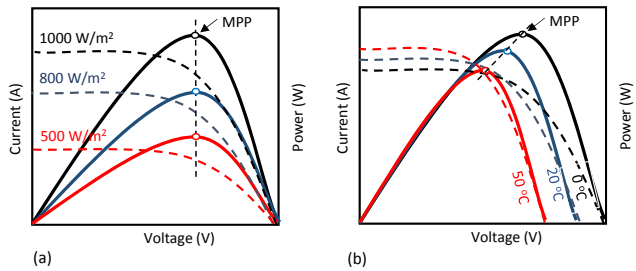

Figure 4.3: P-V and V-I curves of the PV array model for (a) variable solar irradiance and $T_a = 25^oC$, (b) variable temperature and $G = 1000W/m^2$

$$i_o = (i_{sc} - \frac{v_{oc}}{R_p}) \times e^{\frac{v_{oc}}{v_t}} \tag{4.15}$$

$$i_d = i_o + e^{\frac{v_{pv}+i_{pv}*R_s}{v_t}-1} \tag{4.16}$$

Then, the total current (i_{pv}) of the PV panel can be written as:

$$i_{pv} = i_{ph} - i_o\left(e^{\left(\frac{v_{pv}.N_{par}+R_s.i_{pv}}{N_s.A_d.k_B.T_c/q}\right)} - 1\right) - i_p.N_{ser} \tag{4.17}$$

According to the equations developed in this section, the curves characteristics of the PV array are illustrated in Fig. 4.3 at different solar irradiance and temperature. From these characteristics three main points can be observed: (i) short circuit current (i_{sc}), (ii) open circuit voltage (v_{oc}), (iii) maximum power point voltage (v_{mpp}) . When the solar irradiance changes, (i_{sc}) varies accordingly. But, when the temperature changes, v_{oc} and v_{mpp} vary more significantly than the current. The general equation to calculate the value of v_{mpp} is similar to the one used in eq. 4.14 and is written as:

$$v_{mpp} = v_{mpp_{stc}} + k_v \cdot (T_c - 25) \tag{4.18}$$

Finally, the current and voltage values of the PV array are written in equations 4.19 and 4.20 and depend on the number of PV panels interconnected in series and parallel. The total power is calculated as equation (4.21) shows.

$$i_{array} = i_{pv} \cdot N_{par} \tag{4.19}$$

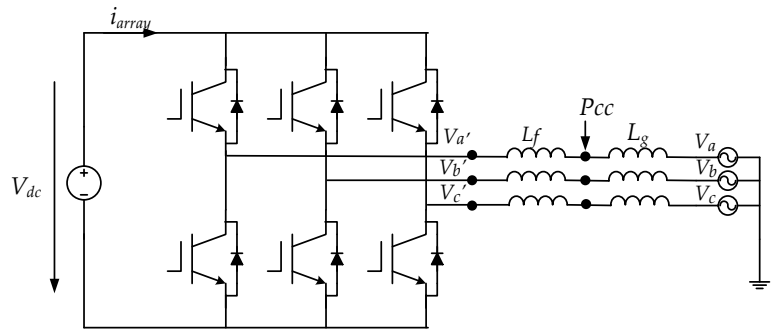

Figure 4.4: PV inverter interconnected with the grid

$$v_{array} = v_{pv} \cdot N_{ser} \tag{4.20}$$

$$p_{array} = i_{array} \cdot v_{array} \tag{4.21}$$

It can be seen the PV array has dual behaviour: (i) as a current source when the voltages are lower than v_{mpp} and (ii) as a voltage source when the voltages are higher than v_{mpp}. The inverter connected to this PV array should deal with this duality.

4.2.2 PV inverter

The PV inverter under analysis is a VSC converter that exchanges power from the PV array (DC side) to the grid (ac side). This inverter has two IGBTs per branch and a phase reactor per line (L_f). Furthermore, the transformer is modelled as an inductor. The grid is modelled as three voltage sources with their corresponding inductance (L_g) and the total resistance is neglected (Fig. 4.4).

The conversion from dc to ac developed by the inverter uses a modulation technique that permits an ac current as similar as possible to a sinusoidal waveform. For the current analysis sinusoidal PWM technique (SPWM) is considered, in which the output line to line voltage ($V_{a'b'}$) depends on the dc voltage from the dc bus ($V_{dc} = v_{array}$) and a modulation index (M) (Fig.4.5). The relationship between the ac and the dc voltage is linear if the modulation index varies between 0 to 1 as equation (4.22) shows. However, after this value, the relationship is not linear and the power quality of the sine-wave is reduced.

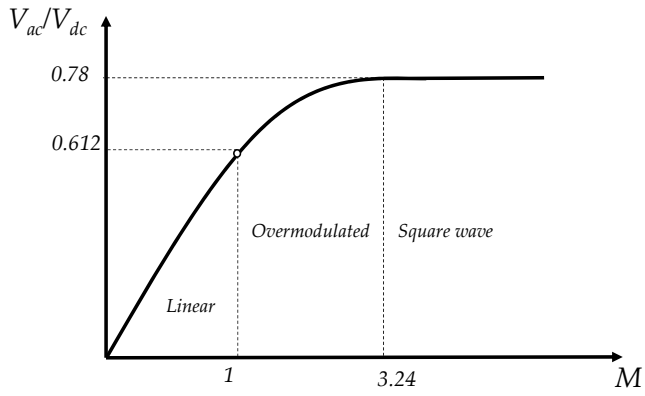

Figure 4.5: Output voltage and dc voltage in relation with Modulation index

$$V_{a'b'} = M \cdot \frac{\sqrt{3} \cdot V_{dc}}{2\sqrt{2}} \qquad 0 \leq M \leq 1 \tag{4.22}$$

To connect the PV array and the inverter, a dc capacitor is used. Its function and model is explained in the following section.

4.2.3 DC capacitor

In a PV inverter, the dc capacitor has two mains tasks: i) to smooth the dc voltage ripple and ii) to permit a fast dc voltage control. The ripple at the dc side is caused by the normal operation of the IGBTs. This ripple affects to the normal operation of the PV generator, as the power extracted from the PV array depends directly on the dc voltage at the PV array terminal (Fig. 4.6)[173]. The capacitor should be large enough to reduce the ripple at the terminals of the PV array. However, the power flow and the direct voltage control depends on the fast variation of the dc voltage.

The equivalent circuit for the dc side of the inverter is illustrated in Fig. 4.7, where the PV array is the dc generator acting on the dc link capacitor. The energy stored in the capacitor is given by equation 4.23 and the power flowing through the dc circuit is written in equation 4.24.

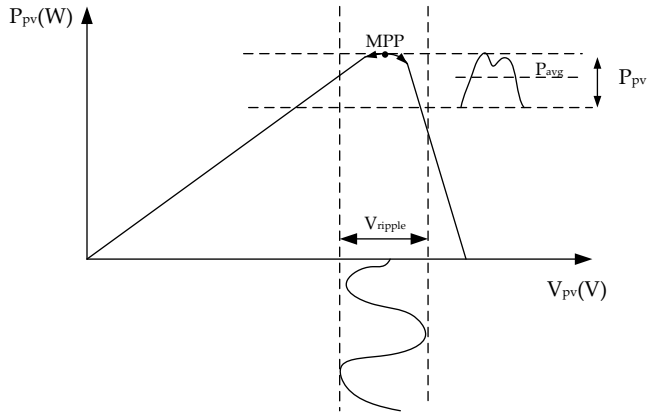

Figure 4.6: Ripple voltage effect on PV panel output power

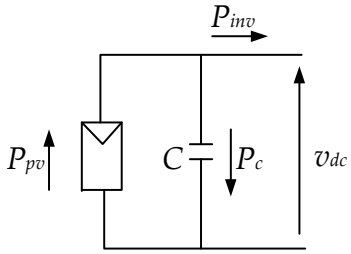

Figure 4.7: Equivalent dc circuit of a PV generator

$$W_c = \frac{1}{2} C_{dc} V_{dc}^2 \tag{4.23}$$

$$P_c = P_{pv} - P_{inv_{in}} \tag{4.24}$$

where; P_{pv} is the output power of the PV array [W] and; $P_{inv_{in}}$ is the active power flowing into the PV inverter.

4.2.4 Phase reactor

A phase reactor is usually connected to the ac side of the inverter and has the following purposes [174]:

- to reduce the high frequency harmonic of the ac side.
- to control of active and reactive power can be done independently.
- to limit sudden changes of power due to the solar irradiance at the dc side.
- to limit over-current due to short circuit currents

The design of these phase reactors depends on the control characteristics of the PV inverter. In the case that the modulation of the PV inverter is SPWM, the modulation index (M) and the dc voltage are part of the phase reactor design. The rated current (I_{rated}), the ripple (Δ_{ripple}) and the switching frequency (f_{sw}) is also considered as equation 4.25 shows [175].

$$L_f = \frac{V_{dc}.(1-M).M}{4.I_{rated}.\Delta_{ripple}.f_{sw}} \tag{4.25}$$

4.2.5 Transformer

The task of the transformer is to step up the ac voltage of the PV inverter to an appropriate value for the LS-PVPPs internal grid. Besides, the transformer also offers a galvanic isolation to the PV inverter. But also it works as a current filter and as a limiter of fault currents. For PV applications, a three-phase three winding transformer is commonly used. The existing vector group for these type of transformers are: Dy_ny_n, Dd_nd_n, YNy_ny_n, YNd_nd_n, YNy_nd_n as it was mentioned in section 2.2.3.

A simplified model of the PV inverter ac side is illustrated in (Fig. 4.8), where X represents the total reactance due to the filter, the transformer, and the grid. For the purpose of the present study, the capacitance effect is neglected.

After the model has been developed, the analysis of the capability curves and the limitations of the PV generator are analysed in the following section.

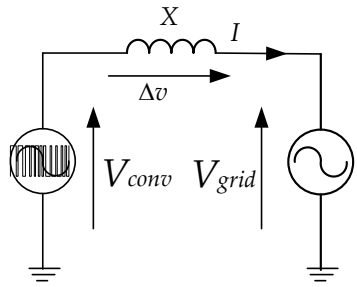

Figure 4.8: Simplified model of the Inverter

4.3 Capability curves of the PV generator

To analyse the capability curves of the PV generator it is necessary to understand the limitations of voltage, current and power of each component. This section presents the equations that represent the limitations of the PV generator related to the transfer of active and reactive power at the point of common coupling (PCC).

4.3.1 Voltage limitation

The dc voltage can vary from 0 to the maximum possible in order to extract different values of power from the PV array. However, the inverter sets the limitations of the dc voltage due to its operation. The minimum dc voltage (v_{min}) accepted by the inverter that will allow the ac voltage to be inside the values permitted by the grid codes is calculated in equation (4.26). In this equation, the maximum modulation index is considered (M = 1).

$$v_{min} = \frac{2\sqrt{2}}{\sqrt{3}} \cdot \frac{V_{a'b'}}{1} \tag{4.26}$$

In the case that the PV inverter is working at MPP, the minimum solar irradiance accepted to keep the voltage higher than the minimum value is calculated as:

$$G_{min} = \left(\frac{v_{dc_{min}} - v_{oc_{stc}}}{k_v} + 25 - T_a\right) \cdot \frac{800}{NOCT - 20} \tag{4.27}$$

Besides the minimum voltage, the maximum dc voltage v_{max} must also be determined. This value depends on the open circuit voltage of each panel times the number of panels connected in series (Equation 4.29). If the dc voltage is higher than the maximum of the PV array, the power supplied will be zero. The maximum v_{oc} of the PV array is dependent on the minimum temperature possible at the location chosen. These voltage limitations are written as:

$$v_{oc_{max}} = v_{oc_{stc}} + k_v \cdot (T_{a_{min}} + G_{min} \cdot \frac{NOCT - 20}{800} - 25) \tag{4.28}$$

$$v_{max} = v_{oc_{max}} \cdot Nser \tag{4.29}$$

4.3.2 Current limitation

The limitations of the dc current of the PV array depend specifically on the solar panel characteristics and the solar irradiance. The temperature does not play an important role in the variation of the current and thus this factor is not considered. The maximum current depends on the maximum solar irradiance and the i_{sc} value at standard conditions as:

$$i_{dc_{max}} = isc_{stc} \cdot \frac{G_{max}}{G_{stc}} \cdot Npar \tag{4.30}$$

The PV inverter current at the dc side should handle the current of the PV array at the highest irradiance. This current and the voltage determine the inverter operation area on the dc side.

4.3.3 Active power limitation

The PV curve of the PV array illustrated in Fig. 4.9 shows the behaviour of power vs the dc voltage. Three important points are necessary to analyse as: (i) $P_{dc_{vmin}}$, (ii) $P_{dc_{vmpp}}$ and (iii) $P_{dc_{vmax}}$. The minimum value of Power ($P_{dc_{vmin}}$), at the left side of the curve, considers the minimum dc voltage possible and the current at any ambient condition. In this case, if the solar irradiance is too low, the current will be close to 0 and the PV array will not be supplying enough active power to the grid. The maximum power ($P_{dc_{vmpp}}$) is obtained when the dc voltage is equal to the value of v_{mpp} for each

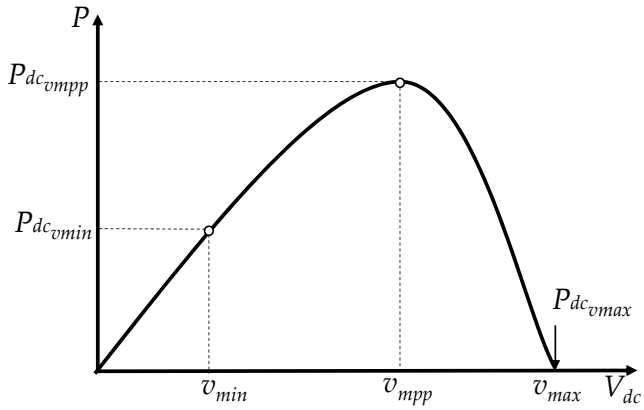

Figure 4.9: Power vs Voltage at the dc side. Main power points to analyse

solar irradiance and the corresponding temperature. The final point of power $P_{dc_{vmax}}$ is when the dc voltage is equal to the open circuit voltage that depends especially on the temperature. For any solar irradiance and temperature, the values of $P_{dc_{vmin}}$, $P_{dc_{vmpp}}$ and $P_{dc_{vmax}}$ are defined as:

$$P_{dc_{vmin}}(G, T_a) = v_{min} \cdot I_{dc}(G, T_a) \tag{4.31}$$

$$P_{dc_{vmpp}}(G, T_a) = v_{mpp}(G, T_a) \cdot I_{dc}(G, T_a) \tag{4.32}$$

$$P_{dc_{vmax}}(G, T_a) = v_{max}(G, T_a) \cdot I_{dc}(G, T_a) \tag{4.33}$$

Considering these power variations due to the solar irradiance and temperature, the maximum possible power ($P_{max_{array}}$) that can be extracted from the PV array is determined at the highest solar irradiance and the lowest temperature possible at the location of the PVPP (equation 4.34). With this limitation of power, the PV inverter should be designed for this active power taking into account an overrate of 25 % (equation 4.35).

$$P_{max_{array}}(G_{max}, T_{a_{min}}) = V_{mpp}(G_{max}, T_{a_{min}}) \cdot I_{dc}(G_{max}, T_{a_{min}}) \tag{4.34}$$

$$P_{max_{inverter}} = P_{max_{array}} \cdot 1.25 \tag{4.35}$$

From the analysis developed above, a safe operation area (S.O.A) is determined as illustrated in Fig. 4.10.

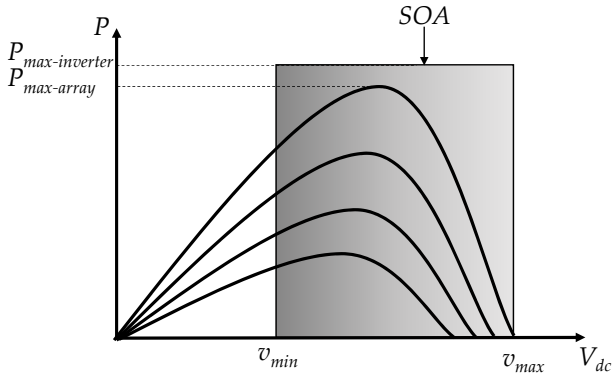

Figure 4.10: Safe operation area (SOA) of a PV generator

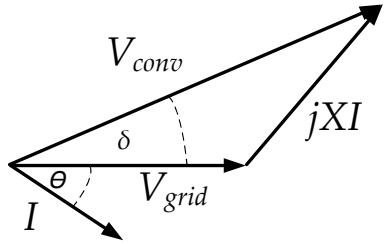

Figure 4.11: Phasor diagram of the PV inverter interconnected with the grid.

4.3.4 Reactive power limitations

From the model and the phasor diagram, illustrated in (Fig. 4.11), the equations of the active and the reactive power are:

$$P = 3\frac{V_{grid} \cdot V_{conv}}{X} \cdot \sin(\delta) \tag{4.36}$$

$$Q = 3\frac{V_{grid}}{X}\left(V_{conv}\cos(\delta) - V_{grid}\right) \tag{4.37}$$

The maximum apparent power that the PV generator can inject into the grid is given by the rated power of the inverter. Graphically, this limitation is illustrated as a circumference centred in the origin (Fig. 4.12). The equations for these limitations are:

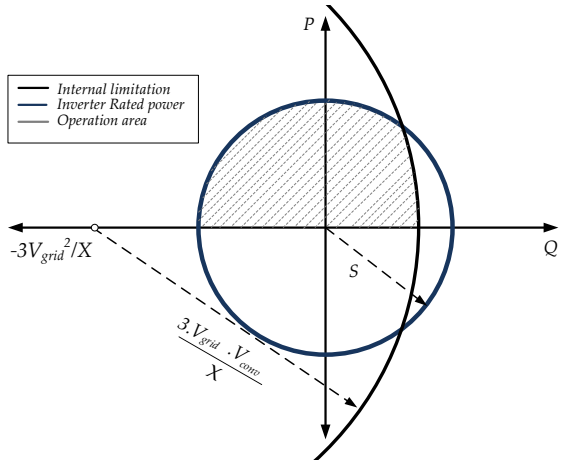

Figure 4.12: Basic PQ capability curve of the PV generator

$$S = \frac{3}{\sqrt{3}}.V_{grid} \cdot I_{grid} \tag{4.38}$$

$$S^2 = P^2 + Q^2 \tag{4.39}$$

If V_{grid} is multiplied by each variable of the phasor diagram, a new equation is obtained:

$$P^2 + \left(Q + \frac{3.V_{grid}^2}{X}\right)^2 = \left(3.\frac{V_{grid} \cdot V_{conv}}{X}\right)^2 \tag{4.40}$$

From this equation, the new curve is a circle that has a centre in $\frac{-3V_{grid}^2}{X}$ in the Q axis with a radius of $\frac{3 \cdot V_{grid} \cdot V_{conv}}{X}$ (Fig. 4.12). This curve represents the voltage limitation of the inverter. The radius of this curve varies due to the modulation index and the dc voltage. Also, the total reactance value at the PCC influences the final value for this radius. Drawing both equations together, the basic PQ capability of the converter is obtained and illustrated in Fig. 4.12.

4.4 Influence of ambient conditions

In this section, the influence of ambient conditions on the limitations of active and reactive power is analysed considering the PV array and the PV inverter. According to the model of the PV array, its characteristic curves are illustrated in Fig.4.3 at different solar irradiance, temperature and dc voltage. It can be stated that the instantaneous value of power (p_{inst}) and current depends on the instantaneous value of irradiance, temperature and dc voltage (equation 4.41).

$$p_{inst}(G, T, V_{dc}) = i_{array}(G, T, v_{array}) \cdot v_{array} \tag{4.41}$$

W In the case that the PV inverter works at the MPP, then the dc voltage (v_{mpp}) varies depending on the solar irradiance and temperature. Thus, the active power at this point has the following equation:

$$p_{mpp}(G, T, v_{mpp}) = i_{array}(G, T, v_{mpp}(G, T)) \cdot v_{mpp}(G, T) \tag{4.42}$$

Considering the equations for the dc power explained before and the inverter's efficiency (η), the ac output power equations at the PCC are written in (4.43) and (4.44).

$$p_{ac_{inst}}(G, T, V_{dc}) = I(G, T_a, Vdc) \cdot v_{array} \cdot \eta(G, T_a, v_{array}) \tag{4.43}$$

$$P_{ac_{mpp}}(G, T, V_{dc}) = I_{mpp}(G, T_a) \cdot v_{mpp}(G, T_a) \cdot \eta(G, T_a, v_{mpp}) \tag{4.44}$$

Depending on the ambient conditions, the active power that the PV generator can supply has two limitations. The first limitation corresponds to the highest solar irradiance, the minimum temperature of the plant location and the corresponding v_{mpp}. The second limitation corresponds to the maximum solar irradiance and the maximum temperature with the corresponding v_{mpp}. The difference between these values depends a lot on the difference of temperature that the geographical location has. These two limitations are formulated as:

$$P_{ac_{max_1}} = P_{dc}(G_{max}, T_{min}, v_{mpp}) \cdot \eta(G_{max}, T_{min}, v_{mpp}) \tag{4.45}$$

$$P_{ac_{max_2}} = P_{dc}(G_{max}, T_{max}, v_{mpp}) \cdot \eta(G_{max}, T_{max}, v_{mpp}) \tag{4.46}$$

The limitation of the reactive power is calculated considering the two circles that dominate the PQ capability curve. If the curve is dominated by $S^2 = P^2(G, T_a) + Q^2$, then the reactive power will depend on the active power variation that was defined in the previous equations. In the case the curve is dominated by the equation (4.40), then the limitation of the reactive power depends on the dc voltage and the modulation index as it is expressed in equation (4.47). Considering the variation of the dc voltage, the reactive power can be written as (4.48) or (4.49).

$$Q = \frac{3\sqrt{3}}{2\sqrt{2}} \times \frac{V_{grid} \cdot V_{dc} \cdot M}{X} \tag{4.47}$$

$$Q_{inst}(G, T, V_{dc}) = \frac{3\sqrt{3}}{2\sqrt{2}} \cdot \frac{V_{grid} \cdot v_{array} \cdot M}{X} \tag{4.48}$$

$$Q_{mpp}(G, T, V_{dc}) = \frac{3\sqrt{3}}{2\sqrt{2}} \cdot \frac{V_{grid} \cdot v_{mpp}(G, T) \cdot M}{X} \tag{4.49}$$

The modulation index varies depending on the dc voltage value, meaning that the reactive power remains almost constant. In order to manage the reactive power, M can be imposed. This affects the ac voltage value of the converter, thus M only can vary between two permitted values: M_{min} and M_{max}. These values depend on the ac voltage dead band set by the grid codes. For instance, Romania, Germany, South Africa and China have the same deadband of $\pm 10\%$. Considering the dc voltage equal to v_{mpp} for a single value of solar irradiance and temperature with an imposed M, the minimum and the maximum reactive power are defined as:

$$Q_{min} = \frac{3\sqrt{3}}{2\sqrt{2}} \cdot \frac{V_{grid} \cdot v_{mpp}(G, T_a) \cdot M_{min}}{X} \tag{4.50}$$

$$Q_{max} = \frac{3\sqrt{3}}{2\sqrt{2}} \cdot \frac{V_{grid} \cdot v_{mpp}(G, T_a) \cdot M_{max}}{X} \tag{4.51}$$

With the analysis developed previously, some interesting capability curves are obtained. For a variable dc voltage, the PQ curve that is obtained is shown in Fig. 4.13. In the case that the dc voltage is equal to v_{mpp}, the PQ capability curve is illustrated in Fig.4.14. Finally, Fig.

4.15 illustrates the PQ curve when the dc voltage is equal to v_{mpp} and M is imposed to vary the reactive power.

4.5 Validation of the system

To validate the PQ capability curves obtained in the previous section, a PVPP of 1 MW is designed, modelled and simulated in DiGSILENT PowerFactory ®. The PVPP has two PV generators of 0.5 MW each. The main characteristics of these PV generators are detailed in Table A.1.

PV panel characteristics		**PV array characteristcs**	
V_{oc}	58.8 [V]	P_{array}	0.5 [MW]
I_{sc}	5.01 [A]	N_{ser}	15
I_{mpp}	4.68 [A]	N_{par}	175
V_{mpp}	47 [V]	T_{min}, T_{max}	0-70 [°C]
k_v	0.45 [1/°C]	G_{max}	1100 [W/m^2]

Table 4.1: PV panel and array characteristics

The PVPP will work in underexcited or overexcited operation[3]. To test the PVPP under different solar radiation and temperature, three study cases are analysed: (a) Variation of dc voltage from v_{min} to v_{max}, (b) Variation of the v_{mpp} value, and (c) the variation of the modulation index.

4.5.1 Variation of the dc voltage

The PQ capability curve is analysed by the variation of the dc voltage under different ambient conditions. To understand the performance of the PV generator, two solar irradiance values are tested: 400 and 1000 W/m^2. Each solar irradiance is tested with three different temperature values: 10, 20 and 40 °C. The results are plotted in Fig. 4.16 to Fig. 4.17

[3]Underexcited: absorbs reactive power. Overexcited: supplies reactive power. In both cases, the PVPP supplies active power

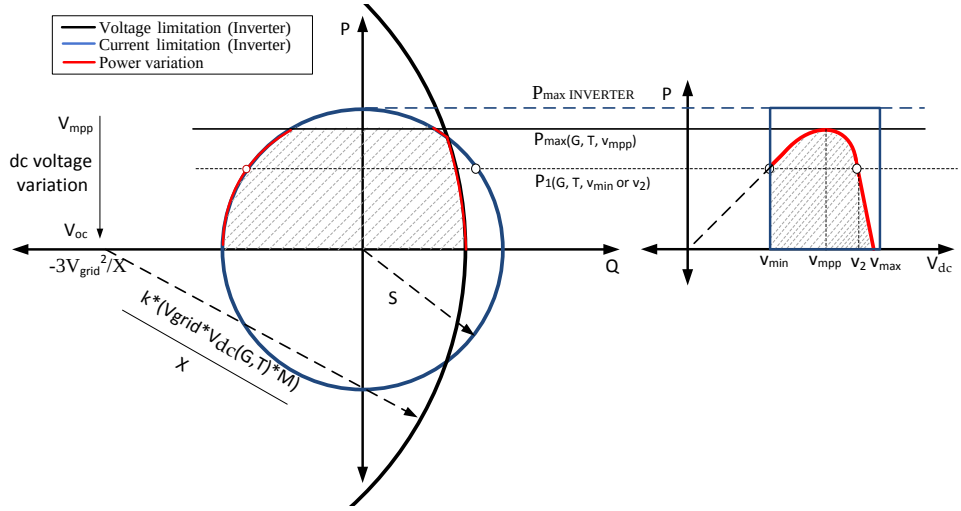

(a)

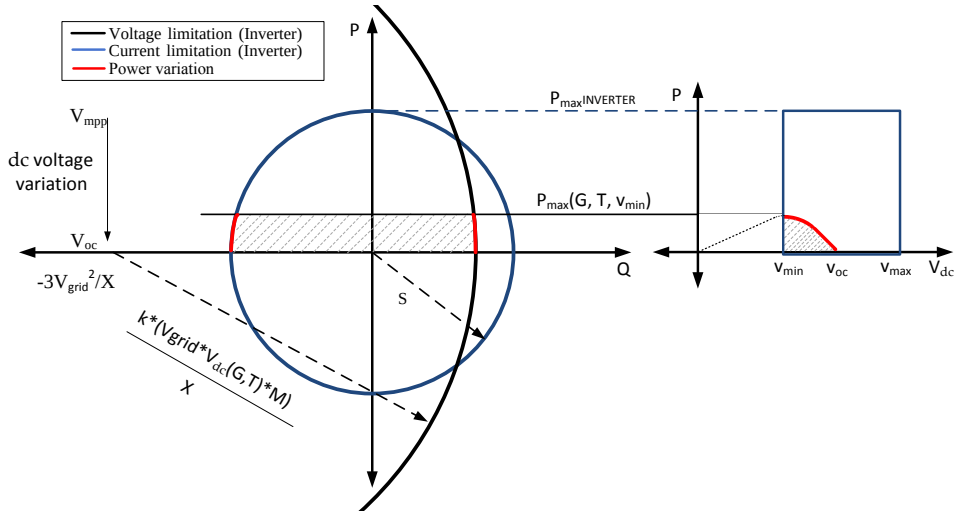

(b)

Figure 4.13: PQ capability curve of a PV generator for V_{dc} variable at maximum solar irradiance. (a) Minimum temperature (b) Maximum Temperature.

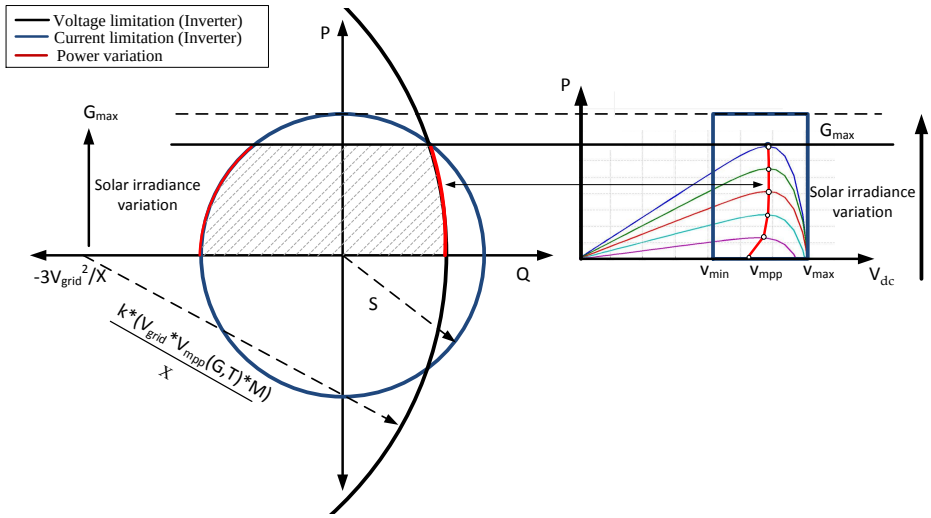

(a)

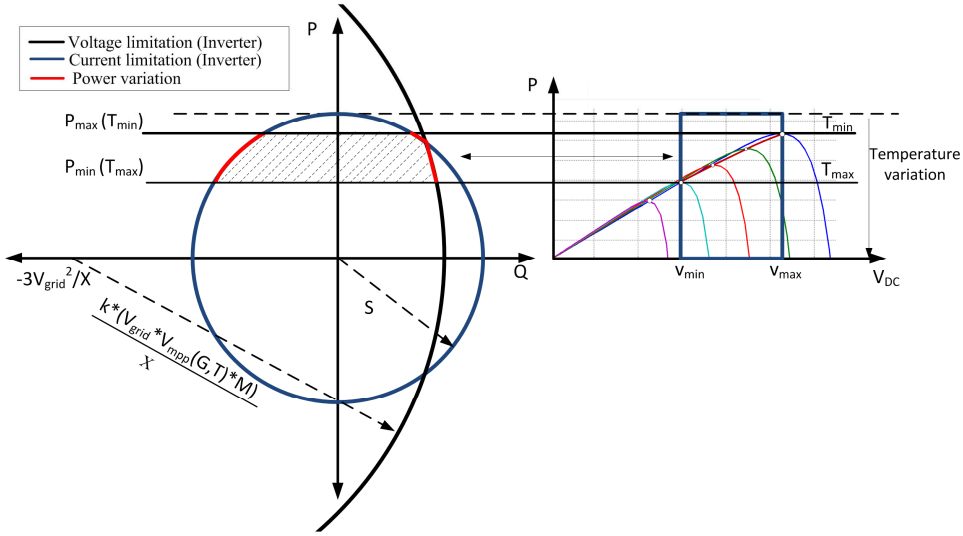

(b)

Figure 4.14: PQ capability analysis of the PV generator considering (a) Constant Temperature and variable solar irradiance (b) Constant solar irradiance and variable Temperature.

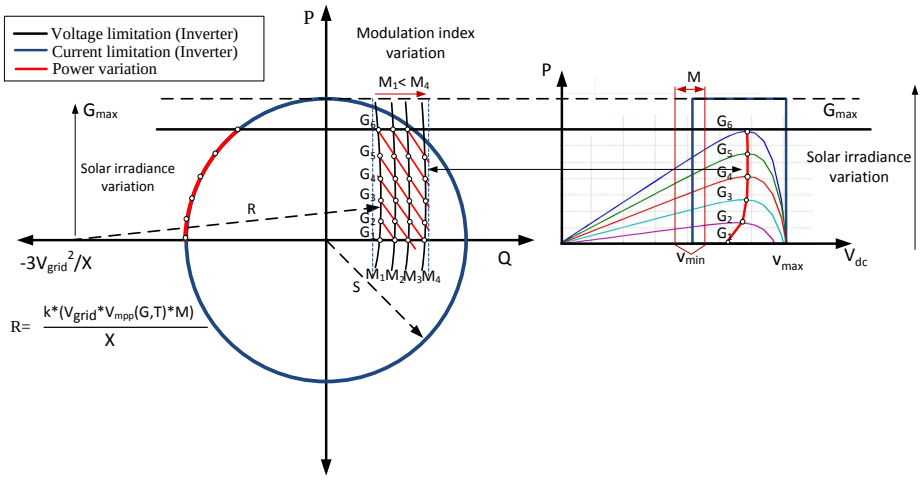

(a)

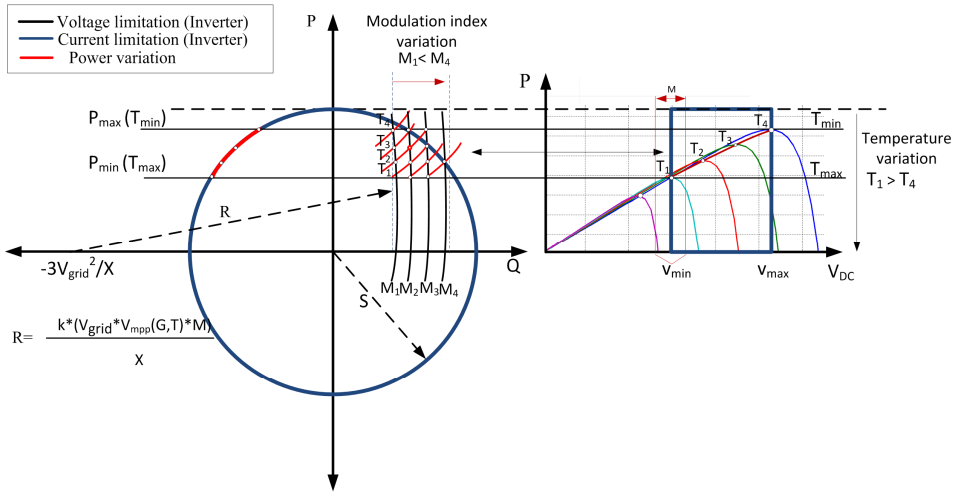

(b)

Figure 4.15: PQ capability curve of a PV generator for M variable. (a) Constant Temperature and variable solar irradiance (b) Constant solar irradiance and variable Temperature.

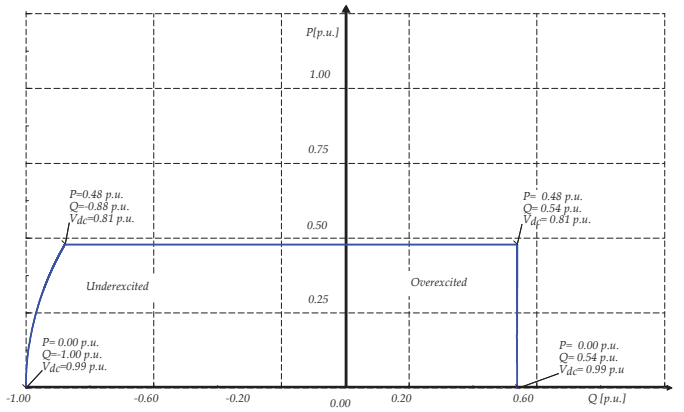

(a)

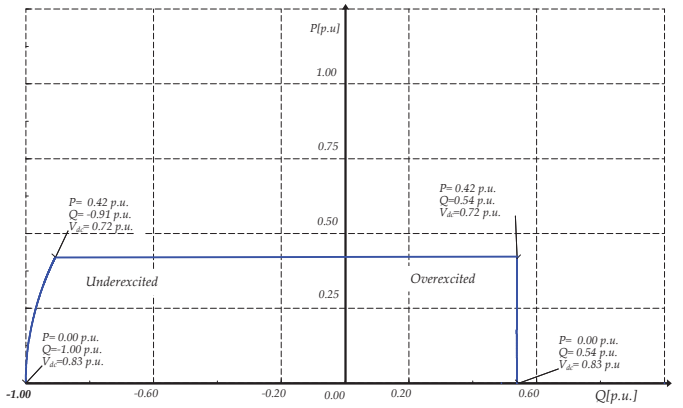

(b)

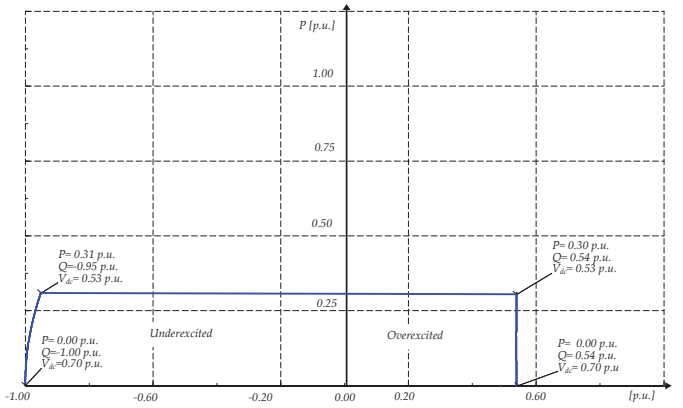

(c)

Figure 4.16: PQ capability analysis of the PV generator (G=400 W/m^2) for a variable V_{dc} (a) Ta=10 °C (b) Ta=20 °C(c) Ta=40 °C

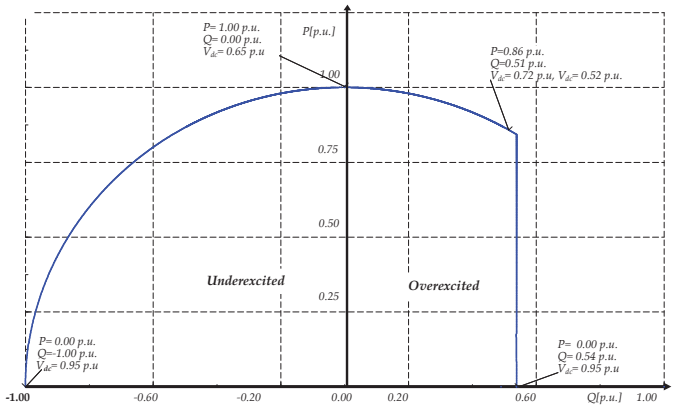

(a)

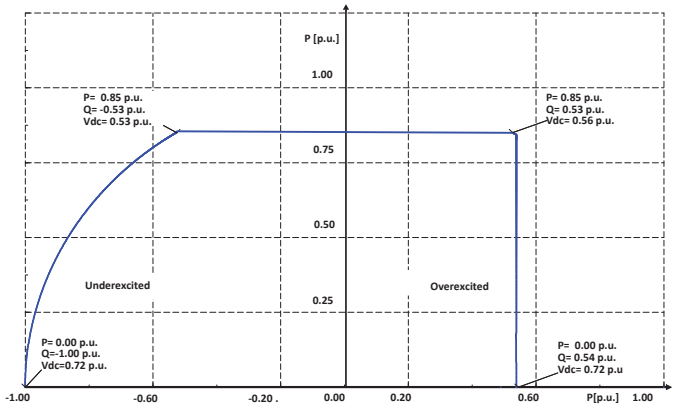

(b)

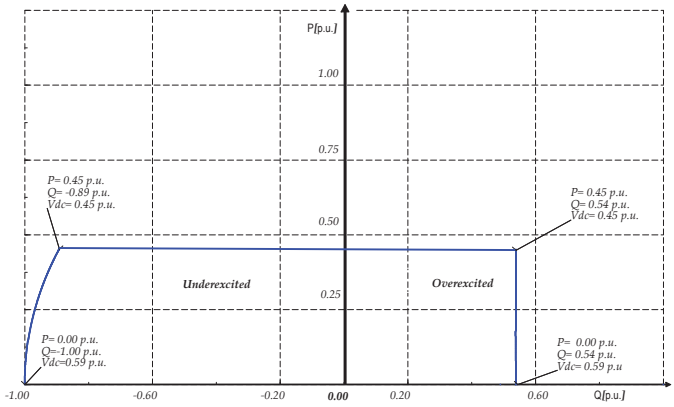

(c)

Figure 4.17: PQ capability analysis of the PV generator (G=1000 W/m^2) for a variable V_{dc} (a) Ta=10 °C (b) Ta=20 °C (c) Ta=40 °C.

4.5.2 Variation of v_{mpp} value

In this case the v_{mpp} value varies according to the solar irradiance and temperature that permits extraction of the maximum active power for each ambient conditions. In this case, three scenarios are considered:

- Scenario 1: The solar irradiance will vary from 0 to 1000 W/m^2 with steps of 1 W/m^2. The ambient temperature is constant T_a = 10 °C.
- Scenario 2: The ambient temperature will vary from 10 to 40 °C with steps of 0.1 °C. The solar irradiance has a unique value of 1000 W/m^2.
- Scenario 3: The solar irradiance will vary from 0 to 1000 W/m^2 with steps of 1 W/m^2. The ambient temperature is constant T_a = 40 °C.

The PQ curve of the PVPP at the PCC, for each scenario, when the voltage is v_{mpp}, is illustrated in Fig.4.18.

4.5.3 Variation of the modulation index

In this case, the dc voltage is equal to the v_{mpp} that varies according to the solar irradiance and temperature. The scenarios analysed considers the variation of solar irradiance, temperature and modulation index. In each scenario, the step size of the modulation index variation is 0.01 and it varies from 0.5 to 1.5. For these scenarios, the PQ curve is illustrated in Fig. 4.19.

- Scenario 1: The solar irradiance will vary from 0 to 1000 W/m^2 with steps of 1 W/m^2. The ambient temperature is constant T_a = 10 °C.
- Scenario 2: The ambient temperature will vary from 10 to 70 °C with steps of 0.1 °C. The solar irradiance has a unique value of 1000 W/m^2.

4.6 Conclusions

This chapter has studied the capability curves of the PV generator considering the variation of solar irradiance, temperature as well as

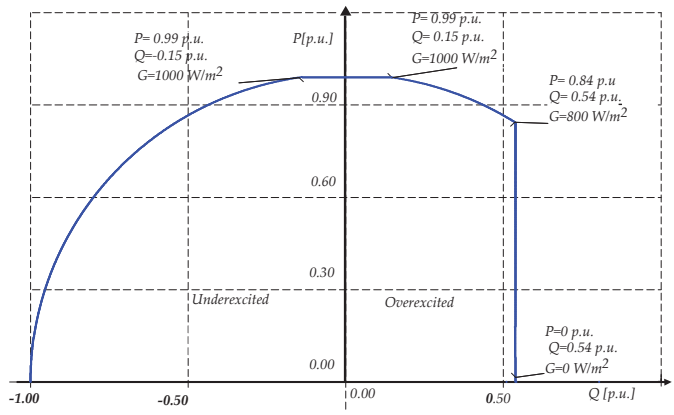

(a)

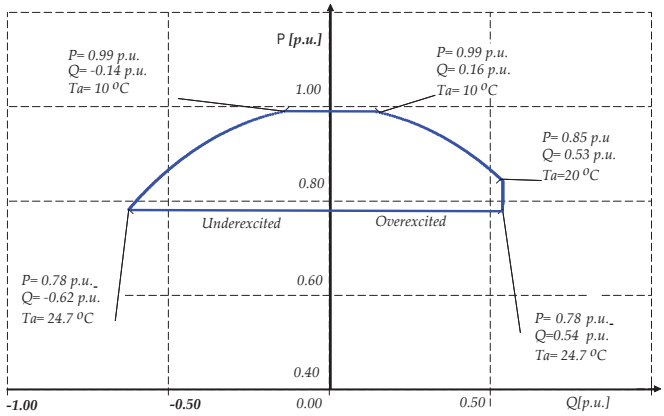

(b)

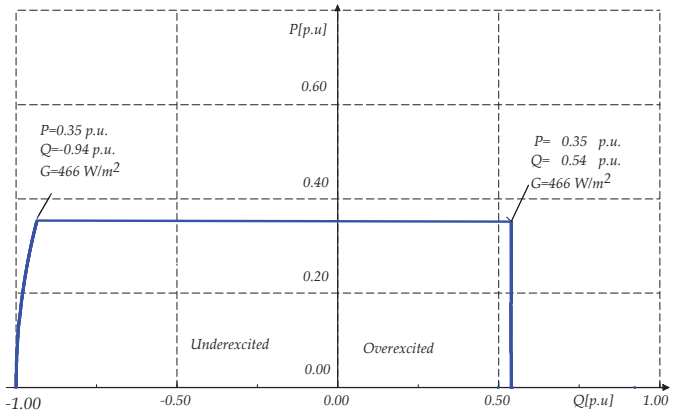

(c)

Figure 4.18: PQ capability analysis of the PV generator when $V_{dc} = v_{mpp}$ (a) G = 0 to 1000 W/m^2, T_a = 10 °C (b) T_a = 10 to 40 °C, G = 1000 W/m^2 (c) G = 0 to 1000 W/m^2, T_a = 40 °C

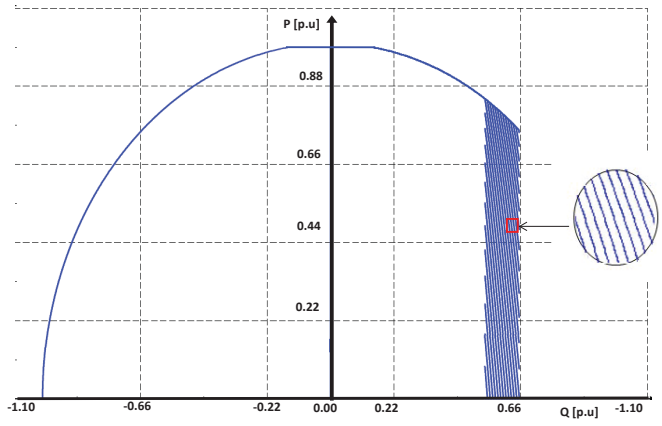

(a)

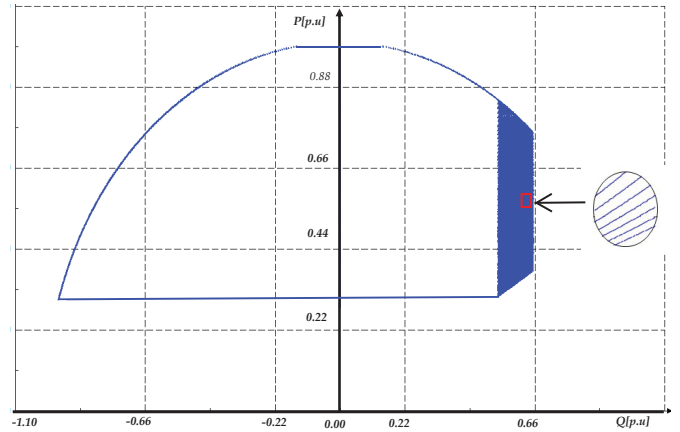

(b)

Figure 4.19: PQ capability analysis of the PV generator for a variable modulation index (a) G = 0 to 1000 W/m^2, T_a = 10 °C (b) T_a = 10 to 70 °C, G = 1000 W/m^2.

some electrical characteristics such as the dc voltage and the modulation index. Figures 4.13 to 4.15 summarize these curves. For this purpose, the current chapter has presented the corresponding mathematical model of the PV array and the PV inverter. It has also presented the limitations of voltage, current, and active power for the PV generator where Fig.4.10 was presented. Finally, a validation study was conducted in DIgSILENT PowerFactory® where the complete model has been introduced and simulated under different conditions. From the mathematical analysis and the simulation, some conclusions are discussed.

- The PQ capability curves of the PV inverter are characterized by four main parameters: solar irradiance, temperature, dc voltage and the modulation index. These values are dependent on each other in order to obtain the complete PQ curve. In the case where the dc voltage is equal to a single value, the active power and the reactive power will depend mainly on the solar irradiance, temperature, and modulation index. But in the case the dc voltage is variable, the complete curve can be obtained for a single solar irradiance and temperature.
- The solar irradiance and the temperature are important parameters to identify the SOA of the PV inverter. First, the highest solar irradiance and the lowest temperature determine the highest active power that the PV inverter can supply to the grid. It is necessary to mention that the highest temperature limits the output active power that the PV generator can supply to the system.
- The dc voltage and the modulation index are also parameters that affects the PQ capability curve and the operation of the PV inverter. In this chapter, it has been shown that the dc voltage can vary between v_{min} and v_{max}. The first value depends on the ac voltage value at the output of the PV inverter and the modulation index. The second value depends specifically on the highest solar irradiance and the lowest temperature.
- In the case that the dc voltage chosen is equal to v_{mpp}, the maximum active power can be obtained for a determined solar irradiance and temperature. However, this single point of operation does not permit the PV inverter to work in all of the PQ curves at any moment. Only a variation of solar irradiance will permit

the change of point of operation. This characteristic is not desirable in LS-PVPPs as it is necessary to provide ancillary services to the system.

- In overexcited operation, the limits of reactive power depend more on the modulation index than the solar irradiance or temperature. But it continues to depend on the dc voltage. Thus, its drastic variation could affect the ac voltage at the PV inverter terminals. The control should consider these limitations to vary the modulation index together with the reactive power.

After the capability curves have been analysed taking into account the solar irradiance, the ambient temperature, and the dc voltage effect, the next chapter deals with the dynamic control of the PV generator. In addition, Chapter 6 will present a discussion about the compliance of the PQ capability curves required by grid codes taking into account the curves analysed in this chapter.

Part III

Dynamic model and control

Chapter 5

Dynamic response of a PV generator considering its capabilities curves

"A 1000-megawatt solar power station occupies square miles (or square kilometres) and works only in the daytime. Even so, the dream of producing electric power from sunlight on a massive scale won't die."
Franklin Hadley Cocks, Energy Demand and Climate Change

This chapter analyses how the dynamic response of a photovoltaic (PV) generator is affected by its PQ capability curves under quick variations of solar irradiance and different temperature values. For this purpose, the dynamic model of the PV generator is detailed considering the base model explained in Chapter 4. The dynamic control of the PV generator is implemented taking into account the active and reactive power control limitations. The study is completed by a dynamic simulation in DiGSILENT PowerFactory®, where quick changes of solar irradiance are tested. The effect of the dc voltage, solar irradiance, and temperature in the PV generator operating point is shown together with the corresponding PQ capability curves.[1]

[1]This chapter is based on the following publications:
A. Cabrera-Tobar, E. Bullich-Massagué, M. Aragüés-Peñalba, O. Gomis-Bellmunt, "Dynamic response of a PV generator considering its capabilities curves", *Submitted to IET Renewable Power Generation*.
A. Cabrera-Tobar, O. Gomis-Bellmunt, "Dynamic study of a photovoltaic power plant interconnected with the grid", *PES Innovative Smart Grid Technologies Conference Europe (ISGT-Europe)*, Ljubljana, Slovenia. 9-12 Oct. 2016. pp. 1-6.
A. Cabrera-Tobar, O. Gomis-Bellmunt, "Performance of a small photovoltaic power plant under different meteorological conditions", *16th International conference on environmental and electrical engineering (EEIC)*, Florence, Italy. 7-10 June. 2016. pp. 1-6.

5.1 Introduction

The PV generator's inverter can already provide reactive power under some constraints of current and voltage [176]. However, it is necessary to analyse the PQ capability curve of this generator considering ambient conditions and the performance of the PV inverter. In [177],[178], the reactive power response of a PV generator has been studied but these do not consider the effect of the ambient condition on the capability curves.

The capability curves studied in Chapter 4 can influence in the control of the LS-PVPP. Thus, a proper study of the dynamic response of the PV generator considering its capability is necessary. Some authors have studied the dynamic performance of the PV generator when variable radiation occurs, however, these do not consider the limitations of the PV generator for future integration to the transmission system [179], [180], [48]. The purpose of this chapter is to analyse how the capability curves affects the dynamic performance of the PV generator when quick changes of solar irradiance occur at different ambient conditions.

This chapter is structured in four main topics: the dynamic model, control of the PV generator and lastly some dynamic simulations. This study has the purpose to show the performance of the PV generator under quick variations of solar irradiance when the PQ capability curve is considered.

5.2 Dynamic model

For the present study, the dynamic model relates the different components of the PV generator presented in Chapter 4, with the dynamic variation of solar irradiance, temperature, and electrical variables.

To develop the dynamic model, a modular system is used, where each module has its own characteristics and model, but the interaction between them is what defines the PV generator's performance. In this way, each of the models can be developed in parallel and the performance of each of them can be tested individually. The modular dynamic model proposed for this thesis is illustrated in Fig.5.1,

and consists in five modules: (i) forecasting, (ii) PV array, (iii) Bus dc, (iv) PV inverter, and (v) ac side.

The first module is related to the forecasting of solar irradiance and temperature during the day. The accuracy of the forecasting permits to enhance the performance of the PV generator. Knowing the solar irradiance and temperature in advance can permit to know the available maximum power at each instant during the day, and thus the control of the PV generator can be improved according to plant operator's requirements. The techniques used for an accurate forecasting model for different scale times can be developed using: various meteorological data such as pressure, relative humidity, temperature, wind speed– combined with past observed data [181, 182]. For the purpose of the PV generator model, the output of this module should be the solar irradiance and the ambient temperature.

The second module is the PV array, which input is the data given by the forecasting module and the output are the output power (P_{pv}) and the v_{mpp} at each solar irradiance. As it was explained in Section 4.2, the model of the PV array depends on the dc voltage at its terminals. Thus, another input for the model is the dc voltage that comes from the dc bus model. The output power will be varying according to this voltage and the solar irradiance at each time set during the day.

The third module is the DC bus voltage, which is based on a capacitor behaviour. Its dynamic model can be characterised as:

$$V_{dc}(s) = \frac{i_c(s)}{sC} \tag{5.1}$$

Then, the third module is the PV inverter which model was explained in Section 4.2.2. The dynamic behaviour depends on the conversion from dc to ac voltage considering as well its dc and ac limitations (see Fig. 4.4). The modulation index varies accordingly the dc voltage value at its input and the reference ac voltage. The inverter, however, also is the one that performs the dynamic control of the PV generator playing with the variables given by all the modules presented in Fig. 5.1.

The ac system module compresses the behaviour of the grid, phase reactor and transformer. The outputs of this module are: the ac

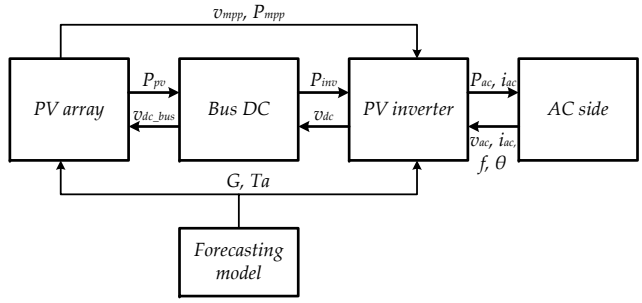

Figure 5.1: Modular dynamic model of a PV generator

voltage, the ac current, the frequency and the phase angle. [2]

By taking into account all these models, the control of the PV generator is developed in the following section.

5.3 Dynamic control

A VSC converter is used to control active and reactive power as well as to set the amplitude, the angle and the frequency of the output phase voltages. For these, there are three control strategies commonly used for grid tied PV inverters: (i) direct control, (ii) vector control and (iii) power synchronization control [183].

In PV inverters, the most used technique is the vector control, where the current and three phase voltages are transformed to the rotating direct-quadrature frame. This will be synchronised with the ac grid

[2] A detailed model of this system will be explained in AppendixA.

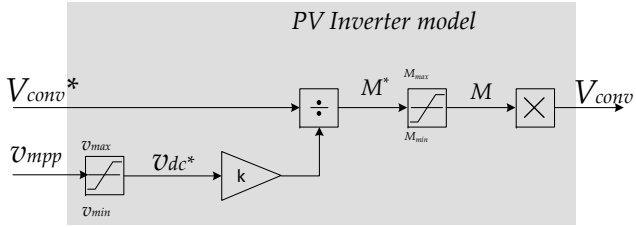

Figure 5.2: PV inverter model

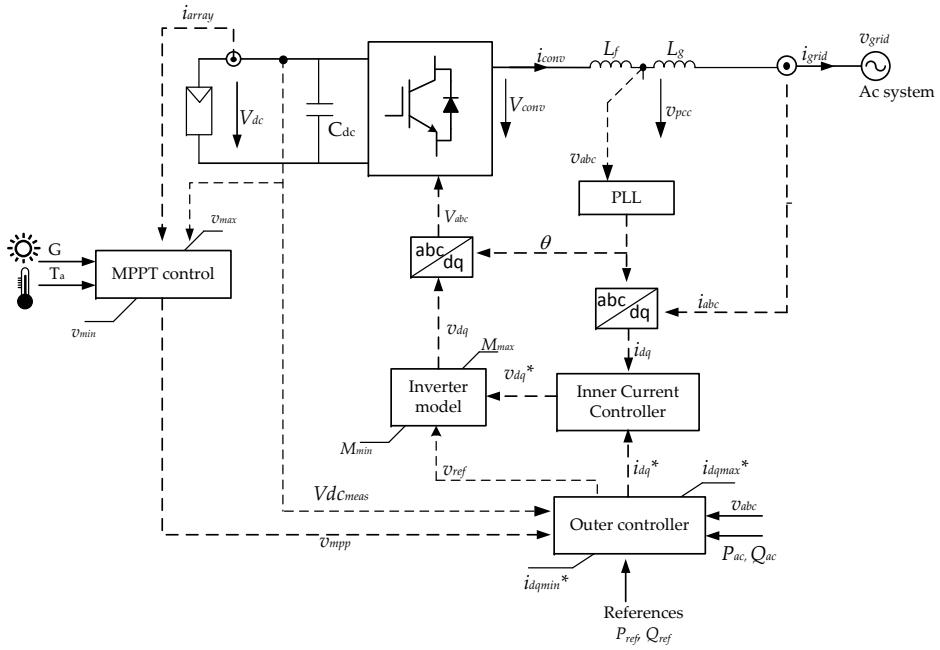

Figure 5.3: PV generator general control

voltage by a phase locked loop (PLL). The general control of a PV generator for grid-tied systems is illustrated in Fig. 5.3. This control consists of a maximum power point tracker (MPPT), phase locked loop (PLL), inner current loop, outer control, and voltage modulation. Each of these blocks are explained in the following section.

5.3.1 MPPT

PV generators commonly work at maximum power point at each solar irradiance and temperature. The tracking of this point (MPPT) is often developed by an algorithm that its main purpose is to find the voltage (v_{mpp}) or current (i_{mpp}). Several type of algorithms have been used to solve this issue as Perturb and Observe (P&O), hill climbing, beta method, incremental conductance, fractional short circuit current, fractional open circuit voltage, pilot cell, current sweep, soft computing methods[3] and several others [184], [185] [130], [131].

[3]Soft computing methods for MPPT are artificial neural network, fuzzy logic control, genetic algorithm, differential evolution and chaos search method

All of these methods have to deal with quick changes of irradiance, PV panel's aging, number of sensors used and partial shading conditions [184]. One of the most popular is the one called " Perturb and Observe" where the sensed variables are voltage and current. This algorithm is based on the calculation of power by using the current and voltage measured. It is based on the variation of the dc voltage at each time step and thus a perturbation of active power occurs in the system. If the active power increases with respect to the previous value, then the control should reduce the dc voltage considering a Δv value. But in the case the active power reduces, the next Δv should be added to the previous value of dc voltage. Its popularity is because it is easy to implement, it does not need a periodic tuning and it is not PV array dependent. The drawbacks of this algorithm are: oscillations around the MPP and tracking deviation when quick changes of solar irradiance occur [131].

In this thesis, however, a modification of the algorithm is developed. Instead of being comparing the previous value of active power with the measured in the new time step, it is compared with the one calculated in the PV array model thanks to the forecasting data (Fig. 5.4). Each time step, the change of dc voltage (Δv) is equal to 0.02 p.u and the output voltage from the algorithm (v^*_{dc}) can vary inside the limits of v_{min} and v_{max}.

5.3.2 Inner current control

The inner current control is the one that gives the signal references (v^*_d and v^*_q) to the voltage modulation block which has to transform this voltage references to three phase voltages with the corresponding modulation technique. The inner current control improves the performance of the VSC as it uses as feedback the current of the converter and compares it with the current references that come from the outer controller (Fig. 5.5).

5.3.3 Outer controller

The outer controller defines the current reference signals (i^*_d and i^*_q) for the inner current controller. In the case of PV generators for LS-PVPPs these signals are related with the active and reactive power

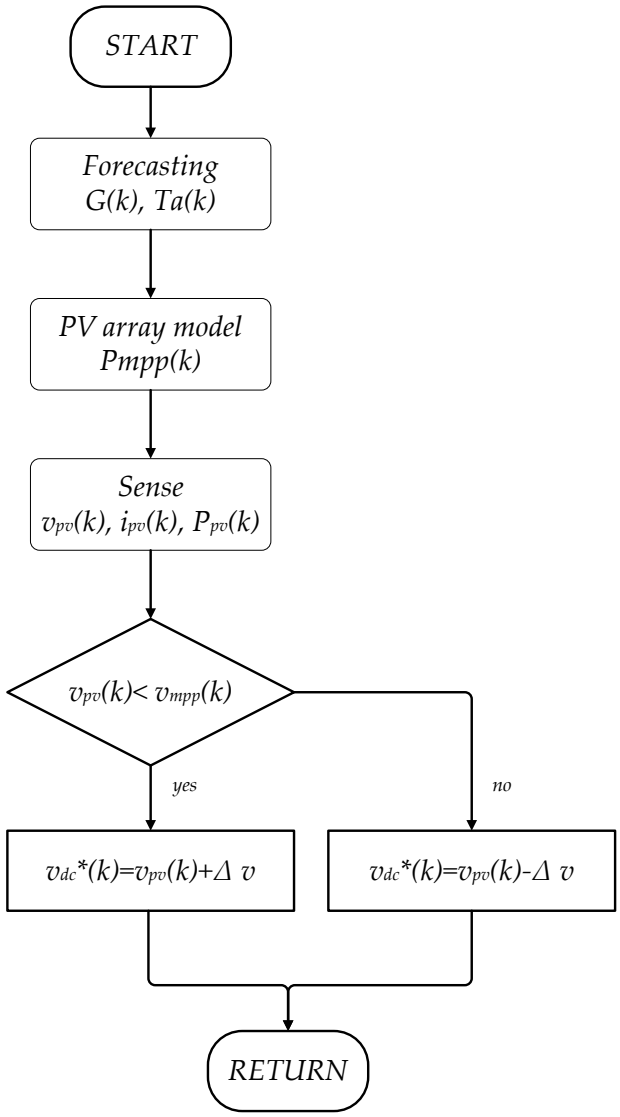

Figure 5.4: Algorithm implemented for MPPT

[4]. For the active power, three types of controllers can be part of the system: active power controller, direct voltage controller, and the frequency controller. For reactive power, the reactive power controller

[4]The active power is related with i_d^* and the reactive power with i_q^* as the d_{axis} of the dq rotating frame is aligned with ac network voltage phasor

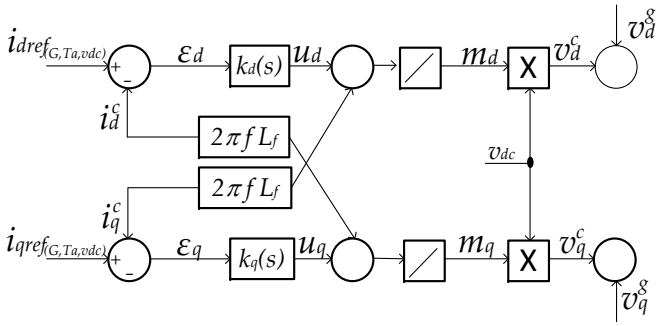

Figure 5.5: General inner current control of a PV generator

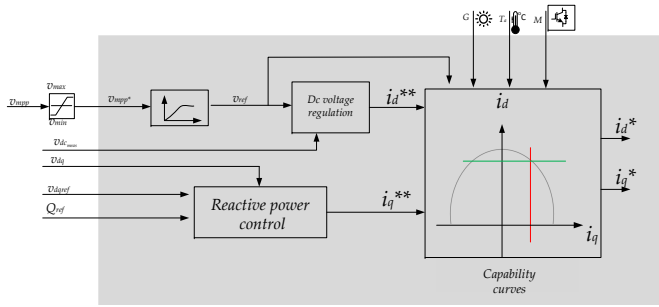

Figure 5.6: General outer control of a PV generator

and the ac voltage controller can also be designed.

In this case, the dc voltage controller and the reactive power controller are designed to test the dynamic response of the PV generators considering its capability curves. This control is illustrated in Fig. 5.6

dc voltage controller

The dc voltage controller ensures the power balance between the source (PV array) and the ac power injected into the grid. For this the main equation is the relationship between in the input and output power in a lossless PV generator:

$$P_{pv} = P_{ac} \tag{5.2}$$

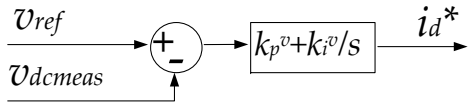

Figure 5.7: PV inverter's dc voltage control

where:

$$P_{pv} = i_{pv} * v_{pv} \tag{5.3}$$

$$P_{ac} = v_{pcc_d} i_d^g + v_{pcc_q} i_q^g \tag{5.4}$$

Taking into account the model of the dc side presented in Section 4.2.3, the energy stored at the capacitor side is equal to eq. (5.5). Then the square of the dc voltage (v_{pv}^2) can be assumed equal to the dc energy (W_{dc}) transferred from the dc to the ac side.

$$W_c = \frac{1}{2} C v_{pv}^2 \rightarrow v_{pv}^2 = W_{dc} = \frac{2}{C} W_c \tag{5.5}$$

Thus, the dc voltage control operates on the error of the stored energy $\delta W_{dc} = W_{dc}^* - W_{dc}$. For the control, a PI is used, which its dynamics not only depends on the energy stored at the capacitor side but also on the MPPT time response plus the limitations due to the inverter and the ambient conditions. The diagram of this control is illustrated in Fig. 5.7

Reactive power controller

The expression to evaluate the reactive power flowing to the ac grid can be formulated as:

$$Q_{ac} = v_{pcc_q} \cdot i_d^g - v_{pcc_d} \cdot i_{g_q} \tag{5.6}$$

In the dq frame when it is synchronized with the grid $v_{pcc_q} = 0$, so the reactive power reference can be controlled by i_q^* (eq.5.7). To control this reactive power and to cancel the steady state error a PI control is used (Fig. 5.8)

$$i_q^* = \frac{2/3 Q_{ref}}{v_{pcc_q}} \tag{5.7}$$

In this case, the reactive power control has the main task of injecting or absorbing reactive power when it is needed: ac voltage variations

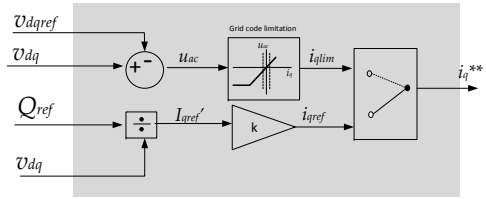

Figure 5.8: Reactive power control

or grid support (Q_{ref}). In any of the cases, the PV inverter can only surplus these requirements inside the PQ capability curve. The reactive power should follow the reference given by the first control, this is limited by the PQ capability curve that depends on solar irradiance, temperature, and the dc voltage. The i_q^* limitations are written in the equations (A.21) and (A.22). In the case, that the reactive power required is higher than the limitation, the PV inverter will only provide the maximum permitted at that conditions, as the voltage chosen at each time is equal to v_{mpp} that only can vary from v_{min} to v_{max}. The block diagram of the reactive power control is illustrated in Fig. 5.8.

$$i_{q_{min}} = \sqrt{i_{inv}^2 - i_d^2(G, T_a, v_{mpp})} \tag{5.8}$$

$$i_{q_{max}} = \frac{2/3 Q_{max}(G, T, v_{mpp})}{v_q} \tag{5.9}$$

5.4 Phase locked loop

The final block is the PLL structure, which is a feedback control system that has the task to adjust the phase angle between the grid reference (dq) frame and the converter (dq) reference frame (Fig. 5.9). To do this, the controller has to align the grid voltage phasor with one of the two dq axes. In this case, it is aligned with the d-axis which means that the $v_q^g = 0$. With this new angle, the VSC becomes synchronised with the grid, so $v_q^c = 0$ in steady state [186]. When the PLL angle is obtained, then the voltages and currents can be transformed from abc frame to dq rotating frames and vice-versa.

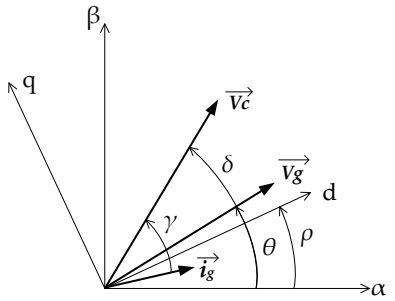

Figure 5.9: dq diagram for AC side inverter

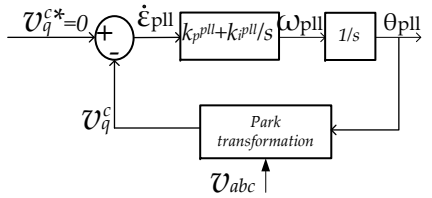

Figure 5.10: Phase lock loop controller diagram

The feedback control structure of the PLL uses commonly a PI which compensates the error between the reference voltage $v_q^{c*} = 0$ and the new v_q^c considering the new phase angle (Fig. 5.10) [5].

In this section, the dynamic control was presented considering the capability curves. The following section will present the simulation of this PV generator under different scenarios.

5.5 Dynamic simulation

In this section, the dynamic model of the PV generator is simulated in DiGSILENT PowerFactory ® under different scenarios to present its performance when the capability curve is considered. The PV generator under study has a power capacity of 0.6 MVA and its main characteristics are detailed in Table A.1. Additionally, the corresponding P-V curves for variable solar radiation and temperature are presented in Fig. 5.11

[5] The PLL used in this thesis can be improved by using an estimator. This is explained in Appendix A

PV panel characteristics		PV array characteristcs	
V_{oc}	58.8 [V]	P_{array}	0.5 [MW]
I_{sc}	5.01 [A]	N_{ser}	15
I_{mpp}	4.68 [A]	N_{par}	175
V_{mpp}	47 [V]	T_{min}, T_{max}	0-70 [°C]
k_v	0.45 [1/°C]	G_{max}	1100 [W/m^2]

Table 5.1: PV panel and array characteristics

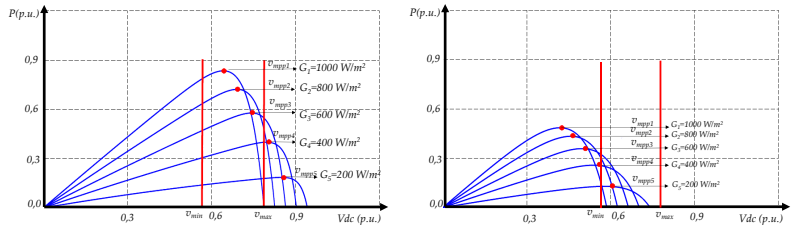

Figure 5.11: P-V curves for variable solar irradiance (a) T_a = 10°C , (b) T_a = 40°C

The first case study is when the solar irradiance varies from a low irradiance (200 W/m^2) to a high value (1000 W/m^2) in a small period of time and then it comebacks to (200 W/m^2) (Case study A). The second case study considers the change of solar irradiance from high (1000 W/m^2) to low (200 W/m^2) and then it comebacks to (1000 W/m^2) (Study case B) (see Fig. 5.12). In each case, the simulation is developed for two different temperatures (a) T_a = 10°C and (b) T_a = 40°C. Additionally, a reference of reactive power is applied and is equal to –0.6 MVAr that is the same as the nominal power of the PV generator. Thus, the PV generator will work close to the limit given by the PQ capability curves.

For case study A, the results of active and reactive power for each ambient temperature are presented in Fig. 5.13 and Fig. 5.14. When the ambient temperature is T_a = 10°C, the active power expected is 0.176 and 0.825 p.u. for a solar irradiance of 200 and 1000 W/m^2 respectively. When the solar irradiance changes suddenly from 200 to 1000 W/m^2, the expected active power cannot be fulfilled instantaneously. In fact, after 0.5 seconds, the active power is 0.304 p.u. instead of 0.825 p.u. As the solar irradiance changes again from 1000 to 200 W/m^2, the active power returns to a value close to 0.176 p.u.

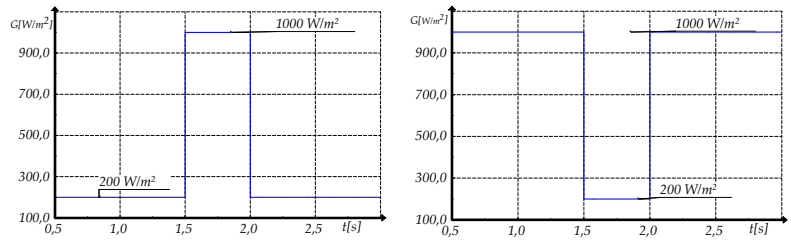

Figure 5.12: Quick changes of solar irradiance tested in the present application (a) Study case A, (b) Study case B

In this study case, the absorbed reactive power is close to 0.985 p.u and 0.951 when the solar irradiance goes from 200 to 1000 W/m^2 and vice-versa. However, the expected range of reactive power is from 0.98 to 0.57 p.u. When the ambient temperature is T_a = 40^{o}C, the active power expected is 0.129 and 0.486 p.u. for a solar irradiance of 200 and 1000 W/m^2 respectively. However, the active power reached by the PV generator when the solar irradiance is 1000 W/m^2, it is close to 0 p.u. Then, the absorbed reactive power is around 1 p.u.

For case study B, the results of active and reactive power for each ambient temperature are presented in Fig. 5.15 and Fig. 5.16. When the ambient temperature is T_a = 10^{o}C, the active power expected is 0.825 and 0.176 p.u. for a solar irradiance of 1000 and 200 W/m^2 respectively. The active power that the PV generator injects when the solar irradiance is 1000 W/m^2 during 1.5 seconds goes from 0.22 to 0.6 p.u. The absorbed reactive power also changes from 0.959 to 0.798 p.u. However, when the solar irradiance changes instantaneously to 200 W/m^2 , the active power reduces at the same speed from 0.6 to 0.117 p.u. The reactive power also changes instantaneously from 0.798 to 0.935 p.u When the ambient temperature is T_a = 40^{o}C, the active power expected is 0.486 and 0.129 p.u. for a solar irradiance of 1000 and 200 W/m^2 respectively. However, the active power reached by the PV generator when the solar irradiance is 1000 W/m^2, it is 0 p.u. Then, the absorbed reactive power is around 1 p.u.

According to these results, the operational area in dynamic mode together with the capability curves is illustrated in Fig. 5.17 and Fig. 5.18. The capability curve when the ambient temperature is 10^{o}C for a variable solar irradiance from 0 to 1000 (W/m^2) with a

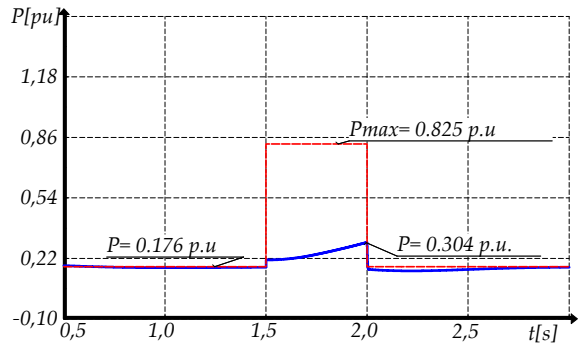

(a)

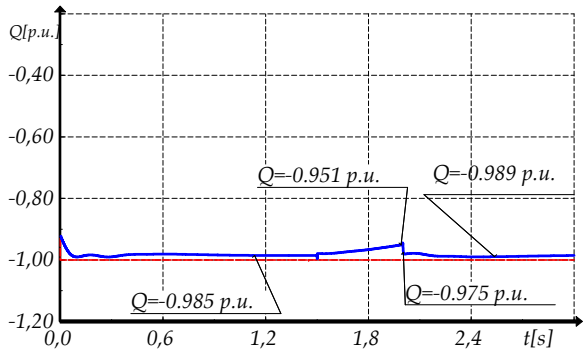

(b)

Figure 5.13: Dynamic response of a PV generator for case study A and T_a = 10°C (a) Active Power, and (b) Reactive power

dc voltage equal to the correspondingv_{mpp} shows a wide range of operation. However, when the ambient temperature is 40°C, the maximum active power that the PV generator can inject is 0.3 p.u corresponding to a solar irradiance of 470 W/m^2. For study case A, it can be seen that the area of operation is very close to the limitation curve as it tries to absorb the maximum reactive power possible. The active power goes from 0.176 p.u to 0.304 p.u. but when the ambient temperature is 40°C, the active power goes from 0.176 to 0 p.u. Thus the area of operation is reduced. For study case B, the area of operation inside the capability curve increases as the active power is closed to the maximum when the solar irradiance is equal to 1000 (W/m^2) but when the ambient temperature is 40°C the operational area is similar to study case A.

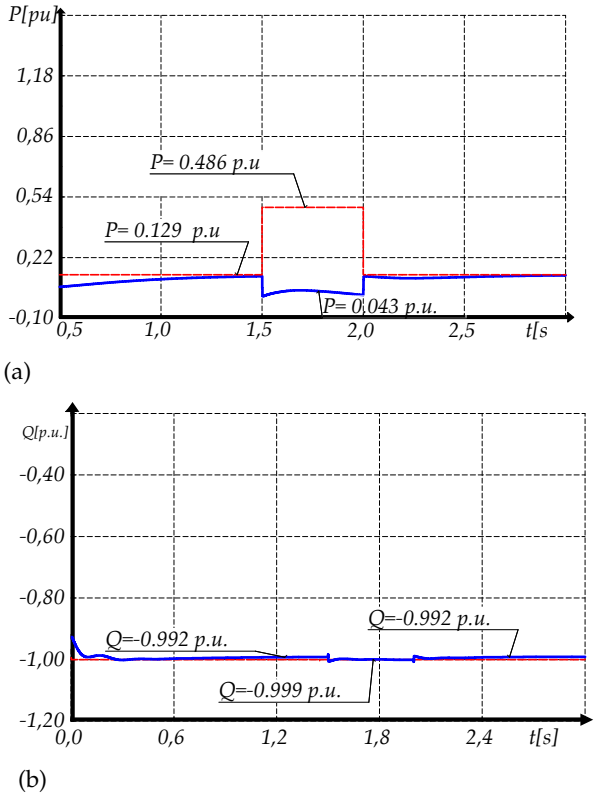

Figure 5.14: Dynamic response of a PV generator for case study A and T_a = 40°C (a) Active Power, and (b) Reactive power

Considering the results of the dynamic simulation together with the capability curves a broad discussion is presented in the following section.

5.6 Discussion

From the dynamic simulation of the PV generator under the case study A and B with different ambient temperature, some important points can be addressed.

MPPT dynamics: The MPP for each solar irradiance and temperature is illustrated in the P-V curve (Fig. 5.11). These power points correspond to the ideal point of operation at the PQ curve (Fig. 5.17).

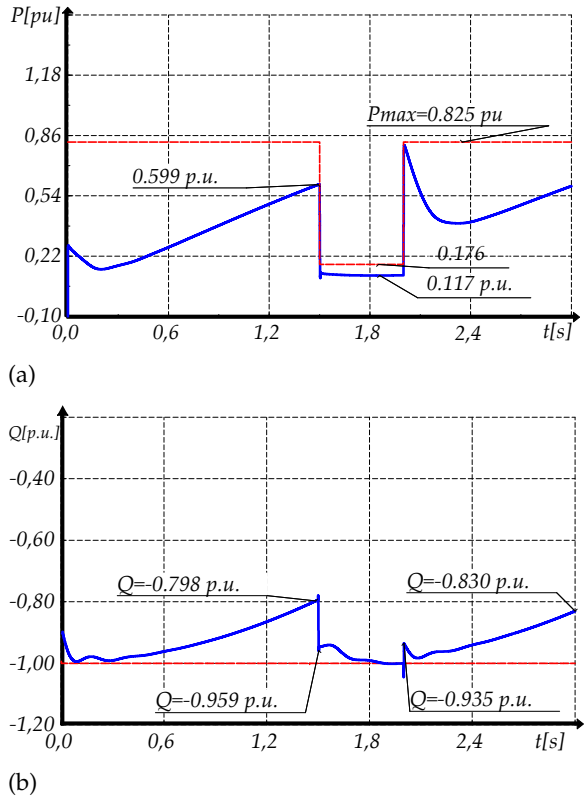

Figure 5.15: Dynamic response of a PV generator for case study B and T_a = 10°C (a) Active Power, (b) Reactive power

However, it can be seen that these points are not reached in case A or B. When the solar irradiance varies from low to high value, the dc voltage value at that instant influences on the active power value (Fig. 5.11). Then, the MPPT starts to work to reach the MPP, but as its time response is higher than the disturbance, the MPP is not reached. In the other hand, when the solar irradiance decreases instantaneously, the active power does it at the same speed and only depends on the value of dc voltage that is set at the moment of the change and not due to the MPPT time response.

Effect of temperature: The cell temperature plays an important role in the PV generator's performance as it varies not only depending on the ambient temperature but also on the solar irradiance. The PQ curve is affected when the ambient temperature increases and

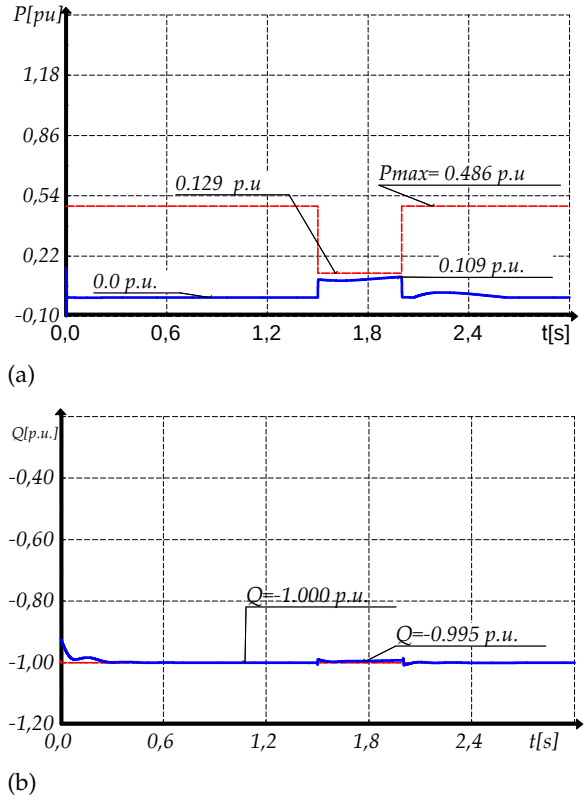

Figure 5.16: Dynamic response of a PV generator for case study B and T_a = 40°C (a) Active Power, (b) Reactive power

the voltage are equal to v_{mpp}. In the case the ambient temperature is 40°C, the PV generator can inject active power only if the solar irradiance is varying from 0 to 470 W/m^2. For higher solar irradiance the value of v_{mpp} is lower than the v_{min}, so the inverter cannot inject active power as it is working outside the safe operation area. In this chapter, when the v_{mpp} is lower than v_{min}, then the dc voltage chosen is equal to v_{min}. In this way, the PV inverter can still inject active power. However, this makes that the active power will be less than the maximum possible at that solar irradiance and depends on the P-V curves of the PV array. In this case, for a voltage equal to v_{min} and solar irradiance equal to 1000 W/m^2 the active power that the PV generator can inject is close to zero as v_{min} is close to the open circuit voltage for the given temperature (Fig. 5.11).

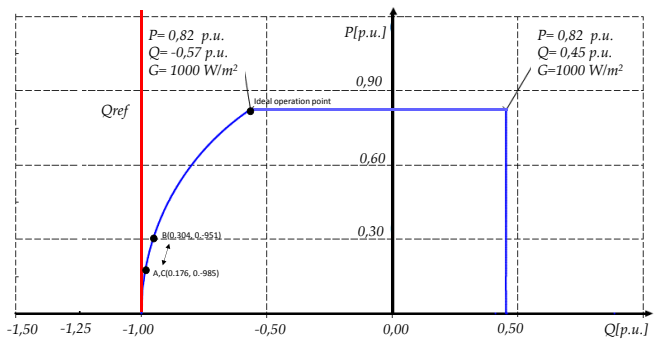

(a)

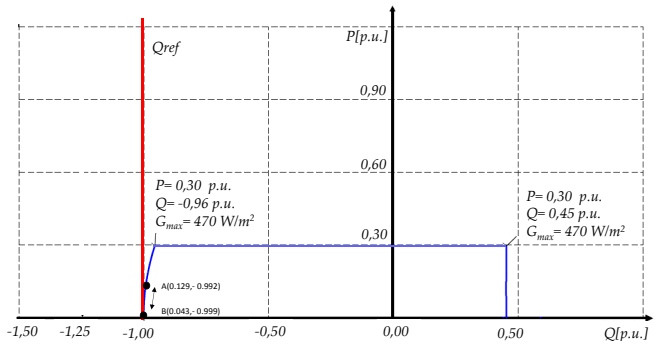

(b)

Figure 5.17: Dynamic area of operation inside the capability curves for Case study A (a) $T_a = 10^oC$, and (b) $T_a = 40^oC$

Reactive power limitation: in any of the study cases, the reference of reactive power is higher than the rated power of the PV generator. This makes that the PV generator works close to the capability curve. In this case, the operation area is in the four quadrants where the PV generator can absorb reactive power and inject active power. In this area, the limitation is given by the PV generator nominal current and depends basically on the variation of active power. As it was discussed before, the variation of active power depends on the solar irradiance, temperature and dc voltage. Thus, the reactive power has to change each time the solar irradiance or temperature changes. It can be seen that despite the quick changes of ambient conditions (for study case A) the PV generator can absorb reactive power around 1 p.u. But for study case B the reactive power can go from 0.75 p.u to 0.99 p.u instantaneously as the solar irradiance decreases.

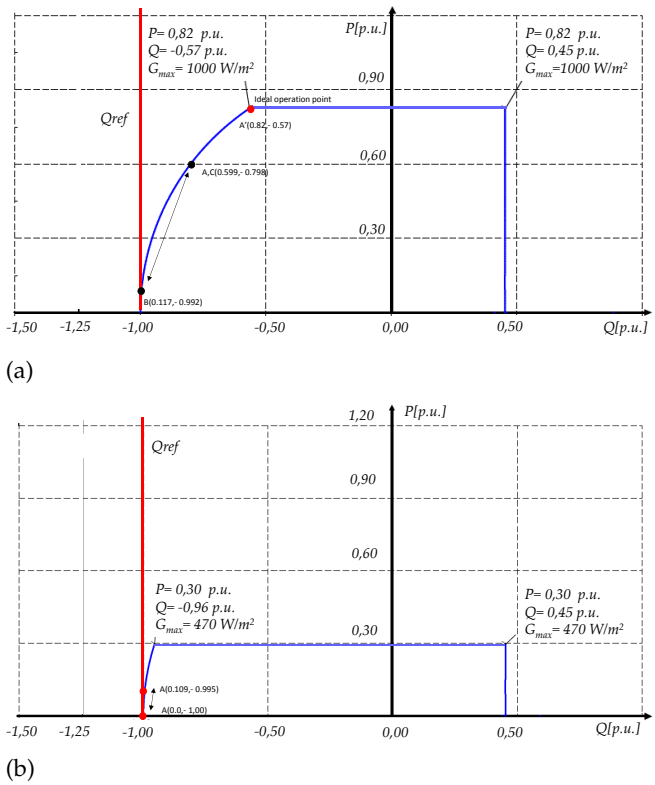

Figure 5.18: Dynamic area of operation inside the capability curves for Case study B (a) T_a = 10°C , and (b) T_a = 40°C

5.7 Conclusions

In the current chapter, the modelling and the control of the PV generator were presented in detail considering the P-V and the PQ curves for the corresponding ambient conditions. Then, the dynamic simulation together with an analysis of the results were presented. According to this study, some conclusions can be drawn.

- When the dc voltage is equal to v_{mpp}, then the ambient conditions play an important role in the active power that the system can deliver and the same occurs with the value of reactive power that the PV generator can absorb or inject. However, due to the dynamic response of the MPPT, the changes of active and reactive power can go smoothly around the capability curves.

- The use of the PQ and the P-V curves helps to develop the control at any ambient condition and to understand the dynamic performance when quick changes of solar irradiance occur. However, it is important to notice that when the solar irradiance is high and changes quickly to a lower value, the reduction of active power occurs instantaneously.

Taking into account this dynamic control that considers the capability curves presented in Chapter 4.3, the management of active and reactive power can be enhanced in order to comply with grid code requirements. Therefore, the next chapter proposes a new control considering the dynamic model, the basic control and the results presented in the current chapter.

Chapter 6

Active and reactive power control of a PV generator for grid code compliance

"I'd put my money on the sun and solar energy. What a source of power! I hope we don't have to wait until oil and coal run out before we tackle that"
Thomas Edison, 1931

The grid codes reviewed in Chapter 3 explains that the LS-PVPPs should provide ancillary services as voltage and frequency regulation as well as a good response under fault conditions. For this reason, the enhancement of the local control of the PV generators is necessary. Thus, the aim of this chapter is to propose a local controller of active and reactive power to comply with the grid codes restrictions. For this purpose, the control considers the capability curves, studied in Chapter 4, which vary due to the change of solar irradiance, temperature, and some electrical characteristics. To validate the control, the PV generator is modelled led in DIgSILENT PowerFactory® and tested under different ambient conditions. The results show that the control developed can manage the active and the reactive power in the desired point at different solar irradiance and temperature[1].

[1]This chapter is based on the following publication:
A. Cabrera-Tobar, E. Bullich-Massagué, M. Aragüés-Peñalba, O. Gomis-Bellmunt, "Topologies for large scale photovoltaic power plants", *Renewable and Sustainable Energy Reviews.*, 59 (2016),pp. 309-309.

6.1 Introduction

PV inverters have been used in small PV systems where ancillary services were not necessary to address. However, with the development of LS-PVPPs the control of active and reactive power during the day has become an issue. Thus, the control of the PV generator should be improved considering the grid codes and the capability curves analized in Chapters3 and 4 respectively.

Commonly, in small PV systems, the control of active power has been developed by tracking the maximum power point (MPPT) and many techniques around this topic have been used as it is explained in [184]. However, in LS-PVPPs this approach is no longer valid due to their new operational requirements. One of the solutions for active power control is the use of energy storage but this causes the increment of cost installations [187]. Much research has been done in this direction, where the main challenge is limiting the active power variations [155, 188, 189, 190, 191, 192]. An alternative solution is the improvement of the control by considering the characteristics of the PV generator. So far, there is limited research in this area and few work has been developed. For instance, Y. Yang et al. [166] explain how a constant power generation can be achieved without using energy storage for a limited part of the day. The control is developed for a two stage inverter (dc-dc and dc-ac) and other grid requirements are not studied. Furthermore, the study presented in [193] explains the control of active power for frequency regulation using a two stage PV inverter (dc-dc and dc-ac). The proposed control varies the duty cycle at the dc-dc converter when a frequency deviation occurs. The same approach has been presented by various authors like [187] and [194]. However, none of them includes the variation of solar irradiance or the capability curves of the PV generator used. For a single stage of inversion, a study has been presented by [195] where the control of active and reactive power is developed by the variation of the dc link voltage reference as well as the modulation index. However, this technique was not applied under variable solar irradiance.

On the other hand, for the reactive power control of PV systems in LS-PVPPs few work has been developed. For instance, Rakibuzzaman et al. [111] explain the control of reactive power and how the capability curve could influence in the response. However, the

variation of ambient conditions is not considered in this approach. Additionally, R. Varma et al. are working on the control of the LS-PVPPs as STATCOM to support the grid when power oscillation occurs [196]. However, in this work, it is considered the remaining inverter capacity and depends on the solar irradiance behavior. From a general point of view without any specific source of energy, new types of reactive power control for grid tied inverters have been presented in [197], [198]. These studies do not take into account the variation of solar irradiance during the day or the corresponding capability curves of the PV generator. In the case of wind power plants, the control of active and reactive power has been developed in previous years. For instance, the study developed by R. Almeida et. al [199] proposes an optimized control strategy to manage the active and reactive power by a wind generator. This strategy combines the pitch control and the inverter's control to manage the rotor's speed for the required point of operation.

It is worth to point out that the control of active and reactive power in a LS-PVPP has not commonly been developed considering the capability curves of the PV generator or the combined performance limitations between the PV inverter and the PV array Fig.6.1. As it is explained in Chapter 4, these curves are characterized by four main parameters: solar irradiance, temperature, dc voltage, and the modulation index. In the case where the dc voltage is equal to a single value, the active power and the reactive power will depend mainly on the solar irradiance, temperature and modulation index. But in the case the dc voltage is variable, the complete curve can be obtained for a single solar irradiance and temperature. Thus, an improved control of active and reactive power for grid code compliance can be developed.

The aim of this chapter is to propose a new control of active and reactive power for a PV generator considering the corresponding capability curves and the grid code requirements. For active power, two main targets are accomplished: (i) Power curtailment, and (ii) Power reserves, by using an adaptation of the MPPT. For the reactive power control, two considerations are addressed: (i) preference of active over reactive power and (ii) preference of reactive over active power. Then, the control is validated by a simulation of a LS-PVPP modeled in DIgSILENT PowerFactory® under different ambient conditions. Finally, the results and the discussion are presented together with

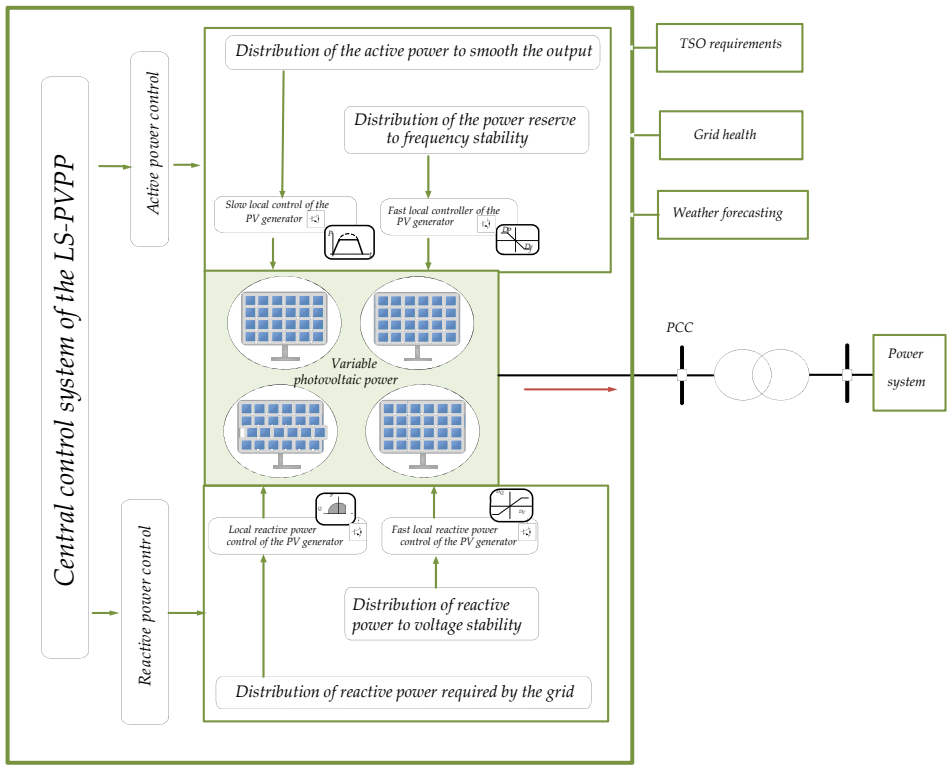

Figure 6.1: Conceptual diagram of the scope of this chapter

the conclusions.

6.2 Control of a LS-PVPP

The control of the LS-PVPP permits its integration to the electrical system considering the requirements given by the grid codes, consequently, these type of power plants can participate in ancillary services. The challenges that LS-PVPPs have to overcome were discussed in section 3.3, and in summary, it can be stated that the main objectives of the control for the LS-PVPP are the control of active and reactive power to manage voltage and to be part of primary and secondary frequency control.

To address these objectives, a hierarchical control architecture is considered, as it is illustrated in (Fig. 6.2), where the first stage is the electrical system operator who sends the requirements, then the second stage is the power plant control and the third stage is the PV generator. The control of the LS-PVPP is focused on the reference calculation of active and reactive power according to the transmission system operator [192, 151]. It is also responsible to apply grid support actions, for example in case of disturbances. In this control, a PI is added to reduce the error between the reference and the power available in the grid. The total active or reactive power calculated by the controller is divided by the total number of PV generators in the LS-PVPP and this is the reference value under which the PV generators should respond (Fig. 6.3 and 6.4) [151],[200].

After these references are calculated, the PV generator develops its corresponding control according to grid code requirements and the behaviour of the internal grid to keep ac voltage and frequency constant. A general control structure of a PV generator is illustrated in Fig. 6.5, where three main blocks can be seen: active and reactive power controller, and inverter control. The task that the active and the reactive power controller has is to deliver the power demanded by the power plant controller. This control should consider the variation of ambient conditions and the PQ capability curves of the PV generator analysed in Chapter 4and Chapter 5. Meanwhile, the inverter control is in charge of grid synchronisation, voltage modulation, dc voltage regulation and the current loop as it was explained

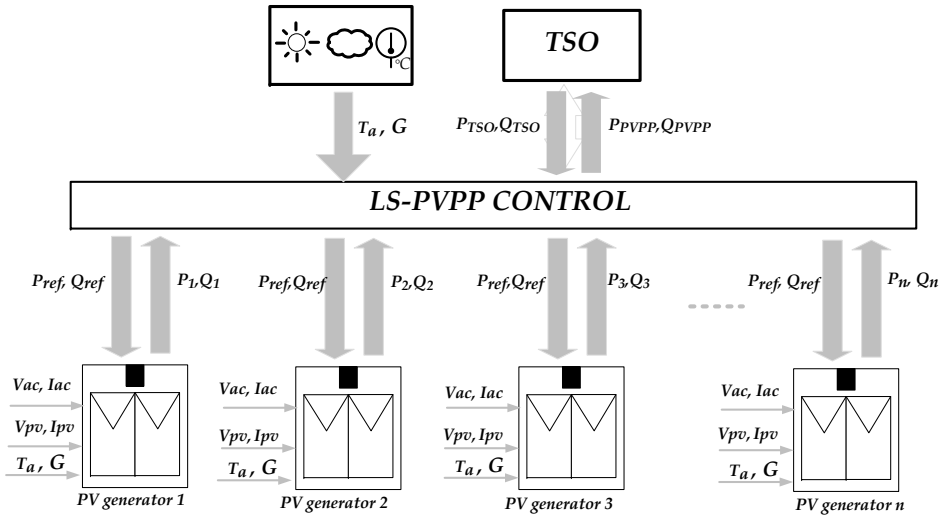

Figure 6.2: Proposed control architecture for a LS-PVPP

in Chapter 5. The detail block diagram of the PV generator control is presented in Fig. 5.3.

The control of active and reactive power in a PV generator for LS-PVPPs is explained in the following sections.

6.3 Active power control

According to the grid codes reviewed in Chapter 3, the active power management for LS-PVPPs should consider: power curtailment, ramp rate control and active power reserves. In this section, the active power control of a PV generator is explained in detail with emphasis on power curtailment and active power reserves.

6.3.1 Power curtailment

In section 5.3, the dynamic control of the PV generator was explained in detail. However, in that control, it was assumed that the PV generator was working at the MPP. So the active power control depends on the solar irradiance, temperature, and the dc voltage. However, to have an active power management less dependent on the ambient

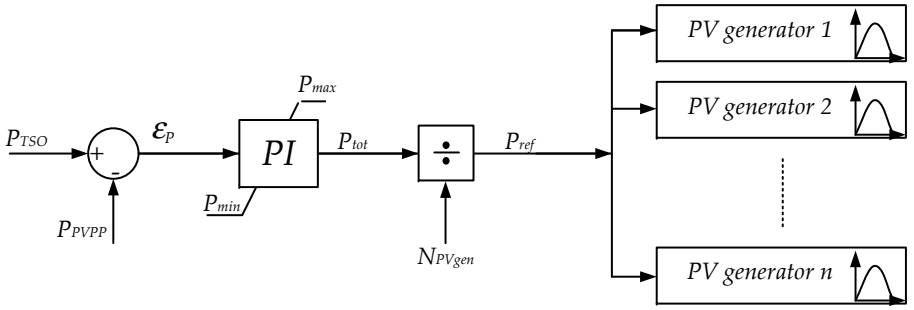

Figure 6.3: Active power plant control

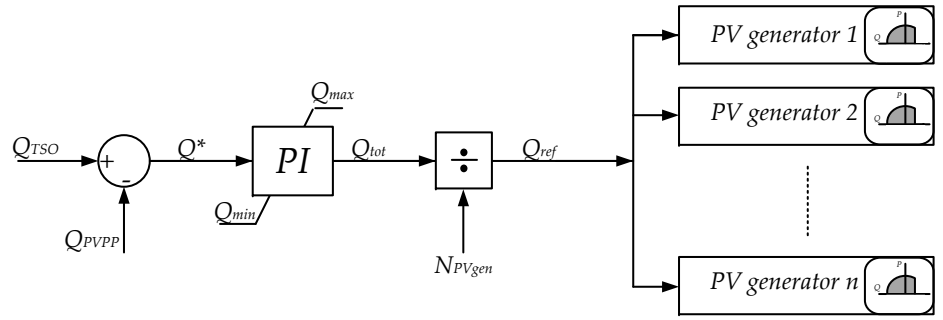

Figure 6.4: Reactive power plant control

conditions and to comply with the grid codes, this control should be changed.

In the present chapter, to address this power curtailment, the PV generator cannot be working at MPPT. Instead, the control has to work close to the reference of active power (P_{ref}) set by the PPC. Thus, a reference power point tracker is used (RPPT), which aim is to look for the P_{ref} at each instant. For that purpose, any algorithm used for MPPT can also be used in RPPT but the target point is what changes. In this case, as P&O is used, the dc voltage is changed by steps (Δv) until the active power supplied by the PV array is the same as the power reference. Each time the solar irradiance changes, the algorithm should only decide if the dc voltage reference should increase or decrease its value (Fig. 6.6(a)). However, as the solar irradiance changes, the reference of active power could be higher than the max-

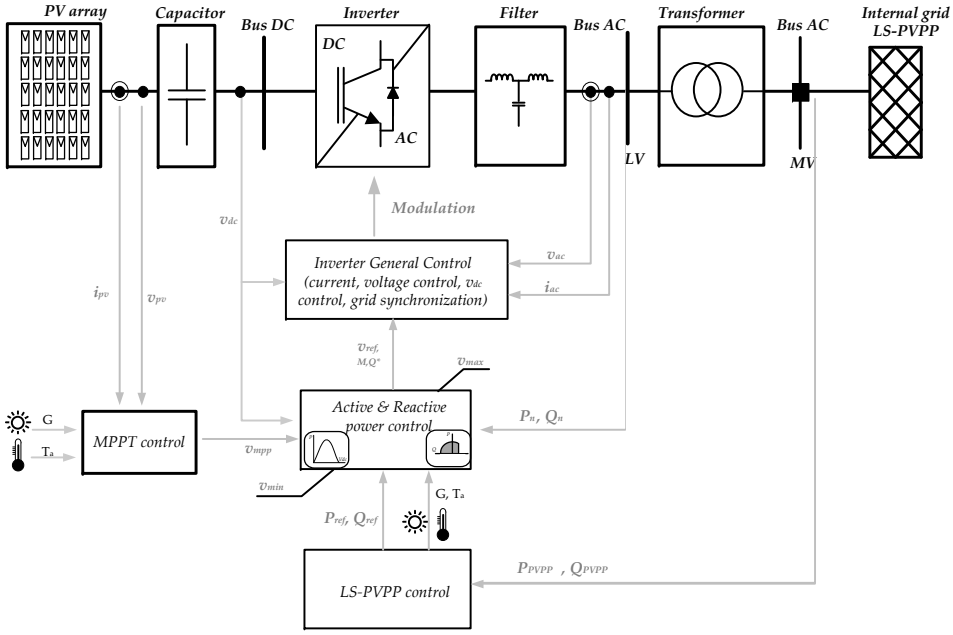

Figure 6.5: General control structure of a three phase grid connected PV generator in a LS-PVPP.

imum possible power that the PV generator can supply. In this case, the algorithm starts to work as a normal MPPT (Fig.6.6(b)).

Considering this approach and the curve of active power versus irradiance (PG curve), two operation zones can be distinguished: (I) MPPT control, (II) RPPT control. On this curve, three main points are considered: cut in, cut out, and nominal solar irradiance (Fig. 6.7). When the value of solar irradiance is too low (less than 50 W/m^2), the PV generator cannot work properly as the dc voltage could be lower than the v_{min}. The solar irradiance at which the PV generator firsts starts to generate power is named as "cut-in solar irradiance". As the solar irradiance increases, the PV generator starts to work with the MPPT control, when the power reference is fulfilled, the point of solar irradiance is the one named as "cut-out solar irradiance". After this point, the RPPT control is used in order to keep the reference power. However as the solar irradiance increases, the cell temperature as well, then the dc voltage could be again out of the dc voltage limitation and the power generated by the PV generator will not reach the reference. This point is called, the nominal solar

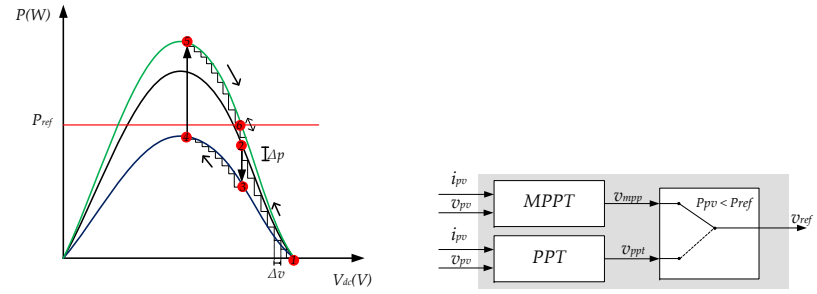

Figure 6.6: Power curtailment control: (a) RPPT operation in a PV generator, (b) logic between MPPT and RPPT

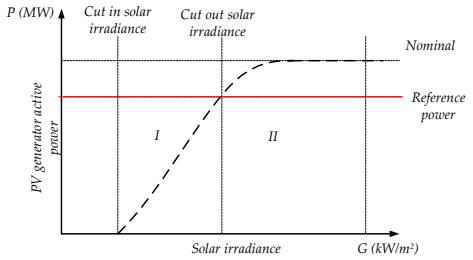

Figure 6.7: Control areas of a PV generator in a PG curve when a reference is given

irradiance and another active power reference should be calculated.

6.3.2 Active power reserves

The fluctuation of solar irradiance during the day together with the cloud coverage may cause fluctuation of frequency due to the variation of the generated active power. This situation could happen in a scenario where the most of the generation comes from renewable energy. This problem can be seen especially in countries or islands that are not connected with the continent generation. Thus, the grid codes from these countries requires that the power plants have power reserves in order to give a response of active power for primary and secondary frequency control [2].

[2]Primary frequency control takes place in the period of up to 30 s after a frequency deviation occurs and secondary frequency control takes place between 5 seconds to 10

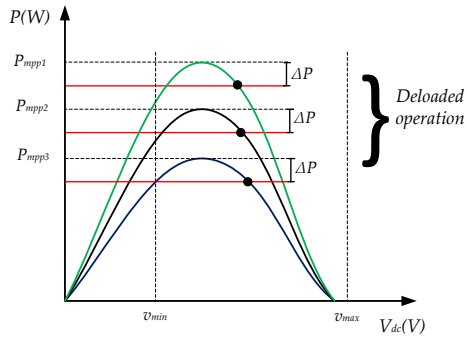

Figure 6.8: Deloading operation in PV generators

To have this type of response, it is necessary that the PV generator does not supply the maximum power and instead it should work in a suboptimal operating point according to grid characteristics. The power reserve could be from 10 % to 20 % of the power plant capacity (deloaded operation) [125] (Fig.6.8).

To control the PV generator for active power reserves, it is necessary to calculate at each time step the possible maximum active power that the PV generator can supply. Then, the reference power should be given by the percentage required by the TSO of the maximum possible active power (eq. (6.1) and eq.(6.2)). With this new reference, the RPPT control explained in Section 6.3.1 can be applied.

$$P_{reserve} = \Delta P_{tso} * P_{dc_{mpp}}(G, T_a) \tag{6.1}$$

$$P_{ref} = P_{dc_{mpp}}(G, T_a) - P_{reserve} \tag{6.2}$$

After the active control has been addressed, the reactive power control is explained in the following section.

6.4 Reactive power control

Taking into account the grid code requirements studied in Chapter 3, it is necessary that LS-PVPPs could supply or absorb reactive power

minutes [122]

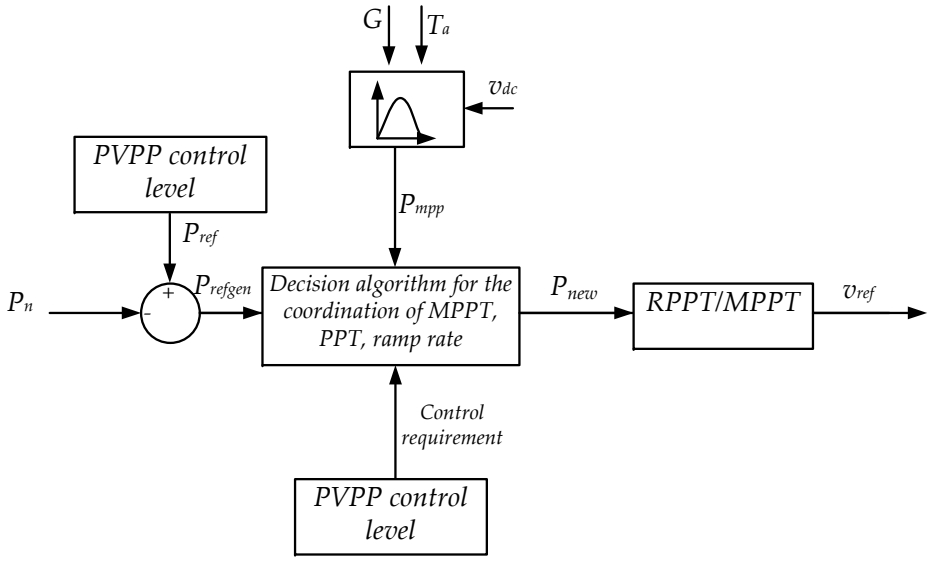

Figure 6.9: Control scheme for control of active power in PV generators

due to voltage disturbance or grid requirements. As it was explained in Section 6.2, the central control of the PVPP is the one who calculates the reference of reactive power. Then, the PV generator has to reach this value.

However, due to the limitations and the capability curves (see Chapter 4) could not be feasible to supply or absorb reactive power at a given reference. Hence, the possible reactive power that the PV generator can supply or absorb depends mainly on the active power that varies with solar irradiance, temperature, dc voltage, and modulation index (see Fig. 4.13 to 4.15). If the reference of reactive power is small (less than 0.4 p.u), the PV generator could reach this value for almost any solar irradiance or temperature, except for higher solar irradiance (Fig. 6.10). Meanwhile, for higher values then it could not be possible to provide the reactive power for almost any solar irradiance (Fig. 6.11).

The grid codes, however, require that the PV generator could inject or absorb reactive power according to the Fig.3.4, and in the case of voltage disturbance it is necessary to respond according to Fig. 3.7. In case of disturbance the amount of reactive power that the PV generator should be capable to provide, should not depend on the

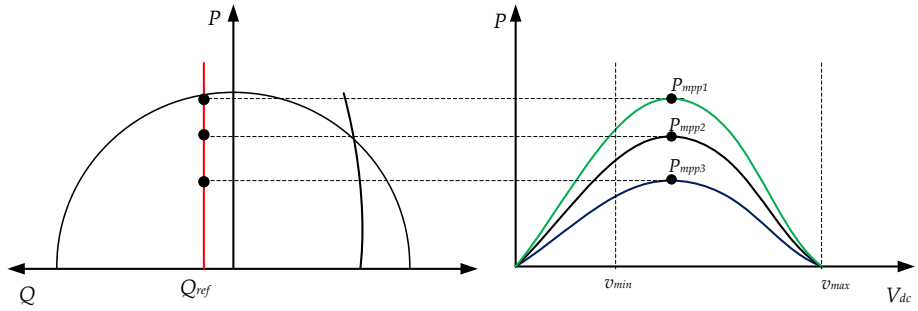

Figure 6.10: Low reference of reactive power

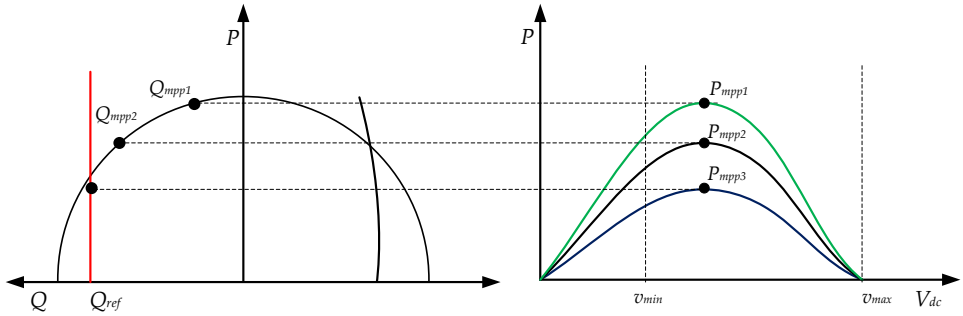

Figure 6.11: High reference of reactive power

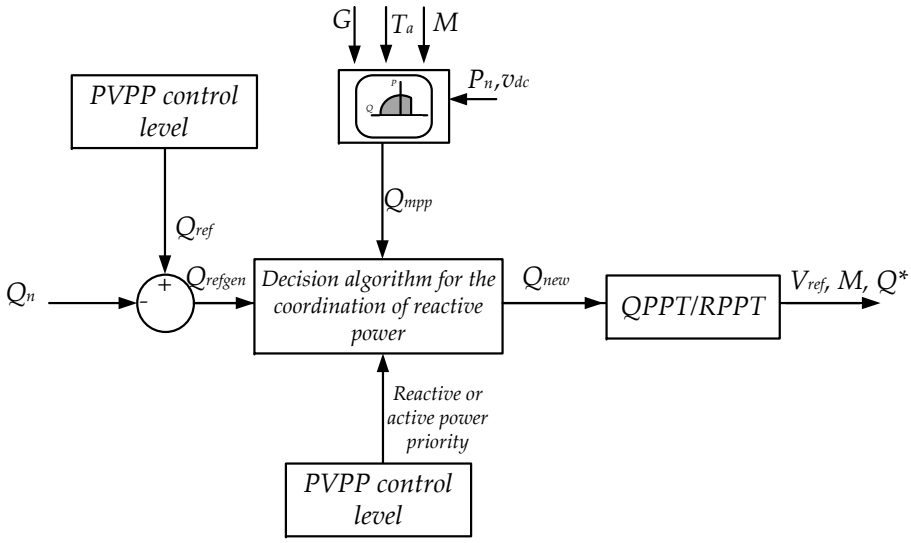

Figure 6.12: Control scheme for control of reactive power in PV generators

solar irradiance and temperature at that instant.

Thus, this section presents a novel control to address this issue in order to provide reactive power despite the ambient conditions when the reactive power control is set as a priority (Fig. 6.12). This control reads the reference of reactive power given by the plant operator, then if the reactive power control is not a priority the control is developed as it was explained in Section 5.3 with a conventional reactive power regulation. But if the reactive power is set as a priority, then the PV generator has to calculate the maximum reactive power (Q_{mpp}) that the PV generator can supply in that moment. If the reference is lower than this value, the normal control of reactive power can be applied (Fig.5.8 (Chapter 5))

However, if the reference of reactive power is higher than the Q_{mpp} , then the active power should be reduced according to equation 6.3 or 6.4 depending if it is absorbing or injecting reactive power respectively. The new reference of active power is reached by RPPT control.

$$P_{ref} = \sqrt{S^2 - Q_{ref}^2} \tag{6.3}$$

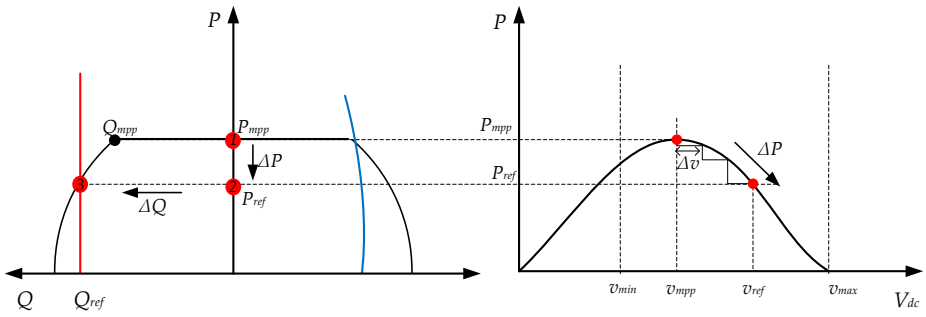

Figure 6.13: Reactive power control for one solar irradiance

$$P_{ref}^2 + \left(Q_{ref} + \frac{3.V_{grid}^2}{X}\right)^2 = \left(3.\frac{V_{grid} \cdot V_{conv}}{X}\right)^2 \tag{6.4}$$

It is important to notice that each time the solar irradiance changes, the generated active power varies depending on the dc voltage value. The RPPT control should again track the reference of active power calculated due to reactive power reference. This behavior is illustrated in Fig. 6.13, where the first point is for a given solar irradiance (A). At this point, the active power that the PV generator can supply is P_{MPPT} in the case any curtailment or power reserve is activated. In this instant, a reference of reactive power is given to the generator's control. However, with this power, the Q_{MPPT} is lower than the reference. Thus a new reference of active power is calculated (P_{ref1}). To achieve this point the dc voltage has to change from v_{mpp} to v_{ref} and the PV generator starts to work at point B. Then the generator can supply the value of reactive power equal to the reference (point 3). In the case the solar irradiance changes a new PV curve is generated (blue line), because of the dc voltage value, the new active power is P_2 and the PV generator starts to work in point C (PV curve) and 4 (PQ curve). As the RPPT control has to follow the reference of reactive power, then the dc voltage reduces to reach the reference (Point D and point 3). Thus, this new control is called reactive power point tracker (QPPT).

In the following section, a study case is presented to implement this new control of reactive for different scenarios.

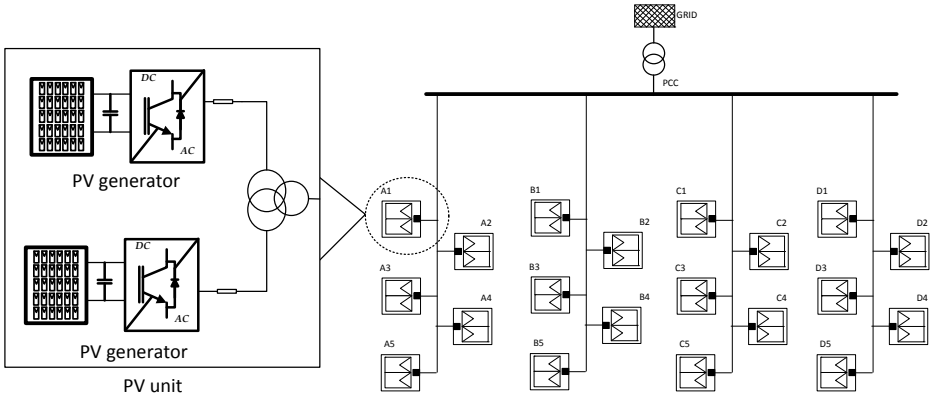

Figure 6.14: PVPP diagram under study

6.5 Case study

A LS-PVPP of 24 MW is designed and modelled in DIgSILENT PowerFactory® and has the configuration presented in Fig. 6.14. For the present study, the results for a single PV generator is presented and its main characteristics are summarized in Table A.1. The design of this power plant was developed according to the solar irradiance and temperature data are taken from Urcuqui-Ecuador in 2014. Besides, the inverter has been oversized 20 % of the maximum active power capacity of the PV array. Each PV generator has a nominal power capacity of 0.6 MVA.

Two cases studies are considered: (i) testing the active power control (case study A) and (ii) testing the reactive power control (case study B). For each type of control, the PPC is the one that sends the references of active or reactive power to the local controller. For these tests, three days are chosen with different solar irradiance and an ambient temperature around 10°C to 25°C.

6.5.1 Case study A

For this case study, three different active power values are set as references during the day:

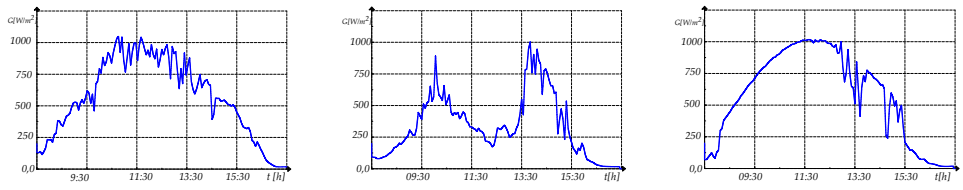

Figure 6.15: Solar irradiance data (a) Day 1 (b) Day 2, and (c) Day 3

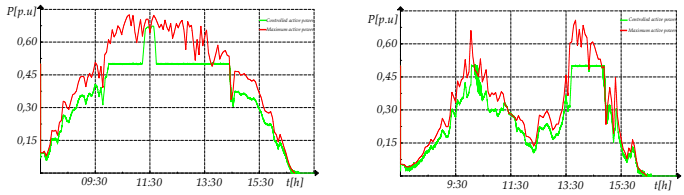

Figure 6.16: Control of active power for different power references. (a) Day one, (b) Day two

- Set a power reserve of 20 % of the maximum power capacity from 6:00 to 10:00 and from 15:00 to 18:00.
- Set a power curtailment of 50 % of the maximum capacity from 10:00 to 15:00.
- Deactivate the power curtailment to reach the maximum power point during 10 minutes (11:25 to 11:35).

The test is developed for day one and two, and the results are illustrated in Fig. 6.16. For any of the days tested, it can be seen that the control of active power makes possible to keep the power reserve equal to 20 % of the maximum power capacity for an active power higher than 0.20 p.u. When the generated active power is lower than 0.2 p.u, the power reserve is not reached and instead is equal to the maximum possible.

However, in the case of power curtailment, there are some differences between the first and the second day. On day 1, the active power reference is reached easily with the control due to the sufficient solar irradiance. On day 2, however, the new reference of power is only reached during ten minutes in the morning and 80 minutes in the afternoon. This behavior is due to the drastic changes in solar irradiance during the day.

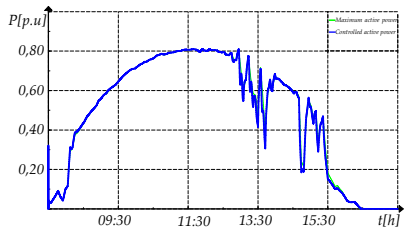

Figure 6.17: Active power response for day 3 considering MPPT

The deactivation of the power curtailment in order to get the maximum power during 10 minutes is successful on day 1 and day 2. It is important to notice that due to the MPPT control, the ramp rate to get the maximum power is 0.05 MW/min on day 1 and 0.026 MW/min on day 2.

6.5.2 Case study B

In this case study, the reactive power control is tested considering the solar irradiance of day 3. To understand the performance of this control, some tests are developed: (a) active power priority and (b) reactive power priority.

Active power priority

When the priority is given to the active power, the MPPT control is used. The total active power supplied by the PV generator is illustrated in Fig. 6.17. Considering the variation of solar irradiance and temperature during the day, the maximum reactive power that the PV generator can absorb is illustrated in Fig.6.18 together with the operational area. It can be seen, that the maximum reactive power that the PV generator can absorb is variable in the time. For instance, from 10:00 to 12:00, the minimum reactive power absorbed is close to 0.6 p.u. From 12:00 to 14:00, there are important solar irradiance variations which produce quick changes of active and reactive power.

In the case that a reference of reactive power is required (Q_{ref} = –0.8p.u) by the PV generator and the MPPT is still used, the response of it is illustrated in Fig. 6.19 together with the operational

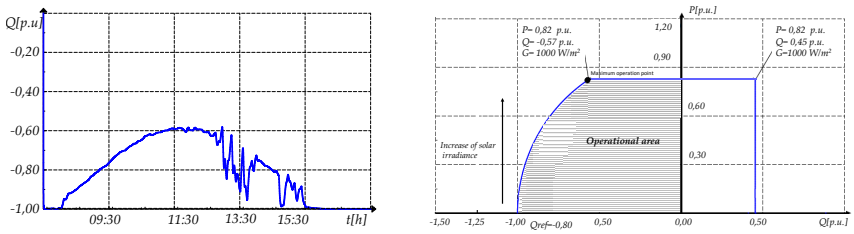

(a) (b)

Figure 6.18: Absorbed reactive power when MPPT is considered (a) Maximum possible reactive power and (b) Operational area

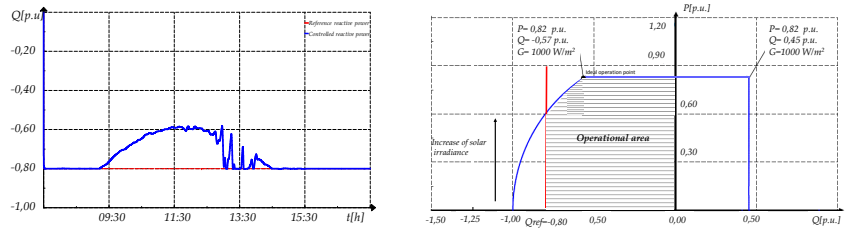

(a) (b)

Figure 6.19: Absorbed reactive power when a reference of reactive power is considered (a) Response of reactive power (b) Operational area

area. With these conditions, the PV generator can follow the reactive power reference between some hours (06:00 to 08:00 and 15:00 to 18:00). However, when the active power exceeds a certain value, the PV generator cannot follow the reference of reactive power.

For a Q_{ref} = 0.8p.u, the PV generator can inject the reactive power depending on the voltage limitation and the modulation index. A modulation index of 1 and 1.75 is tested and illustrated in Fig. 6.20 and Fig. 6.21 respectively together with their operation area. When the modulation index is 1, the reactive power is equal to 0.45 p.u for any solar irradiance. Meanwhile, when the modulation index is 1.75, the reference of reactive power is reached from 07:00 to 10:00 and from 13:30 to 18:00. However, from 10:00 to 13:00, the reference of reactive power is not reached. Instead, the maximum possible reactive power is injected, which depends on the solar irradiance. The curve that limits its behaviour from 10:00 to 13:00 is the current curve, for the rest of the day it is the voltage curve.

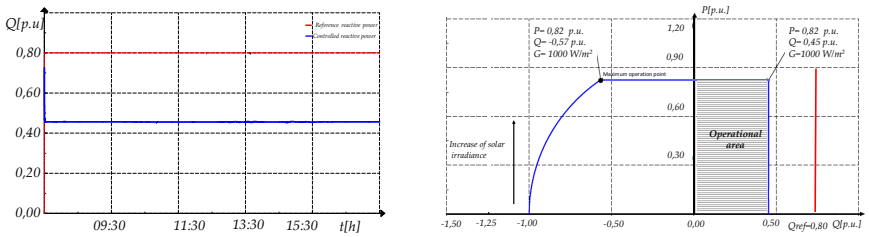

(a) (b)

Figure 6.20: Injected reactive power with MPPT control and M = 1 (a) Response of reactive power and (b) Operational area

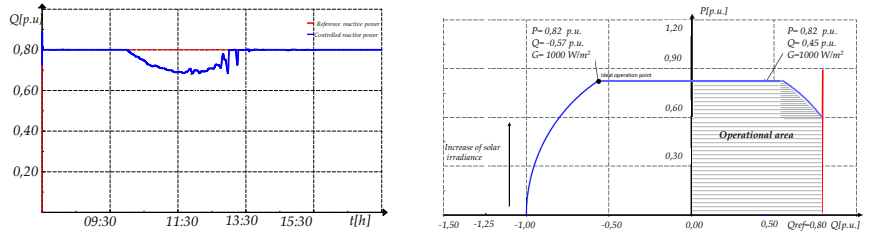

(a) (b)

Figure 6.21: Injected reactive power with MPPT control and M = 1.75 (a) Response of reactive power and (b) Operational area

Reactive power priority

To test this control, two references of reactive power are simulated: (i) Q_{ref} = –0.8p.u and (ii) Q_{ref} = 0.8p.u. For the first reference (absorption of reactive power), the results of active and reactive power are illustrated in Fig. 6.22 with the corresponding capability curve. Due to the reactive power priority, the PV generator absorbs a value of reactive power equal to its reference almost all the time. Due to the changes in irradiance and the response time of the control, there are specific times where there is an error around 0.05 p.u. In order to have this reference of reactive power, the active power is limited to 0.6 p.u between the hours 08:00 to 13:00.

For the second reference (injection of reactive power), two different modulation index are tested: (i) M = 1 and (ii) M = 1.75. The results are shown in Fig. 6.23 and Fig. 6.24 respectively with the corresponding operational area. When M = 1, the reactive power cannot reach the reference of reactive power and stays at the maximum value (0.45

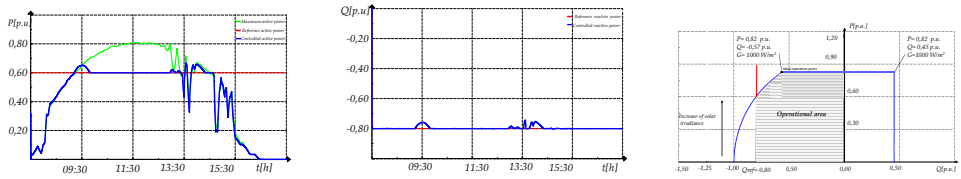

(a) (b) (c)

Figure 6.22: QPPT response when a reactive power reference is applied (a) Active power, (b) Reactive power, and (c) Operational area

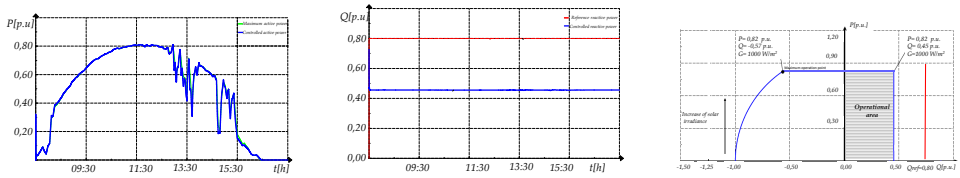

(a) (b) (c)

Figure 6.23: Power response with QPPC for M = 1 (a) Active power and (b) Reactive power , and (c) Operational area

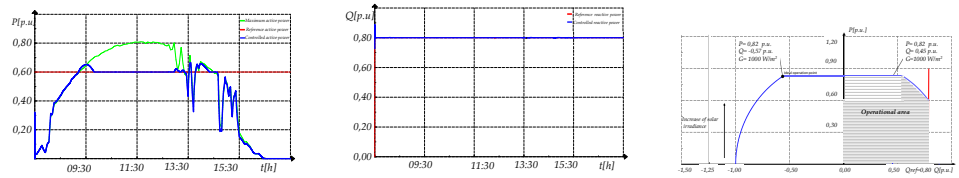

(a) (b) (c)

Figure 6.24: Power response with QPPC for M = 1.75 (a) Active power and (b) Reactive power, and (c) Operational area

p.u). In the case M = 1.75, the PV generator injects a reactive power equal to the reference during all the time by the reduction of active power from 09:00 to 13:30.

6.6 Discussion

From the controller presented in this chapter and from the obtained results, some important issues are necessary to be addressed:

6.6.1 Active power control

The control of active power in a suboptimal point (lower than the MPP) can be developed with an RPPT control. The PV generator can supply power according to an active power reference. The response, however, depends as well on the solar irradiance fluctuations during the day. For instance, on the second day, between 14:00 to 15:00 quick solar irradiance variations are presented and the control tries to respect the 20 % of power reserve but the control does not follow this reference.

The ramp rate due to the MPPT control to reach the maximum power from a given reference is variable depending on the solar irradiance. Two different ramp rates were reached during the two days one close to 0.05 MW/min and the other close to 0.026 MW/min. The first one was obtained due to a variation of active power of 0.146 p.u and 0.0658 p.u for the second one. The difference between them is the maximum active power reached that depends on the solar irradiance variation at that moment. In the first case, the value of solar irradiance for that instant is around 900 W/m^2 and in the second case is around 270 W/m^2.

6.6.2 Reactive power control

For the injection or absorption of reactive power, the response also depends on the solar irradiance when the active power generation is a priority. It can be stated that with a maximum active power, there will be a maximum reactive power that can be injected or absorbed depending on the capability curves. Because of this, if a reference of reactive power is set and at the same time the active power control is a priority, the reference will be reached only if it is lower than the maximum reactive power point possible at that instant. In the case that the reactive power is a priority and there is high solar irradiance, the reference of reactive power can be reached only if the active power point changes to another point of operation lower than the MPP.

It is important to notice that for injection of reactive power, the variation of this value does not present large fluctuation as it depends on the changes of dc voltage together with the modulation index. If the maximum modulation remains fixed, then the reactive power that

the PV generator can inject also remains close to a fixed value. However, this value could be lower than the reference set by the control. Therefore, a change of modulation index helps to fulfil the reference of reactive power demanded by the PPC.

6.6.3 Compliance of grid codes

Considering the grid code requirements regarding the management of active power, it can be stated that working with RPPT for a given reference helps to comply with the basic requirements as power reserves and power curtailment without the addition of energy storage at variable solar irradiance. It can be seen that for quick solar irradiance variations as the ones presented on day 2, the power curtailment helps to reduce the variability of power generated that can affect the grid performance.

Regarding the reactive power, the PV generator has to follow the reference sent by the PPC. However, due to the limitations and the PV generators capability curves, it could not be feasible to inject or absorb reactive power at a given reference [201] when the generation of active power is a priority. For absorption of reactive power, if the reference of reactive power is smaller than 0.57 p.u (corresponding to G = 1000W/m^2), then the PV generator can absorb this reactive power reference at any solar irradiance during the day. However, if the reactive power reference is higher than 0.57 p.u then the PV generator cannot absorb this reference of reactive power at different solar irradiance. In the case of injection of reactive power, the maximum possible reactive power is equal to 0.45 p.u. Thus, the PV generator cannot inject higher reactive power.

When the QPPT is applied, then the results show that the PV generator can reach the reference given. For absorption of reactive power, if the reference is higher than 0.57 p.u then the PV generator can absorb this reactive power by changing the maximum active power generated to 0.6 p.u. Though, this means that there is 20 % of active power losses between 09:30 to 13:00 (Fig. 6.22). For injection of reactive power, the reference of reactive power only can be reached by the increment of the modulation index to 1.75 p.u that can cause the injection of higher harmonics to the grid. For higher solar irradiance (800 to 1000 W/m^2), the power generated has to be limited to 0.6 p.u by the variation of the dc voltage.

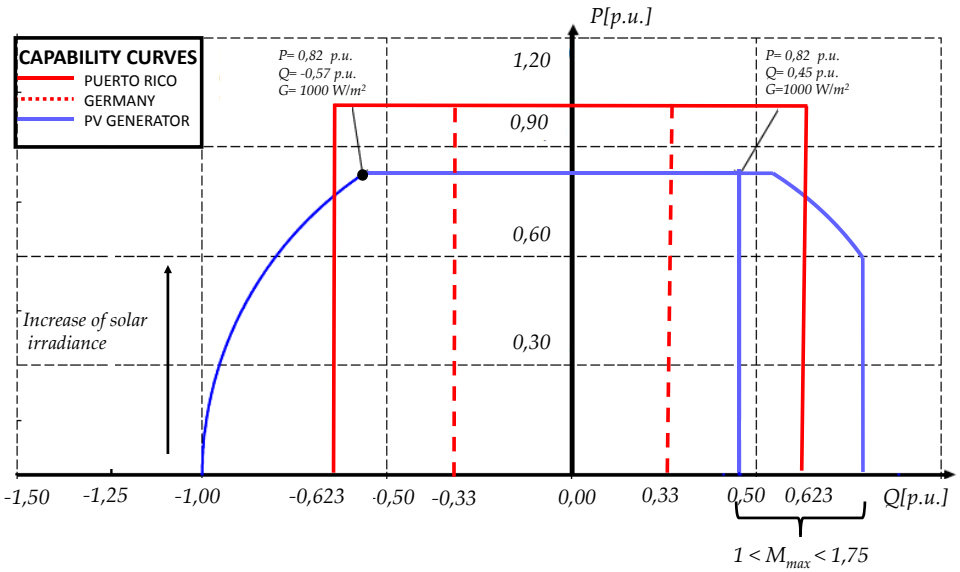

Figure 6.25: Capability curves comparison considering the grid codes of Puerto Rico, Germany and the capability curve extracted from the current study case

Considering the response of the PV generator for the different scenarios for reactive power, it can be analysed if the requirements of the grid codes can be achieved under different scenarios. Fig. 6.25 illustrates the capability curve given by the PV generator together with the capability curve required by Puerto Rico and Germany for steady state conditions. When QPPT is utilized, the PV generator can inject or absorb reactive power according to the requirements but the active power generated could be lower than the P_{mpp}. For absorbed reactive power, if the reference is 0.623 p.u, then the new reference of active power should be 0.78 p.u. For the injection of reactive power, the modulation index has to be higher than 1 to comply with this reference.

However, when the reactive power is not set as a priority then the requirements asked by the grid code of Puerto Rico cannot be fulfilled for higher solar irradiance and maximum modulation index of 1. So, new equipment should be installed in order to give reactive power support as STATCOM, capacitor banks, FACTS. However, for the case of Germany, at any irradiance the PV generator can supply or inject the reference of reactive power as it is lower than 0.57 p.u

without making any change in the operation of active power or the modulation index.

Additionally, it can be seen that for an active power generated lower than 0.78 p.u (corresponding to G = 900W/m^2), the PV generator can absorb or inject reactive power higher than the limitations imposed by the grid codes without reducing the generated active power. Thus, it is necessary that the Grid codes will consider the effect of the PV generator performance at different solar irradiance, temperature, dc voltage and modulation index in order to set higher limitations and improve the performance of the LS-PVPP.

6.7 Conclusions

This chapter has presented the control of active and reactive power for a PV generator considering its capability curves variation applied in a large scale photovoltaic power plant. For this purpose, the current chapter has presented the general configuration and control structure used commonly in a LS-PVPP. Then the active power control for a PV generator has been presented considering active power curtailment and active power reserves. Additionally, the control of reactive power was also studied under two different considerations: active power priority or reactive power priority taking into account the corresponding capability curves. Finally, a simulation of the control proposed was conducted in DIgSILENT PowerFactory ® where the complete model has been introduced and simulated under different conditions. From the control developed and the simulations, some conclusions are discussed.

- The quick variation of solar irradiance affects not only to the active power response but also to the reactive power. When the solar irradiance is high, then the reactive power capability is reduced. Besides, this could disrupt the plant with quick variations of reactive power, this can be diminished with an appropriate control of the reactive power.
- The ambient temperature also affects the total reactive power that the LS-PVPP can provide at the point of common coupling (PCC). When the ambient temperature is higher than (25^{o}C), then the reactive power is increased especially when the reactive power is supplied by the PV generator.

- The modulation index and the dc voltage value play an important role on the point of operation of the PV generator when reactive power is injected. For an appropriate control, the maximum modulation index can vary between 1 to 1.75 to comply with grid code requirements.
- The capability curves play an important role in the control of the PV generator when active and reactive power control are considered. These curves should be taken into account for each solar irradiance, ambient temperature, dc voltage and modulation index. The reactive power reference can be achieved by the consideration of these capability curves together with the control.
- Considering the grid code requirements regarding the management of active power, it can be stated that working with RPPT for a given reference helps to comply with the basic requirements as power reserves and power curtailment. However, a deeper study on ramp rate control must be developed considering variable solar irradiance. In the case of reactive power, grid codes should also consider the behaviour of the PV generator according to ambient conditions in order to set the limitations.

The general control of the PV inverter depends as well on the measured variables as the phase angle and the frequency. The variation of solar irradiance affects directly to the measurements of these variables. Thus, the next chapter will study the improvement of the PLL to have an accurate phase angle and frequency.

Part IV

Future research outcomes and Conclusions

Chapter 7

Conclusions

" I think the future for solar energy is bright"
Ken Salazar

The thesis' main objective was to study to what extent a PV generator can be controlled to comply with the plant operator's requirements considering the capability curves under variable solar irradiance and temperature. Hence, four main challenges were identified and addressed thorough out this thesis.

Chapter 2 examined the available technology to construct a LS-PVPP, as well as what is the most used internal configuration and ac collection grid to accomplish such aim. As LS-PVPPs have to interact with the electrical grid, several grid codes have been adapted to permit their integration in a smooth way. A deep comparison and analysis of the grid codes of Germany, Romania, China, South Africa and Puerto Rico was presented in Chapter 3. Additionally, the chapter discussed the challenges that LS-PVPPs have to face to accomplish these grid codes as well as the necessary technology to do it.

As the basic unit of a LS-PVPP is the PV generator, Chapter 4 presented its capability curves considering variables as the solar irradiance, ambient temperature, dc voltage and the modulation index. The chapter has shown in detail the static model used, the mathematical analysis and the simulations to validate the study. In Chapter 5, a dynamic model of the PV generator was developed to study the dynamic performance of each of the components. The model was developed considering the effect of solar irradiance, ambient temperature and dc voltage on the dc power as well as the behaviour of the PV inverter. Additionally, this chapter presented the dynamic control used where the capability curves were included.

Using the dynamic model and control developed in Chapter 5, a complete control for the active and reactive power in order to comply with grid code requirements is explained in Chapter 6. In the case of active power: power curtailment, ramp-rate control, and power reserve were explained in detail. In the case of reactive power, two types of control were considered: preference of Q over P, preference of P over Q.

This chapter presents the thesis final conclusions and recommendations for future research.

7.1 Final Conclusions

The thesis final conclusions, based on the objectives presented in Chapter 1, are classified according to the four challenges: system integration, technical limitations , dynamic modelling, and dynamic control.

7.1.1 System Integration

Based on the performed literature review for LS-PVPP, the common PV generator configuration is the central one that has a PV array interconnected to a single stage PV inverter through a dc capacitor and then it is connected to a transformer to step up the voltage. This configuration shows low levels of reliability, flexibility, and MPPT efficiency. The mismatching losses due to the PV array configuration are higher than in other configurations. However, its robustness, easier control, and installations' lower cost are the main characteristics that make this configuration the preferred one. However, another configuration which is interesting to study is the multistring topology. This has been used in fewer LS-PVPPs but this topology could be more used in the future. Regarding the ac collection grid, the state of the art shows that radial configuration is the most used as it has the lowest cable cost.

Additionally, the system integration can be performed due to the grid codes. In Chapter 3, a comparison between the grid codes of Germany, Puerto Rico, Romania, China and South Africa was developed. In this comparison it could be seen that the trend of these grid

codes is to ask ancillary services to the LS-PVPPs with a similar behaviour as conventional power plants. From this comparison, it can be stated that Puerto Rico has so far the most strict requirements regarding voltage and frequency regulation, active and reactive power control and also system disturbance response.

For the system integration, the knowledge of the PV generator operation is essential in order to develop an adequate control for the LS-PVPP and at the same time comply with the grid code requirements. In this thesis, the focus was to enhance the knowledge of the PV generator considering its limitations, and control when solar radiance varies for different values of ambient temperatures as it was presented in Chapter 4 and Chapter 6.

The addition of equipment as energy storage, STATCOMs or FACTs could be necessary in order to comply with the grid code requirements presented in Chapter 3. However, the improvement of the PV generator's control presented in Chapter 6 showed that the grid codes could be accomplished without the use of extra equipment. This is true for grid codes of Germany, South Africa, China but not Puerto Rico as it requires higher values of reactive power.

7.1.2 Technical limitations & Capability curves

The PV generator -PV array, inverter, and transformer- is the basic unit of the entire LS-PVPP. An adequate analysis regarding its limitation considering as a single unit was presented in Chapter 4.

To develop the technical limitations and capability curves, the understanding of the PV generator performance regarding the solar irradiance, ambient temperature, power and dc voltage was necessary. On this premise, it is important to notice that the active power of the PV array depends not only on the ambient conditions but also on the dc voltage.

Besides, the ambient temperature together with the solar irradiance affects the PV solar cell temperature. As it was explained in Section 4.3.1, the increase of solar cell temperature affects the point of operation in the P-V curve. The power extracted could be lower than expected and could affect the overall performance of the PV generator and the LS-PVPP. Higher solar irradiance means higher solar cell temperature that is translated in lower expected active power.

This behaviour of the PV array has not been broadly considered in the understanding of the PV generator as a unit in previous studies. Thus, in this thesis the different studies developed in Chapters 4 to 6 consider the effect of the ambient temperature as well as the solar irradiance.

The capability curves were extracted considering the behaviour of the PV generator on the dc and the ac side. Besides, the limitations of each parameter for the capability curves were studied taking into account the variation of solar irradiance and ambient temperature. The capability curve is being limited when the PV generator works only in the MPP. However, when the dc voltage is variable, the active and reactive power can vary around the complete capability curve for that condition. The capability curves and the limitations were considered as well in the control of the PV inverter and were tested under variable conditions in Chapter 5 and Chapter 6.

7.1.3 Dynamic Modelling

In order to understand the performance of the PV generator in a LS-PVPP considering the variation of solar irradiance, temperature and other electrical characteristics, the present thesis relied on the development of a detailed model of the PV generator.

The model developed in this thesis is modular, which implies that each component can be modelled independently. In this sense, the PV array is a module, where the model considers the variation of solar irradiance, ambient temperature, and dc voltage. The data for solar irradiance or ambient temperature can be taken for a complete day if a day analysis is necessary. Also, the model accepts quick changes of solar irradiance under a determined ambient temperature as it was discussed in Chapter 5.

Other modules are the DC capacitor, PV inverter, transformer and the grid. Each of them has been modeled accordingly. Any change developed inside the modules will not affect the performance of the independent modules. The inputs and outputs of each module are clearly identified in Chapter 5. Thus, the model can be changed depending on the analysis developed.

In addition, any test developed on this model showed the influence of the ambient conditions, capability curves, and grid on the general

performance of the PV generator. Besides, the compliance of the grid codes can also be considered.

7.1.4 Dynamic control

Taking into account the dynamic model, the limitations and the grid codes, the control for active and reactive power has been developed (Chapter 6). The control of active power is related directly to the changes in solar irradiance, ambient temperature, and the dc voltage. Considering these variables, the one that can be controlled is the dc voltage. Commonly, the small PV system wanted to control this voltage to be equal to the corresponding v_{mpp}. It was seen that the controllability of the PV generator can be improved if the dc voltage can vary around the corresponding P-V curve. So, power reserves and power curtailment can be achieved when the dc voltage point of operation changes.

Besides, this thesis shows that the reactive power can be managed inside certain limitations. The capability curves and adequate control permit the management of the reactive power at different ambient conditions. Depending on the control chosen, the active power generated could be affected.

Considering this new control, the references of reactive power can be reached by the PV generator. However, this could not be true for the complete LS-PVPP as it depends on the grid strength and also the losses inside the power plant. Thus, the LS-PVPP could still need extra equipment to comply the grid codes requirements. This will happen especially for the case of Puerto Rico, where the reference of reactive power is higher.

7.2 Recommendations for Future Research

This section indicates possible areas for future research on the field of LS-PVPPs and extension of the work performed in this thesis.

- Regarding the PV generator configuration, Multistring topology is one that is attracting to investors. Though now it is not the technology preferred, it could change in the upcoming years. Thus, a deep cost analysis for the same study case should be

developed. Additionally, it is necessary to study the control of the inverter used in this topology as it could present other problems to overcome.

- Additionally, a deep study of LS-PVPPs with dc collection grid could also be developed. As the PV solar cell supplies dc power, it could be more helpful to have the internal grid of the power plant in dc connection. However, a deep analysis of cost, operation, and maintenance is still missing. Additionally, a technical and economical comparison between the dc and the ac collection grid is also necessary.
- Research could focus on the improvement of the grid code requirements taking into account the technology used. This will help to the development of future grid codes in order to permit the integration of LS-PVPP.
- Because of the requirements demanded by grid codes an improvement of technology is mandatory. The use of additional equipment as energy storage systems, diesel generator, FACTS and capacitor banks help to comply the grid codes. A deep study about these technologies inside LS-PVPPs is still necessary.
- As multistring topology in PV generators is possible, it is necessary to extract the capability curves of generators connected through this configuration. The variation relies in the use of the dc-dc converter that regulates the dc part, so the reactive power could be less affected by this value.
- It is necessary to test the control of reactive power for the complete LS-PVPP under variable solar irradiance in each PV array. Besides, the addition of extra equipment to comply grid code requirements is also necessary to be studied.
- With the control proposed in this thesis, the LS-PVPP can participate in voltage and frequency regulation. So, studies considering weak and strong grids together with the control developed in this thesis is still missing.
- Frequency and inertia regulation is an important issue to be solved for future grid code requirements. The control of the PV generator should be enhanced taking into account the capability curves studied in this thesis and the control presented.

Bibliography

[1] IEA, "Trends 2015 in photovoltaic applications," IEA, Tech. Rep., 2015. [Online]. Available: http://www.iea-pvps.org

[2] "Global Market Outlook for solar power 2015-2019." [Online]. Available: http://resources.solarbusinesshub.com

[3] "Major Solar Projects in the United States Operating, Under construction or under development." [Online]. Available: http://www.seia.org

[4] "PV power plants 2014. Industry guide." [Online]. Available: http://www.pv-power-plants.com/

[5] M. Ito, K. Kato, K. Komoto, T. Kichimi, and K. Kurokawa, "A comparative study on cost and life-cycle analysis for 100MW very large-scale PV (VLS-PV) systems in deserts using m-Si, a-Si, CdTe, and CIS modules," *Prog. Photovoltaics Res. Appl.*, vol. 16, no. 1, pp. 17–30, Jan. 2008.

[6] "World Population Prospects The 2015 Revision," United Nations, New York, Tech. Rep., 2015. [Online]. Available: https://esa.un.org

[7] P. R. Ehrlich and J. P. Holdren, "Impact of Population Growth," *Source: Science, New Series*, vol. 171, no. 3977, pp. 1212–1217, 1971.

[8] S. Pye, A. Dobbins, C. Baffert, J. Ivana, R. De Miglio, and P. Deane, "Energy poverty and vulnerable consumers in the energy sector across the EU." Insight energy, Tech. Rep., 2012.

[9] I. Energy Agency, "World energy outlook, 2016," IEA, Paris, Tech. Rep., 2016. [Online]. Available: www.iea.org/t{&}c/

[10] J. Wu, "Goal 7Ensure Access to Affordable, Reliable, Sustainable and Modern Energy for All," *UN Chronicle*, 2015. [Online]. Available: https://unchronicle.un.org

[11] "World energy outlook. Energy access." IEA, Tech. Rep., 2016. [Online]. Available: http://www.worldenergyoutlook

[12] BP, "BP Energy Outlook 2017," Tech. Rep., 2017. [Online]. Available: https://www.bp.com

[13] M. Hubbert, D.C.: National Bureau of Standards, Washington,DC, Tech. Rep., 1982.

[14] J. Delbeke and P. Vis, "EU Climate Policy Explained," European Union, Tech. Rep., 2016.

[15] O. Ellabban, H. Abu-Rub, and F. Blaabjerg, "Renewable energy resources: Current status, future prospects and their enabling technology," *Renewable and Sustainable Energy Reviews*, vol. 39, pp. 748–764, 2014.

[16] "IRENA Resource." [Online]. Available: http://resourceirena.irena.org

[17] EWEA, "The European Wind Energy Association — EWEA." [Online]. Available: http://www.ewea.org/

[18] "Wind Energy Facts at a Glance." [Online]. Available: http://www.awea.org

[19] "U.S. Solar Market Insight — SEIA." [Online]. Available: http://www.seia.org

[20] "Global market outlook for Photovoltaics 2014-2018." [Online]. Available: http://www.epia.org

[21] M. D. Prada-Gil, J. L. Domínguez-García, F. Díaz-González, and A. Sumper, "Offshore Wind Power Plants (OWPPS)," in *HVDC Grids*, dirk van h ed. Hoboken, NJ, USA: John Wiley & Sons, Inc., mar 2016, ch. 6, pp. 109–140.

[22] M. de Prada Gil, O. Gomis-Bellmunt, and A. Sumper, "Technical and economic assessment of offshore wind power plants based on variable frequency operation of clusters with a single power converter," *Applied Energy*, vol. 125, pp. 218–229, jul 2014.

[23] O. N. Bryant, C. C. Sterrett, and D. M. Sauter, "Controls for Operation of Steam Turbine-Generator Units [includes discussion]," *Transactions of the American Institute of Electrical Engineers. Part III: Power Apparatus and Systems*, vol. 73, no. 1, jan 1954.

[24] N. Nilsson and J. Mercurio, "Synchronous generator capability curve testing and evaluation," *IEEE Transactions on Power Delivery*, vol. 9, no. 1, pp. 414–424, 1994.

[25] S. Engelhardt, I. Erlich, C. Feltes, J. Kretschmann, and F. Shewarega, "Reactive Power Capability of Wind Turbines Based on Doubly Fed Induction Generators," *IEEE Transactions on Energy Conversion*, vol. 26, no. 1, pp. 364–372, mar 2011.

[26] L. Schwartfeger, D. Santos-Martin, A. Wood, N. Watson, and A. Miller Presenter, "Review of Distributed Generation Interconnection Standards," *EEA Conference & Exhibition*, pp. 18–20, 2014.

[27] K. Solangi, M. Islam, R. Saidur, N. Rahim, and H. Fayaz, "A review on global solar energy policy," *Renew. Sustain. Energy Rev.*, vol. 15, no. 4, pp. 2149–2163, may 2011.

[28] J. Schallenberg-Rodriguez and R. Haas, "Fixed feed-in tariff versus premium: A review of the current Spanish system," *Renew. Sustain. Energy Rev.*, vol. 16, no. 1, pp. 293–305, jan 2012.

[29] H. M. Liou, "Comparing feed-in tariff incentives in Taiwan and Germany," *Renew. Sustain. Energy Rev.*, vol. 50, pp. 1021–1034, oct 2015.

[30] B. Kumar Sahu, "A study on global solar PV energy developments and policies with special focus on the top ten solar PV power producing countries," *Renew. Sustain. Energy Rev.*, vol. 43, pp. 621–634, mar 2015.

[31] F. Meneguzzo, R. Ciriminna, L. Albanese, and M. Pagliaro, "The great solar boom: a global perspective into the far reaching impact of an unexpected energy revolution," *Energy Sci. Eng.*, vol. 3, no. 6, pp. 499–509, nov 2015.

[32] A. Cabrera-Tobar, E. Bullich-Massagué, M. Aragüés-Peñalba, and O. Gomis-Bellmunt, "Topologies for large scale photovoltaic power plants," *Renew. Sustain. Energy Rev.*, vol. 59, pp. 309–319, jun 2016.

[33] P. Kleneidam, T. Klinge, M. Kaltschmitt, B. Metzger, R. Vorobyev, A. Bindal, C. Rapicano, A. Loosen, J. Dörr, and S. Janczik, "PV market share shifts dramatically in 2013," *Renew. Energy Focus*, vol. 15, no. 4, pp. 26–29, jul 2014.

[34] K. Komoto, K. Kurokawa, Nishimura, and et al., "IEA PVPS Task 8: Project Proposals on Very Large Scale Photovoltaic Power Generation (VLS-PV) Systems in Deserts," in *2006 IEEE 4th World Conf. Photovolt. Energy Conf.*, vol. 2. IEEE, 2006, pp. 2359–2362.

[35] D. Picault, B. Raison, and S. Bacha, "Guidelines for evaluating grid connected PV system topologies," in *2009 IEEE Int. Conf. Ind. Technol.* IEEE, Feb. 2009, pp. 1–5.

[36] A. Ghafoor and A. Munir, "Design and economics analysis of an off-grid PV system for household electrification," *Renew. Sustain. Energy Rev.*, vol. 42, pp. 496–502, Feb. 2015.

[37] A. Cabrera-Tobar, H. U. Banna, C. Koch-ciobotarus, and G. Siddharta, "Optimization of an Air Conditioning Unit according to Renewable Energy availability and Users Comfort," in *ISGT, 2014*, Istanbul, 2014.

[38] J. Weniger, T. Tjaden, and V. Quaschning, "Sizing of Residential PV Battery Systems," *Energy Procedia*, vol. 46, pp. 78–87, 2014.

[39] J. Widén, E. Wäckelgå rd, J. Paatero, and P. Lund, "Impacts of distributed photovoltaics on network voltages: Stochastic simulations of three Swedish low-voltage distribution grids," *Electr. Power Syst. Res.*, vol. 80, no. 12, pp. 1562–1571, Dec. 2010.

[40] J. V. Paatero and P. D. Lund, "Effects of large-scale photovoltaic power integration on electricity distribution networks," *Renew. Energy*, vol. 32, no. 2, pp. 216–234, Feb. 2007.

[41] L. Hassaine, E. OLias, J. Quintero, and V. Salas, "Overview of power inverter topologies and control structures for grid connected photovoltaic systems," *Renew. Sustain. Energy Rev.*, vol. 30, pp. 796–807, Feb. 2014. [Online]. Available: http://www.sciencedirect.com

[42] Z. Zeng, H. Yang, R. Zhao, and C. Cheng, "Topologies and control strategies of multi-functional grid-connected inverters for power quality enhancement: A comprehensive review," *Renew. Sustain. Energy Rev.*, vol. 24, pp. 223–270, Aug. 2013.

[43] V. Salas and E. Olías, "Overview of the state of technique for PV inverters used in low voltage grid-connected PV systems: Inverters above 10kW," *Renew. Sustain. Energy Rev.*, vol. 15, no. 2, pp. 1250–1257, Feb. 2011.

[44] A. Stranix and A. Firester, "Conceptual Design Of A 50 Mw Central Station Photovoltaic Power Plant," *IEEE Trans. Power Appar. Syst.*, vol. PAS-102, no. 9, pp. 3218–3225, Sep. 1983.

[45] E. Simburger and R. Fling, "Engineering Design for a Central Station Photovoltaic Power Plant," *IEEE Trans. Power Appar. Syst.*, vol. PAS-102, no. 6, pp. 1668–1677, Jun. 1983.

[46] K. Papastergiou, P. Bakas, and A. Marinopoulos, "Overview of Alternative System Configurations for Very Large Scale PV Power Plants," *27th Eur. Photovolt. Sol. Energy Conf. Exhib.*, pp. 3805–3810, Oct. 2012.

[47] D. Gallo, R. Langella, A. Testa, J. C. Hernandez, I. Papic, B. Blazic, and J. Meyer, "Case studies on large PV plants: Harmonic distortion, unbalance and their effects," in *2013 IEEE Power Energy Soc. Gen. Meet.* IEEE, Jul. 2013, pp. 1–5. [Online]. Available: http://ieeexplore.ieee.org

[48] A. Marinopoulos, F. Papandrea, M. Reza, S. Norrga, F. Spertino, and R. Napoli, "Grid integration aspects of large solar PV installations: LVRT capability and reactive power/voltage support requirements," in *2011 IEEE Trondheim PowerTech*. Trondheim: IEEE, jun 2011, pp. 1–8.

[49] M. Morjaria, D. Anichkov, V. Chadliev, and S. Soni, "A Grid-Friendly Plant: The Role of Utility-Scale Photovoltaic Plants in Grid Stability and Reliability," *IEEE Power Energy Mag.*, vol. 12, no. 3, pp. 87–95, May 2014.

[50] A. Hoke and D. Maksimovic, "Active power control of photovoltaic power systems," in *2013 1st IEEE Conference on Technologies for Sustainability (SusTech)*. IEEE, aug 2013, pp. 70–77.

[51] E. Bullich-Massagué, M. Aragüès-Peñalba, L. Serrano, P. Carlos, R. Ferrer-San-José, and O. Gomis, "Power Plant Control Experience in Large Scale PV Plant . Modelling, Control, Simulation and Implementation." in *4th Sol. Integr. Work. 2014*, Berlin, 2014.

[52] T. Markvart, *Solar electricity*, 2nd ed., T. U. o. S. Markvart, Ed. Southampton: Wiley, 2009.

[53] ——, *Practical Handbook of Photovoltaics*. Elsevier, 2012.

[54] M. A. Green, K. Emery, Y. Hishikawa, W. Warta, and E. D.

Dunlop, "Solar cell efficiency tables (version 39)," *Prog. Photovoltaics Res. Appl.*, vol. 20, no. 1, pp. 12–20, Jan. 2012.

[55] L. Stolt, J. Hedstrom, J. Kessler, M. Ruckh, K.-O. Velthaus, and H.-W. Schock, "ZnO/CdS/CuInSe2 thin-film solar cells with improved performance," *Appl. Phys. Lett.*, vol. 62, no. 6, p. 597, Feb. 1993.

[56] V. Tyagi, N. A. Rahim, N. Rahim, and J. A. Selvaraj, "Progress in solar PV technology: Research and achievement," *Renew. Sustain. Energy Rev.*, vol. 20, pp. 443–461, Apr. 2013.

[57] M. Z. Rahman, "Advances in surface passivation and emitter optimization techniques of c-Si solar cells," *Renew. Sustain. Energy Rev.*, vol. 30, pp. 734–742, Feb. 2014. [Online]. Available: http://www.sciencedirect.com/science/article/pii/S1364032113007740

[58] A. Metz, D. Adler, S. Bagus, H. Blanke, M. Bothar, E. Brouwer, S. Dauwe, K. Dressler, R. Droessler, T. Droste, M. Fiedler, Y. Gassenbauer, T. Grahl, N. Hermert, W. Kuzminski, A. Lachowicz, T. Lauinger, N. Lenck, M. Manole, M. Martini, R. Messmer, C. Meyer, J. Moschner, K. Ramspeck, P. Roth, R. Schönfelder, B. Schum, J. Sticksel, K. Vaas, M. Volk, and K. Wangemann, "Industrial high performance crystalline silicon solar cells and modules based on rear surface passivation technology," *Sol. Energy Mater. Sol. Cells*, vol. 120, pp. 417–425, Jan. 2014.

[59] W. Hoffmann and T. Pellkofer, "Thin films in photovoltaics: Technologies and perspectives," *Thin Solid Films*, vol. 520, no. 12, pp. 4094–4100, Apr. 2012.

[60] M. Hussin, S. Shaari, A. Omar, and Z. Zain, "Amorphous silicon thin-film: Behaviour of light-induced degradation," *Renew. Sustain. Energy Rev.*, vol. 43, pp. 388–402, Mar. 2015.

[61] C. Candelise, J. F. Speirs, and R. J. Gross, "Materials availability for thin film (TF) PV technologies development: A real concern?" *Renew. Sustain. Energy Rev.*, vol. 15, no. 9, pp. 4972–4981, Dec. 2011. [Online]. Available: http://www.sciencedirect.com/science/article/pii/S136403211100298X

[62] T. Hoff and J. Iannucci, "Maximizing the benefits derived from

PV plants: Selecting the best plant design and plant location," in *IEEE Conf. Photovolt. Spec.* IEEE, 1990, pp. 892–897.

[63] S. Yilmaz, H. R. Ozcalik, S. Kesler, F. Dincer, and B. Yelmen, "The analysis of different PV power systems for the determination of optimal PV panels and system installationA case study in Kahramanmaras, Turkey," *Renew. Sustain. Energy Rev.*, vol. 52, pp. 1015–1024, Dec. 2015.

[64] IRENA, "Renewable Energy technologies: cost analysis series (Solar Photovoltaics)," IRENA, Tech. Rep., 2012. [Online]. Available: https://www.irena.org/DocumentDownloads/Publications/RE_Technologies_Cost_Analysis-SOLAR_PV.pdf

[65] J. Tao and S. Yu, "Review on feasible recycling pathways and technologies of solar photovoltaic modules," *Sol. Energy Mater. Sol. Cells*, vol. 141, pp. 108–124, Oct. 2015.

[66] S. Kjaer, J. Pedersen, and F. Blaabjerg, "A Review of Single-Phase Grid-Connected Inverters for Photovoltaic Modules," *IEEE Trans. Ind. Appl.*, vol. 41, no. 5, pp. 1292–1306, Sep. 2005.

[67] M. S. Agamy, M. Harfman-Todorovic, A. Elasser, R. L. Steigerwald, J. A. Sabate, S. Chi, A. J. McCann, L. Zhang, and F. Mueller, "A high efficiency DC-DC converter topology suitable for distributed large commercial and utility scale PV systems," in *2012 15th Int. Power Electron. Motion Control Conf.* IEEE, Sep. 2012, pp. LS2d.3–1–LS2d.3–6.

[68] M. Taghvaee, M. Radzi, S. Moosavain, H. Hizam, and M. Hamiruce Marhaban, "A current and future study on non-isolated DCDC converters for photovoltaic applications," *Renew. Sustain. Energy Rev.*, vol. 17, pp. 216–227, Jan. 2013.

[69] W. Li and X. He, "Review of Nonisolated High-Step-Up DC/DC Converters in Photovoltaic Grid-Connected Applications," *IEEE Trans. Ind. Electron.*, vol. 58, no. 4, pp. 1239–1250, Apr. 2011.

[70] M. Ciobotaru and V. G. Agelidis, "Large-scale PV system based on the multiphase isolated DC/DC converter," in *2012 3rd IEEE Int. Symp. Power Electron. Distrib. Gener. Syst.* IEEE, Jun. 2012, pp. 801–807.

[71] M. Rashid, *Power electronics handbook.*, A. Press, Ed., 2001.

[72] J. Rodriguez, L. Franquelo, S. Kouro, J. Leon, R. Portillo, M. Prats, and M. Perez, "Multilevel Converters: An Enabling Technology for High-Power Applications," *Proc. IEEE*, vol. 97, no. 11, pp. 1786–1817, Nov. 2009.

[73] S. Rivera, S. Kouro, B. Wu, J. I. Leon, J. Rodriguez, and L. G. Franquelo, "Cascaded H-bridge multilevel converter multistring topology for large scale photovoltaic systems," in *2011 IEEE Int. Symp. Ind. Electron.* IEEE, Jun. 2011, pp. 1837–1844.

[74] S. Kouro, K. Asfaw, R. Goldman, R. Snow, B. Wu, and J. Rodriguez, "NPC multilevel multistring topology for large scale grid connected photovoltaic systems," in *2nd Int. Symp. Power Electron. Distrib. Gener. Syst.* IEEE, Jun. 2010, pp. 400–405.

[75] S. Ozdemir, N. Altin, and I. Sefa, "Single stage three level grid interactive MPPT inverter for PV systems," *Energy Convers. Manag.*, vol. 80, pp. 561–572, Apr. 2014.

[76] S. Testa, A. De Caro and T. Scimone, "Sizing of step-up transformers for PV plants through a Probabilistic Approach." [Online]. Available: http://www.wseas.org

[77] B. Engel, G. Bettenwort, V. Sakschewski, O. Glitza, T. Fawzy, and D. Premm, "How to Represent PV Plants in Grid Integration Studies - A Generic Approach," *26th Eur. Photovolt. Sol. Energy Conf. Exhib.*, pp. 3862–3868, Oct. 2011.

[78] D. A. Trevas, A. Peterson, K. J. Rapp, and J. Luksich, "Optimal sizing of solar energy transformers using natural ester fluid," in *2012 11th Int. Conf. Environ. Electr. Eng.* IEEE, May 2012, pp. 1006–1010.

[79] "Transformers for Solar Power Solutions." [Online]. Available: http://www.energy.siemens.com

[80] DunHuang China Solar Power, "Gansu Dunhuang 50MWp Solar PV Power Station Project," China, Tech. Rep., 2006.

[81] "Requirements for Medium-Voltage Transformers and Transformers for Internal Power Supply for the SUNNY CENTRAL Series CP XT and CP-JP and for Sunny Central Storage." [Online]. Available: http://files.sma.de

[82] "Application paper tripple linx inverter for large rooftop." [Online]. Available: http://www.danfoss.com

[83] A. Testa, S. De Caro, R. La Torre, and T. Scimone, "Optimal size selection of step-up transformers in PV plants," in *XIX Int. Conf. Electr. Mach. - ICEM 2010*. IEEE, Sep. 2010, pp. 1–6.

[84] B. Hafez, H. S. Krishnamoorthy, P. Enjeti, U. Borup, and S. Ahmed, "Medium voltage AC collection grid for large scale photovoltaic plants based on medium frequency transformers," in *2014 IEEE Energy Convers. Congr. Expo.* IEEE, Sep. 2014, pp. 5304–5311.

[85] M. Meinhardt, G. Cramer, B. Burger, and P. Zacharias, "Multi-string-converter with reduced specific costs and enhanced functionality," *Sol. Energy*, vol. 69, pp. 217–227, Jul. 2001.

[86] M. Ciobotaru and V. G. Agelidis, "High gain DC/DC converter for the grid integration of large-scale PV systems," in *2012 IEEE Int. Symp. Ind. Electron.* IEEE, May 2012, pp. 1011–1016.

[87] M. Díez-Mediavilla, M. Dieste-Velasco, M. Rodríguez-Amigo, T. García-Calderón, and C. Alonso-Tristán, "Performance of grid-tied PV facilities based on real data in Spain: Central inverter versus string system," *Energy Convers. Manag.*, vol. 86, pp. 1128–1133, Oct. 2014.

[88] M. Brenna, R. Faranda, and S. Leva, "Dynamic analysis of a new network topology for high power grid connected PV systems," in *IEEE PES Gen. Meet.* IEEE, Jul. 2010, pp. 1–7.

[89] S. Brenna, Morris and Dolara, Alberto and Foiadelli, Federica and Lazaroiu, George C. and Leva, "Transient Analysis of Large Scale PV systems with Floating DC section," *Energies*, vol. 5, no. 10, pp. 3736–3752, 2012.

[90] G. Cramer, M. Ibrahim, and W. Kleinkauf, "PV system technologies," *Refocus*, vol. 5, no. 1, pp. 38–42, Jan. 2004.

[91] B. Lave, H. Grau, and U. Borup, "String Inverters for PV Power Plants," *24th Eur. Photovolt. Sol. Energy Conf. 21-25 Sept. 2009, Hamburg, Ger.*, pp. 4173–4175, Nov. 2009.

[92] E. Karatepe and T. Hiyama, "Performance enhancement of photovoltaic array through string and central based MPPT system under non-uniform irradiance conditions," *Energy Convers. Manag.*, vol. 62, pp. 131–140, Oct. 2012.

[93] A. Woyte, J. Nijs, and R. Belmans, "Partial shadowing of photovoltaic arrays with different system configurations: literature

review and field test results," *Sol. Energy*, vol. 74, no. 3, pp. 217–233, Mar. 2003.

[94] M. Pau, N. Locci, and C. Muscas, "A tool to define the position and the number of irradiance sensors in large PV plants," in *2014 IEEE Int. Energy Conf.* IEEE, May 2014, pp. 374–379.

[95] P. Guerriero, V. D'Alessandro, L. Petrazzuoli, G. Vallone, and S. Daliento, "Effective real-time performance monitoring and diagnostics of individual panels in PV plants," in *2013 Int. Conf. Clean Electr. Power*. IEEE, Jun. 2013, pp. 14–19.

[96] Danfoss, "Danfoss FLX String Inverters for PV power Plants," Danfoss, Denmark, Tech. Rep., 2014. [Online]. Available: http://www.danfoss.com

[97] ——, "String inverters for PV power plants," Danfoss, Denmark, Tech. Rep., 2009. [Online]. Available: http://www.danfoss.com

[98] A. Elis, Y. Kazachkov, and et al., "IEC TF88-WG27-Oct 2009 Wind Modeling Update," Tech. Rep., 2009. [Online]. Available: https://www.wecc.biz

[99] K. Malmedal and P. K. Sen, "Comparison of some randomly selected utilities interconnection requirements and the compliance with the IEEE Std. 1547 - Interconnection guidelines," in *IEEE Rural Electr. Power Conf.* Charleston: IEEE, apr 2008, pp. 1–9.

[100] M. Obi and R. Bass, "Trends and challenges of grid-connected photovoltaic systems A review," *Renew. Sustain. Energy Rev.*, vol. 58, pp. 1082–1094, may 2016.

[101] M. Tsili and S. Papathanassiou, "A review of grid code technical requirements for wind farms," *IET Renew. Power Gener.*, vol. 3, no. 3, p. 308, sep 2009.

[102] B. Magoro and T. Khoza, "Grid connection code for renewable power plants connected to the electricity transmission system or the distribution system in South Africa," South Africa, Tech. Rep., 2012. [Online]. Available: http://www.nersa.org.za

[103] J. Liang, Y. Wang, W. Fubao, W. XiaoFang, A. Chao, L. Zhen, K. XiaoGang, Z. Jian, C. Zhileir, N. ChenHui, and Z. WeiRan, "Comparative study of standards for grid connected PV system in China, the US and European countries," National

Energy Administration of China, Tech. Rep., 2013. [Online]. Available: http://www.uschinaecp.org

[104] I. Banu, M. Istrate, D. Machidon, and R. Pantelimon, "Aspects of Photovoltaic Power Plant Integration in the Romanian Power System," Technical university of Iasi., Tech. Rep., 2014.

[105] A. Ellis, B. Karlson, and J. Wiliams, "Utility scale photovoltaic procedures and interconnection requirements," SANDIA, Albuquerque, New Mexico, Tech. Rep., 2012. [Online]. Available: http://energy.sandia.gov

[106] Vahan Gevorgian; Sarah Booth, "Review of PREPA Technical Requirements for Interconnecting Wind and Solar Generation," NREL, USA, Tech. Rep., 2013. [Online]. Available: http://www.nrel.gov

[107] ASEP, "Código de redes fovoltaico. Panamá 2013." p. 30, 2013. [Online]. Available: http://www.asep.gob.pa/

[108] I.-T. K. Theologitis, "Comparison of existing PV models and possible integration under EU grid specifications," 2011.

[109] M. Mirhosseini and V. G. Agelidis, "Performance of large-scale grid-connected photovoltaic system under various fault conditions," in *2013 IEEE Int. Conf. Ind. Technol.* IEEE, Feb. 2013, pp. 1775–1780.

[110] Xiangqing Jiao and Qi Gao, "Integrated dynamic simulation of photovoltaic installations and its Low Voltage Ride-Through capability analysis," pp. 1–5, 2012.

[111] R. Shah, N. Mithulananthan, R. Bansal, and V. Ramachandaramurthy, "A review of key power system stability challenges for large-scale PV integration," *Renewable and Sustainable Energy Reviews*, vol. 41, pp. 1423–1436, jan 2015.

[112] M. Mohseni and S. M. Islam, "Review of international grid codes for wind power integration: Diversity, technology and a case for global standard," *Renew. Sustain. Energy Rev.*, vol. 16, no. 6, pp. 3876–3890, aug 2012.

[113] R. Yan and T. K. Saha, "Investigation of Voltage Stability for Residential Customers Due to High Photovoltaic Penetrations," *IEEE Trans. Power Syst.*, vol. 27, no. 2, pp. 651–662, may 2012.

[114] M. Thomson and D. Infield, "Impact of widespread photovoltaics generation on distribution systems," *IET Renew. Power Gener.*, vol. 1, no. 1, p. 33, 2007.

[115] W. Pattaraprakorn, P. Bhasaputra, and J. Pattanasirichotigul, "Impacts of PV power plants on distribution grid for voltage stability and economic values," in *2015 12th Int. Conf. Electr. Eng. Comput. Telecommun. Inf. Technol.* IEEE, jun 2015, pp. 1–6.

[116] M. Esmaili, E. C. Firozjaee, and H. A. Shayanfar, "Optimal placement of distributed generations considering voltage stability and power losses with observing voltage-related constraints," *Appl. Energy*, vol. 113, pp. 1252–1260, jan 2014.

[117] W. A. Omran, M. Kazerani, and M. M. A. Salama, "A Clustering-Based Method for Quantifying the Effects of Large On-Grid PV Systems," *IEEE Trans. Power Deliv.*, vol. 25, no. 4, pp. 2617–2625, oct 2010.

[118] L. H. X. H.-h. Wang Yi-Bo, Wu Chun-Sheng, "Study on impacts of large-scale photovoltaic power station on power grid voltage profile," in *2008 Third Int. Conf. Electr. Util. Deregul. Restruct. Power Technol.* IEEE, apr 2008, pp. 2575–2579.

[119] J. Bebic, "Power System Planning: Emerging Practices Suitable for Evaluating the Impact of High-Penetration Photovoltaics," NREL, Tech. Rep., 2008.

[120] E. Muljadi, V. Gevorgian, M. Singh, and S. Santoso, "Understanding inertial and frequency response of wind power plants," in *2012 IEEE Power Electron. Mach. Wind Appl.* IEEE, jul 2012, pp. 1–8.

[121] N. W. Miller, K. Clark, and M. Shao, "Frequency responsive wind plant controls: Impacts on grid performance," in *2011 IEEE Power Energy Soc. Gen. Meet.* IEEE, jul 2011, pp. 1–8.

[122] F. Díaz-González, M. Hau, A. Sumper, and O. Gomis-Bellmunt, "Participation of wind power plants in system frequency control: Review of grid code requirements and control methods," *Renewable and Sustainable Energy Reviews*, vol. 34, pp. 551–564, jun 2014.

[123] P. Tielens and D. Van Hertem, "The relevance of inertia in power systems," *Renew. Sustain. Energy Rev.*, vol. 55, pp. 999–1009, mar 2016.

[124] C. Seneviratne and C. Ozansoy, "Frequency response due to a large generator loss with the increasing penetration of wind/PV generation A literature review," *Renew. Sustain. Energy Rev.*, vol. 57, pp. 659–668, may 2016.

[125] C. Rahmann and A. Castillo, "Fast Frequency Response Capability of Photovoltaic Power Plants: The Necessity of New Grid Requirements and Definitions," *Energies*, vol. 7, no. 10, pp. 6306–6322, sep 2014.

[126] R. Yan, T. K. Saha, N. Modi, N.-A. Masood, and M. Mosadeghy, "The combined effects of high penetration of wind and PV on power system frequency response," *Appl. Energy*, vol. 145, pp. 320–330, may 2015.

[127] A. Abdlrahem, G. K. Venayagamoorthy, and K. A. Corzine, "Frequency stability and control of a power system with large PV plants using PMU information," in *2013 North Am. Power Symp.* IEEE, sep 2013, pp. 1–6.

[128] V. Silva, M. Lopez-Botet-Zulueta, and Y. Wang, "Impact of high penetration of variable renewable generation on frequency dynamics in the continental Europe interconnected system," *IET Renew. Power Gener.*, vol. 10, no. 1, pp. 10–16, jan 2016. [Online]. Available: http://digital-library.theiet.org/content/journals/10.1049/iet-rpg.2015.0141

[129] P. Bhatnagar and R. Nema, "Maximum power point tracking control techniques: State-of-the-art in photovoltaic applications," *Renew. Sustain. Energy Rev.*, vol. 23, pp. 224–241, Jul. 2013.

[130] N. A. Kamarzaman and C. W. Tan, "A comprehensive review of maximum power point tracking algorithms for photovoltaic systems," *Renewable and Sustainable Energy Reviews*, vol. 37, pp. 585–598, sep 2014.

[131] S. Saravanan and N. Ramesh Babu, "Maximum power point tracking algorithms for photovoltaic system A review," *Renew. Sustain. Energy Rev.*, vol. 57, pp. 192–204, may 2016.

[132] E. Ela, M. Milligan, and B. Kirby, "Operating Reserves and Variable Generation," NREL, Tech. Rep., 2011. [Online]. Available: http://www.nrel.gov

[133] R. Guerrero-Lemus, B. González-Díaz, G. Ríos, and R. N. Dib, "Study of the new Spanish legislation applied to an insular system that has achieved grid parity on PV and wind energy," *Renew. Sustain. Energy Rev.*, vol. 49, pp. 426–436, sep 2015.

[134] A. Ellis, R. Nelson, E. Von Engeln, J. MacDowell, L. Casey, E. Seymour, and W. Peter, "Reactive power performance requirements for wind and solar plants," in *2012 IEEE Power Energy Soc. Gen. Meet.* IEEE, jul 2012, pp. 1–8.

[135] A. Cagnano, F. Torelli, F. Alfonzetti, and E. De Tuglie, "Can PV plants provide a reactive power ancillary service? A treat offered by an on-line controller," *Renew. Energy*, vol. 36, no. 3, pp. 1047–1052, mar 2011.

[136] T. Lund, P. Sørensen, and J. Eek, "Reactive power capability of a wind turbine with doubly fed induction generator," *Wind Energy*, vol. 10, no. 4, pp. 379–394, jul 2007.

[137] A. Pathak, M. Sharma, and M. Bundele, "A critical review of voltage and reactive power management of wind farms," *Renew. Sustain. Energy Rev.*, vol. 51, pp. 460–471, nov 2015. [Online]. Available: http://www.sciencedirect.com/science/article/pii/S1364032115005857

[138] A. Mullane, G. Lightbody, and R. Yacamini, "Wind-Turbine Fault Ride-Through Enhancement," *IEEE Trans. Power Syst.*, vol. 20, no. 4, pp. 1929–1937, nov 2005.

[139] A. K. Cabrera, H. U. Banna, C. Koch-Ciobotarus, and S. Ghosh, "Optimization of an air conditioning unit according to renewable energy availability and user's comfort," in *IEEE PES Innovative Smart Grid Technologies, Europe*. Istanbul: IEEE, oct 2014, pp. 1–7.

[140] S. Wang, X. Yao, and J. Zhao, "A novel low voltage ride through strategy of two-stage grid-connected photovoltaic inverter," in *2013 1st Int. Futur. Energy Electron. Conf.* IEEE, nov 2013, pp. 400–405.

[141] L. Yaoyuan, Z. Chengbi, M. Hong, and F. Wenwen, "Research on a new method to achieve low voltage ride through of PV," in *2014 Int. Conf. Power Syst. Technol.* IEEE, oct 2014, pp. 1628–1634.

[142] N. R. Ullah, T. Thiringer, and D. Karlsson, "Voltage and Transient Stability Support by Wind Farms Complying With the E.ON Netz Grid Code," *IEEE Trans. Power Syst.*, vol. 22, no. 4, pp. 1647–1656, nov 2007.

[143] L. Zhou and Y. Chao, "The research of reactive power control strategy for grid-connected photovoltaic plants," in *2013 World Congr. Sustain. Technol.* IEEE, Dec. 2013, pp. 12–17.

[144] Y. Bae, T.-K. Vu, and R.-Y. Kim, "Implemental Control Strategy for Grid Stabilization of Grid-Connected PV System Based on German Grid Code in Symmetrical Low-to-Medium Voltage Network," *IEEE Trans. Energy Convers.*, vol. 28, no. 3, pp. 619–631, sep 2013.

[145] V. Minambres-Marcos, M. A. Guerrero-Martinez, E. Romero-Cadaval, and P. Gonzalez-Castrillo, "Point of common coupling voltage regulation with photovoltaic power plant infrastructures," in *2014 IEEE 23rd Int. Symp. Ind. Electron.* IEEE, Jun. 2014, pp. 2054–2059.

[146] T. Van Dao, H. T. N. Nguyen, S. Chaitusaney, and R. Chatthaworn, "Local reactive power control of PV plants for voltage fluctuation mitigation," in *2014 11th Int. Conf. Electr. Eng. Comput. Telecommun. Inf. Technol.* IEEE, may 2014, pp. 1–6.

[147] W. Xiao, K. Torchyan, M. S. El Moursi, and J. L. Kirtley, "Online Supervisory Voltage Control for Grid Interface of Utility-Level PV Plants," *IEEE Trans. Sustain. Energy*, vol. 5, no. 3, pp. 843–853, jul 2014.

[148] Y. Liu, J. Bebic, B. Kroposki, J. de Bedout, and W. Ren, "Distribution System Voltage Performance Analysis for High-Penetration PV," in *2008 IEEE Energy 2030 Conf.* IEEE, nov 2008, pp. 1–8.

[149] R. K. Varma, S. A. Rahman, A. C. Mahendra, R. Seethapathy, and T. Vanderheide, "Novel nighttime application of PV solar farms as STATCOM (PV-STATCOM)," in *2012 IEEE Power Energy Soc. Gen. Meet.* IEEE, jul 2012, pp. 1–8.

[150] A. Moawwad, V. Khadkikar, and J. L. Kirtley, "A New PQV Droop Control Method for an interline photovoltaic power system." *IEEE Trans. Power Deliv.*, vol. 28, no. 2, pp. 658–668, apr 2013.

[151] O. Gomis-Bellmunt, L. Serrano-Salamanca, R. Ferrer-San-José, C. Pacheco-Navas, M. Aragüés-Peñalba, and E. Bullich-Massagué, "Power plant control in large-scale photovoltaic plants: design, implementation and validation in a 9.4 MW photovoltaic plant," *IET Renew. Power Gener.*, nov 2015.

[152] "GPtech." [Online]. Available: http://www.greenpower.es

[153] F. Díaz-González, A. Sumper, O. Gomis-Bellmunt, and R. Villafáfila-Robles, "A review of energy storage technologies for wind power applications," *Renew. Sustain. Energy Rev.*, vol. 16, no. 4, pp. 2154–2171, may 2012.

[154] IRENA, "Battery storage for renewables: market status and technology outlook," IRENA, Tech. Rep., 2015. [Online]. Available: http://www.irena.org

[155] M. Alam, K. Muttaqi, and D. Sutanto, "A Novel Approach for Ramp-Rate Control of Solar PV Using Energy Storage to Mitigate Output Fluctuations Caused by Cloud Passing," *IEEE Trans. Energy Convers.*, vol. 29, no. 2, pp. 507–518, jun 2014.

[156] M. Ciobotaru and V. Agelidis, "Minimising output power fluctuation of large photovoltaic plant using vanadium redox battery storage," in *6th IET Int. Conf. Power Electron. Mach. Drives (PEMD 2012)*. IET, 2012, pp. D41–D41.

[157] S. Shivashankar, S. Mekhilef, H. Mokhlis, and M. Karimi, "Mitigating methods of power fluctuation of photovoltaic (PV) sources ? A review," *Renewable and Sustainable Energy Reviews*, vol. 59, pp. 1170–1184, jun 2016.

[158] T. Monai, I. Takano, H. Nishikawa, and Y. Sawada, "A Collaborative Operation Method Between New Energy-Type Dispersed Power Supply and EDLC," *IEEE Trans. Energy Convers.*, vol. 19, no. 3, pp. 590–598, sep 2004.

[159] N. Kakimoto, H. Satoh, S. Takayama, and K. Nakamura, "Ramp-Rate Control of Photovoltaic Generator With Electric Double-Layer Capacitor," *IEEE Trans. Energy Convers.*, vol. 24, no. 2, pp. 465–473, jun 2009.

[160] E. Nfah, J. Ngundam, and R. Tchinda, "Modelling of solar/diesel/battery hybrid power systems for far-north Cameroon," *Renew. Energy*, vol. 32, no. 5, pp. 832–844, apr 2007.

[161] A. Mohammed, J. Pasupuleti, T. Khatib, and W. Elmenreich, "A review of process and operational system control of hybrid photovoltaic/diesel generator systems," *Renew. Sustain. Energy Rev.*, vol. 44, pp. 436–446, apr 2015.

[162] R. Tonkoski, L. Lopes, and D. Turcotte, "Active power curtailment of PV inverters in diesel hybrid mini-grids," in *2009 IEEE Electr. Power Energy Conf.* IEEE, oct 2009, pp. 1–6.

[163] M. Datta, T. Senjyu, A. Yona, and T. Funabashi, "A Frequency-Control Approach by Photovoltaic Generator in a PVDiesel Hybrid Power System," *IEEE Trans. Energy Convers.*, vol. 26, no. 2, pp. 559–571, jun 2011.

[164] B.-I. Craciun, S. Spataru, T. Kerekes, D. Sera, and R. Teodorescu, "Power ramp limitation and frequency support in large scale PVPPs without storage," in *2013 IEEE 39th Photovolt. Spec. Conf.* IEEE, jun 2013, pp. 2354–2359.

[165] C. Rahmann, V. Vittal, J. Ascui, and J. Haas, "Mitigation Control Against Partial Shading Effects in Large-Scale PV Power Plants," *IEEE Trans. Sustain. Energy*, vol. 7, no. 1, pp. 173–180, jan 2016.

[166] Y. Yang, F. Blaabjerg, and H. Wang, "Constant power generation of photovoltaic systems considering the distributed grid capacity," in *2014 IEEE Appl. Power Electron. Conf. Expo. - APEC 2014*. IEEE, mar 2014, pp. 379–385.

[167] H. Xin, Y. Liu, Z. Wang, D. Gan, and T. Yang, "A New Frequency Regulation Strategy for Photovoltaic Systems Without Energy Storage," *IEEE Trans. Sustain. Energy*, vol. 4, no. 4, pp. 985–993, oct 2013.

[168] "COMMISSION REGULATION (EU) 2016/ 631 - of 14 April 2016 - establishing a network code on requirements for grid connection of generators." [Online]. Available: http://eur-lex.europa.eu/legal-content/EN/TXT/PDF/?uri=CELEX:32016R0631{&}from=EN

[169] VDE and FNN, "VDE-AR-N 4105:2011-08 Power generation systems connected to the low coltage distribution network," 2011.

[170] R. Albarracin and M. Alonso, "Photovoltaic reactive power lim-

its," in *2013 12th International Conference on Environment and Electrical Engineering*. IEEE, may 2013, pp. 13–18.

[171] F. Delfino, G. Denegri, M. Invernizzi, R. Procopio, and G. Ronda, "A P-Q capability chart approach to characterize grid connected PV-units," pp. 1–8, 2009.

[172] B. Marion, "Comparison of predictive models for photovoltaic module performance," in *2008 33rd IEEE Photovolatic Specialists Conference*. IEEE, may 2008, pp. 1–6.

[173] S. R. Pulikanti, G. Konstantinou, and V. G. Agelidis, "DC-Link Voltage Ripple Compensation for Multilevel Active-Neutral-Point-Clamped Converters Operated With SHE-PWM," *IEEE Trans. Power Deliv.*, vol. 27, no. 4, pp. 2176–2184, Oct. 2012.

[174] R. G. Ramteke and U. V. Patil, "Design and comparative study of filters for multilevel inverter for grid interface," in *2014 International Conference on Power, Automation and Communication (INPAC)*. IEEE, oct 2014, pp. 39–44.

[175] H. Cha and T.-K. Vu, "Comparative analysis of low-pass output filter for single-phase grid-connected Photovoltaic inverter," in *2010 Twenty-Fifth Annual IEEE Applied Power Electronics Conference and Exposition (APEC)*. IEEE, feb 2010, pp. 1659–1665.

[176] S. Weckx, C. Gonzalez, and J. Driesen, "Combined Central and Local Active and Reactive Power Control of PV Inverters," *IEEE Transactions on Sustainable Energy*, vol. 5, no. 3, pp. 776–784, jul 2014. [Online]. Available: http://ieeexplore.ieee.org/document/6755528/

[177] S. Ozdemir, S. Bayhan, I. Sefa, and N. Altin, "Three-phase multilevel grid interactive inverter for PV systems with reactive power support capability," in *2015 First Workshop on Smart Grid and Renewable Energy (SGRE)*. IEEE, mar 2015, pp. 1–6.

[178] K. Turitsyn, P. Sulc, S. Backhaus, and M. Chertkov, "Options for Control of Reactive Power by Distributed Photovoltaic Generators," *Proc. IEEE*, vol. 99, no. 6, pp. 1063–1073, Jun. 2011.

[179] A. Cabrera-Tobar and O. Gomis-Bellmunt, "Performance of a small photovoltaic power plant under different meteorological conditions," in *2016 IEEE 16th International Conference on Envi-*

ronment and Electrical Engineering (EEEIC). IEEE, jun 2016, pp. 1–6.

[180] ——, "Dynamic study of a photovoltaic power plant interconnected with the grid," in *2016 IEEE PES Innovative Smart Grid Technologies Conference Europe (ISGT-Europe)*. Ljubanja: IEEE, oct 2016, pp. 1–6.

[181] "Forecasting of photovoltaic power generation and model optimization: A review," *Renewable and Sustainable Energy Reviews*, vol. 81, pp. 912–928, jan 2018.

[182] J. Antonanzas, N. Osorio, R. Esobar, R. Urraca, F. Martinez, and F. Antonanzas-Torres, "Review of photovoltaic power forecasting," *Solar Energy*, vol. 136, pp. 78–111, oct 2016.

[183] R. Teixeira Pinto, *Multi-Terminal DC Networks: System Integration, Dynamics and Control*, jan 2014.

[184] M. A. Eltawil and Z. Zhao, "MPPT techniques for photovoltaic applications," *Renew. Sustain. Energy Rev.*, vol. 25, pp. 793–813, Sep. 2013.

[185] Y.-H. Liu, J.-H. Chen, and J.-W. Huang, "A review of maximum power point tracking techniques for use in partially shaded conditions," *Renewable and Sustainable Energy Reviews*, vol. 41, pp. 436–453, jan 2015.

[186] A. Yazdani and R. Iravani, *Voltage-sourced converters in power systems : modeling, control, and applications*. IEEE Press/John Wiley, 2010.

[187] A. Hoke and D. Maksimovic, "Active power control of photovoltaic power systems," in *2013 1st IEEE Conference on Technologies for Sustainability (SusTech)*. IEEE, aug 2013, pp. 70–77.

[188] M. Datta, T. Senjyu, A. Yona, and T. Funabashi, "A Coordinated Control Method for Leveling PV Output Power Fluctuations of PVDiesel Hybrid Systems Connected to Isolated Power Utility," *IEEE Transactions on Energy Conversion*, vol. 24, no. 1, pp. 153–162, mar 2009.

[189] R. van Haaren, M. Morjaria, and V. Fthenakis, "An energy storage algorithm for ramp rate control of utility scale PV (photovoltaics) plants," *Energy*, vol. 91, pp. 894–902, nov 2015.

[190] H. Beltran, "Energy storage systems integration into PV power plants," Ph.D. dissertation, Universitat Politècnica de Catalunya, 2011.

[191] I. de la Parra, J. Marcos, M. García, and L. Marroyo, "Control strategies to use the minimum energy storage requirement for PV power ramp-rate control," *Sol. Energy*, vol. 111, pp. 332–343, Jan. 2015.

[192] E. Bullich-Massagué, M. Aragüés-Peñalba, A. Sumper, and O. Boix-Aragones, "Active power control in a hybrid PV-storage power plant for frequency support," *Solar Energy*, vol. 144, pp. 49–62, mar 2017.

[193] A. Okou, O. Akhrif, R. Beguenane, and M. Tarbouchi, "Non-linear control strategy insuring contribution of PV generator to voltage and frequency regulation," in *6th IET International Conference on Power Electronics, Machines and Drives (PEMD 2012)*. IET, 2012, pp. D42–D42.

[194] F. He, Z. Zhao, L. Yuan, and S. Lu, "A DC-link voltage control scheme for single-phase grid-connected PV inverters," in *2011 IEEE Energy Conversion Congress and Exposition*. IEEE, sep 2011, pp. 3941–3945.

[195] A. Moghadasi, A. Sargolzaei, M. Moghaddami, A. I. Sarwat, and K. Yen, "Active and reactive power control method for three-phase PV module-integrated converter based on a single-stage inverter," in *2017 IEEE Applied Power Electronics Conference and Exposition (APEC)*. IEEE, mar 2017, pp. 1357–1362.

[196] H. Maleki and R. K. Varma, "Coordinated control of PV solar system as STATCOM (PV-STATCOM) and Power System Stabilizers for power oscillation damping," in *2016 IEEE Power and Energy Society General Meeting (PESGM)*. IEEE, jul 2016, pp. 1–5. [Online]. Available: http://ieeexplore.ieee.org/document/7741813/

[197] R. Sadnan and M. Z. R. Khan, "Fast real and reactive power flow control of grid-tie Photovoltaic inverter," in *2016 9th International Conference on Electrical and Computer Engineering (ICECE)*. IEEE, dec 2016, pp. 570–573.

[198] S. Weckx, C. Gonzalez, and J. Driesen, "Combined Central and Local Active and Reactive Power Control of PV Invert-

ers," *IEEE Transactions on Sustainable Energy*, vol. 5, no. 3, pp. 776–784, jul 2014.

[199] R. DeAlmeida, E. Castronuovo, and J. PecasLopes, "Optimum Generation Control in Wind Parks When Carrying Out System Operator Requests," *IEEE Transactions on Power Systems*, vol. 21, no. 2, pp. 718–725, may 2006.

[200] D. Van Hertem, O. Gomis-Bellmunt, and J. Liang, *HVDC grids for offshore and supergrid of the future*. Wiley, IEEE Press, 2016.

[201] A. Cabrera-Tobar, E. Bullich-Massagué, M. Aragüés-Peñalba, and O. Gomis-Bellmunt, "Capability curve analysis of photovoltaic generation systems," *Solar Energy*, vol. 140, pp. 255–264, 2016.

[202] M. Mirhosseini and V. G. Agelidis, "Interconnection of large-scale photovoltaic systems with the electrical grid: Potential issues," in *2013 IEEE Int. Conf. Ind. Technol.* IEEE, Feb. 2013, pp. 728–733.

[203] N. Jaalam, N. Rahim, A. Bakar, C. Tan, and A. M. Haidar, "A comprehensive review of synchronization methods for grid-connected converters of renewable energy source," *Renewable and Sustainable Energy Reviews*, vol. 59, pp. 1471–1481, 2016.

[204] C. Li, C. Cao, Y. Cao, Y. Kuang, L. Zeng, and B. Fang, "A review of islanding detection methods for microgrid," *Renewable and Sustainable Energy Reviews*, vol. 35, pp. 211–220, 2014.

[205] S. Patra, S. Agrawal, S. R. Mohanty, V. Agarwal, and M. Basu, "ESPRIT based robust anti-islanding algorithm for grid-tied inverter," in *2016 IEEE Students? Technology Symposium (TechSym)*. Kharagpur: IEEE, sep 2016, pp. 90–95.

[206] G. De Donato, G. Scelba, G. Borocci, F. Giulii Capponi, and G. Scarcella, "Fault-Decoupled Instantaneous Frequency and Phase Angle Estimation for Three-Phase Grid-Connected Inverters," *IEEE Transactions on Power Electronics*, vol. 31, no. 4, pp. 2880–2889, apr 2016.

[207] M. Mojiri, M. Karimi-Ghartemani, and A. Bakhshai, "Estimation of Power System Frequency Using an Adaptive Notch Filter," *IEEE Transactions on Instrumentation and Measurement*, vol. 56, no. 6, pp. 2470–2477, dec 2007.

[208] D. Thomas and M. Woolfson, "Evaluation of frequency tracking methods," *IEEE Transactions on Power Delivery*, vol. 16, no. 3, pp. 367–371, jul 2001.

[209] M. Ciobotaru, V. Agelidis, and R. Teodorescu, "Accurate and less-disturbing active anti-islanding method based on PLL for grid-connected PV Inverters," in *2008 IEEE Power Electronics Specialists Conference*. IEEE, jun 2008, pp. 4569–4576.

[210] J. Kukkola and M. Hinkkanen, "State observer for grid-voltage sensorless control of a grid-connected converter equipped with an LCL filter," in *2014 16th European Conference on Power Electronics and Applications*. IEEE, aug 2014, pp. 1–10.

[211] Y. Park, S.-K. Sul, W.-C. Kim, and H.-Y. Lee, "Phase locked loop based on an observer for grid synchronization," in *2013 Twenty-Eighth Annual IEEE Applied Power Electronics Conference and Exposition (APEC)*. IEEE, mar 2013, pp. 308–315.

[212] H. R. Wickramasinghe, G. Konstantinou, J. Pou, and V. G. Agelidis, "Interactions between Indirect DC-Voltage Estimation and Circulating Current Controllers of MMC-based HVDC Transmission Systems," *IEEE Transactions on Power Systems*, pp. 1–1, 2017.

[213] J. Rafferty, L. Xu, Y. Wang, G. Xu, and F. Alsokhiry, "Frequency support using multi-terminal HVDC systems based on DC voltage manipulation," *IET Renewable Power Generation*, vol. 10, no. 9, pp. 1393–1401, oct 2016.

[214] J. Kukkola and M. Hinkkanen, "Observer-Based State-Space Current Control for a Three-Phase Grid-Connected Converter Equipped With an LCL Filter," *IEEE Transactions on Industry Applications*, vol. 50, no. 4, pp. 2700–2709, jul 2014.

Appendix A

Improvement of a phase locked loop for PV generators

"When there is a big solar energy spill, it's just called ' a nice day ' "

Commonly, small PV systems have been used for residential application where the fluctuation of power during the day has affected drastically to the electrical system operation. However, with the installation of LS-PVPPs together with more power plants based on renewable energy in the transmission system, the fluctuation of solar irradiance can affect the electrical values as frequency and voltage [202] at the PCC.

According to the grid codes reviewed in Chapter 3, LS-PVPPs should provide ancillary services and to support to the grid in case of perturbations. Thus, an adequate measurement of the voltage and frequency at the PCC is an important issue to solve in order to design an adequate control. The measurement or the calculation of these variables should discriminate when the perturbations are caused by the grid or by the same LS-PVPP due to the variation of solar irradiance.

In a PV generator, where the inverter is the basic electronic equipment, a PLL is used to synchronise the generator with the grid by the measurement of the phase angle together with the calculation of the frequency. However, the PLL could present some disturbances when phase angle changes due to the sudden injection or reduction of active power [203], [202], [179],[180]. For instance, when the solar

irradiance changes in a small period of time, the frequency calculation is drastically affected and does not represent the real value at the PCC [179].

The accuracy of the frequency measurement can affect the control and the response time. Some methods - such as active and passive - have been developed to detect frequency or phase deviation for small PV applications (lower than 1 MW) interconnected with a microgrid. On active methods, the inverter adds an error value to the frequency, the voltage or the phase, interfering with the power quality of the system. Commonly, the time response of this method is in between 0.3 to 1 s [204]. However, for PV application this method can present more problems to the control when the solar irradiance varies as it will be difficult to discriminate in a small period of time if the variation of frequency occurs because of the solar irradiance, the grid or the applied method.

For passive methods, the system usually measures voltage, frequency, power or phase distortion at the point of common coupling and compares it with a set threshold. The challenge is to choose the correct parameters to define the threshold value according to the application but still there is a non-detection zone where the PV inverter can fail [205]. Also, the variation of solar irradiance in a small period of time could make that the value of frequency or voltage goes out from the threshold and can be activated by error. The time response of this method is in between 43 to 50 ms [204].

Another method, however, is to develop an algorithm to estimate the variables as voltage and frequency at the PCC. In the case of frequency estimation, the algorithms used can be classified as: zero-crossing-based methods, discrete Fourier transformation, Kalman filtering, adaptive notch filters, and recursive Newton-type algorithm, PLL [206, 207]. All of these methods assume that the voltage waveform is purely sinusoidal, but these algorithms present problems in presence of noise, speed convergence and accuracy [208].

PLL is the most used technique for grid connected inverters, however, for PV applications, it can present problems when solar irradiance varies. The study developed in [209], propose a new PLL structure that is built using a second order generalized integrator. For this, the voltage is measured at the PCC and the inverter current angle is modified intentionally, if there is a difference between the an-

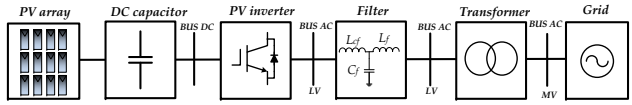

Figure A.1: PV generator model with an LCL filter

gle measured by the PLL and the modified angle, then it is assumed that there is a perturbation in the system. However, this method does not consider the perturbation caused by the PV generator operation when solar irradiance changes.

Another method that was recently studied for grid tied inverters is the development of a state observer to estimate the phase shift and the frequency by an adequate model of the interconnection between the PV inverter and the grid. The study developed by [210] details the observer design for a grid tied inverter with a specific LCL filter for voltage, current and phase shift estimation. Another study was developed in [211] where the observer estimates the phase shift to be used in a PLL and thus the general control is improved. In any of these studies, the observer has not been applied to the integration of PV generators with the electrical system.

Thus, this Appendix presents the evaluation of a state observer for frequency estimation considering the variation of solar irradiance by comparing it with a conventional PLL. This observer will be tested with a PV generator connected to the grid through an LCL filter (Fig. A.1) as this filter reduces the perturbation caused by the solar irradiance and the grid [210].

Analysis of the current Phase locked loop

Considering the dynamic model and control of the PV generator explained in Chapter 5, the output voltage of the inverter is directly affected by the changes of power as it is described in eq. (A.1) and eq.(A.2) [186]. In addition, P and Q depend on the solar irradiance, temperature and dc voltage according to the capability curves described in section 4.3. The output voltage presents small variations when changes of solar irradiance occur that affects directly to the PLL. Thus, the information given by the PLL (frequency and phase

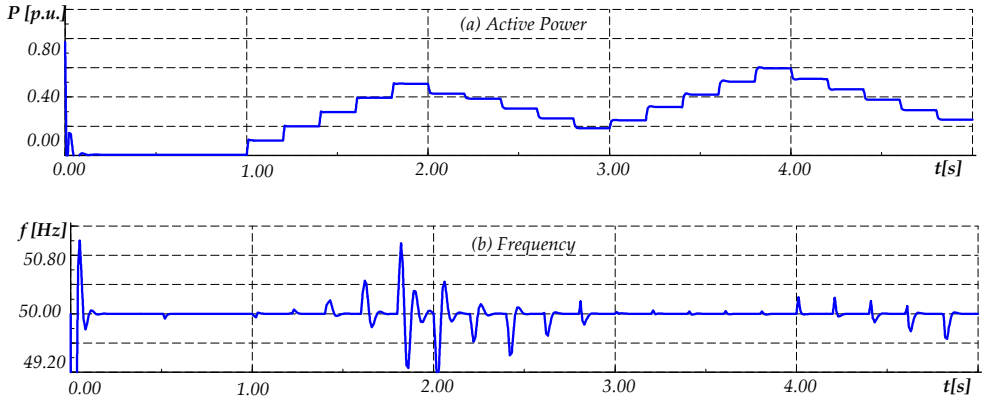

Figure A.2: Active power and frequency perturbations due to changes of solar irradiance when no MPPT is used

angle) suffers from distortion during these moments [179] .

$$v_d^c = \frac{\frac{2}{3}L_f}{v_d^g}.\frac{dP(G,T_a,V_{dc})}{dt} + \frac{\frac{2}{3}L_f\omega_g}{v_d^{pcc}}.Q(G,T_a,v_{dc}) + v_d^g \tag{A.1}$$

$$v_q^c = \frac{\frac{2}{3}L_f}{v_d^g}.\frac{dQ(G,T_a,V_{dc})}{dt} + \frac{\frac{2}{3}L_f\omega_g}{v_d^{pcc}}.P(G,T_a,v_{dc}) \tag{A.2}$$

In the previous equations, the ac voltage depends on the changes of power due to solar irradiance and ambient temperature. Additionally, it also depends on the dc voltage variation which depends on the MPPT or PPT applied. In the case, the algorithm perturb and observe is applied, the dc voltage changes in small steps until the system reach the desired power point. However, in the case the algorithm used does not consider any small steps of dc voltage and only calculates the v_{mpp} at each new solar irradiance, then the PV generator changes the active or reactive power immediately. This behaviour affects the frequency calculated by the PLL as it is illustrated in Fig. A.2.

In this thesis, a MPPT control has been used, though the perturbation has reduced, the frequency calculated by the PLL is not accurate enough and can affect future algorithms. Taking into consideration this behaviour, a solution should be analysed and applied. For this study, the solution chosen is a state observer of frequency which is

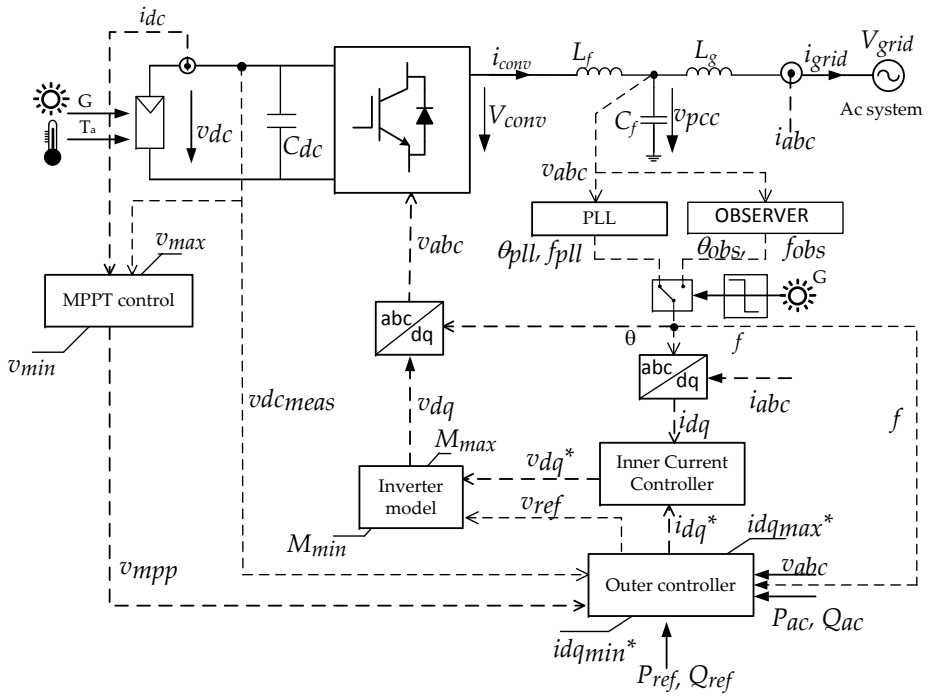

Figure A.3: PV generator general control

added to the PV inverter s control (Fig. A.3). This observer has the main task of supporting the frequency and the phase measured by the PLL when quick changes of solar irradiance occur. The objective of this observer is to calculate the frequency and the phase shift at each instant considering the real interaction between the PV inverter and the grid through the LCL filter.

Frequency steady state observer

In control theory, a steady state observer can be defined as a system which provides information of the internal behaviour of some parameters in a real system. The behaviour of these parameters can be estimated or observed from the inputs, outputs and control variables that identify to a real system. To apply this theory, an accurate steady state model of the real system is necessary. If a system can be

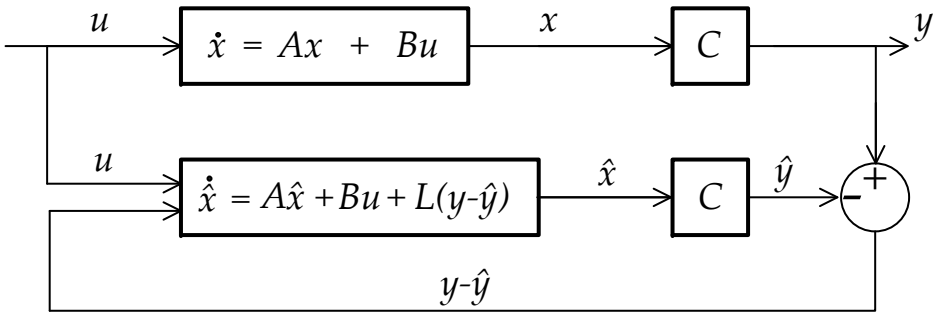

Figure A.4: General Luenberger observer

modelled, then it can be observable.

The steady state of any system can be expressed as:

$$\dot{\mathbf{x}} = \mathrm{A}\mathrm{x} + \mathrm{B}\mathrm{u} \tag{A.3}$$

$$\mathrm{y} = \mathrm{C}\mathrm{x} + \mathrm{D}\mathrm{u} \tag{A.4}$$

where **u** and **y** are the inputs and outputs of the system.

Then, the observer can be designed from these steady state equations. However, extra terms can be included that will be the possible error that has the new system to determine the behaviour of the system. The extra term commonly is a matrix **L** which the main function is to decrease the error between the measured output and the estimated output (Luenberger observer). So, the observer will have the following expression [1]:

$$\dot{\hat{\mathbf{x}}} = \mathrm{A}\hat{\mathbf{x}} + \mathrm{B}\mathbf{u} + \mathrm{L}(\mathrm{y} - \hat{\mathrm{y}}) \tag{A.5}$$

$$\hat{\mathbf{y}} = \mathrm{C}\hat{\mathbf{x}} + \mathrm{D}\mathbf{u} \tag{A.6}$$

Taking into account the expression explained before, the Luenberger observer can be illustrated in block diagrams (Fig. A.6)

[1] For estimated variables the symbol: ˆ will be used in the current chapter

In grid tied inverters, this theory has been applied in order to estimate voltage or current at the ac side in order to decrease the number of sensors, to have a redundant system, or to improve the control. For instance, the work developed in [212] presents the dc voltage estimation using a steady state observer to improve the control. This theory has also been used for frequency support in multi-terminal HVDC system, where the frequency deviation can be estimated through the interaction of the dc converters at the dc side of the grid [213].

A steady state observer for grid tied inverters have been deeply studied in [214] and [210] for voltage and current estimation. However, this theory has not been applied in PV inverters where the phase deviation occurs at each change of solar irradiance and temperature. These studies are going to be applied in the current analysis to observe the frequency and the phase disturbance.

In a PV grid tied inverter, the v_q^{pcc} is imposed to be zero, however when disturbances occur this value could change. Then, as it is shown in Fig. 5.5, the $\mathbf{i_{dq}}$ of the converter is directly affected by the ac voltage, the grid frequency, the LCL filter, and the changes of solar irradiance and dc voltage. Thus, the frequency estimator will be constructed on the premise of this relationship ($\mathbf{i_{dq}}$ vs f). For this, the steady state model of the ac system is needed and then the design of the observer is developed.

AC system model and control

The model of the inverter interconnected with the grid is illustrated in Figure A.5 and can be defined by a state vector, where the state variables for the system are the current from the converter and the grid, besides the voltage at the point of common coupling.

$$x = [\mathbf{i_c} \quad \mathbf{v_{pcc}} \quad \mathbf{i_g}]^T \tag{A.7}$$

where $\mathbf{v_{pcc}}$ is the voltage at the point of common coupling, $\mathbf{i_c}$ and $\mathbf{i_g}$ are the converter and the grid currents, respectively. The state space model of the grid tied inverter can be expressed in the form of: $\frac{dx}{dt} = Ax + Bu$ and $y = Cx$.

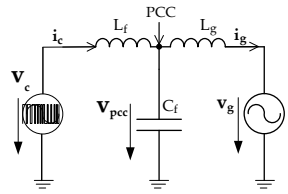

Figure A.5: Grid connected LCL filter considering stationary frame

$$\frac{d}{dt}\begin{bmatrix}\mathbf{i_c}\\ \mathbf{v_{pcc}}\\ \mathbf{i_g}\end{bmatrix} = \begin{bmatrix}-j\omega_g & -\frac{1}{L_c} & 0\\ \frac{1}{C_f} & -j\omega_g & -\frac{1}{C_f}\\ 0 & \frac{1}{L_g} & -j\omega_g\end{bmatrix} x + \begin{bmatrix}\frac{1}{L_c}\\ 0\\ 0\end{bmatrix}\mathbf{v_c} + \begin{bmatrix}0\\ 0\\ \frac{1}{L_g}\end{bmatrix}\mathbf{v_g} \qquad (A.8)$$

$$y = \begin{bmatrix}1 & 0 & 0\end{bmatrix} x \qquad (A.9)$$

In stationary reference frame, the grid voltage is defined as:

$$\mathbf{v_g} = e^{j\vartheta_g} v_g \qquad (A.10)$$

where ϑ_g is the phase angle and equal to $\vartheta_g = \int \omega_g$.

After the ac system model for a PV generator connected to the grid through an LCL filter, the frequency estimator can be designed.

Design of the frequency steady state observe

The design of the current frequency estimator is based on the work developed in [210]. The estimator has two parts: (i) a Luenberger observer and (ii) an adaptive controller. The Luenberger observer has the structure represented in Figure A.6, where the variable to observe is the current in dq frame. Every time the solar irradiance change, the real (i_d^c) and the imaginary component (i_q^c) presents some perturbations.

The full order observer estimates the state variables $\mathbf{x} = \begin{bmatrix}\mathbf{i_c} & \mathbf{v_{pcc}} & \mathbf{i_g}\end{bmatrix}^T$, where an additional term is included: $\mathbf{L} = \begin{bmatrix}l_1 & l_2 & l_3\end{bmatrix}^T$. For this application, the Luenberger observer is written as:

$$\frac{d\hat{\mathbf{x}}}{dt} = A\hat{\mathbf{x}} + B_1\mathbf{v_c} + B_2\hat{\mathbf{v}}_\mathbf{g} + L(\mathbf{y} - \hat{\mathbf{y}}) \tag{A.11}$$

$$\hat{\mathbf{y}} = C\hat{\mathbf{x}} \tag{A.12}$$

As the measured voltage is at the PCC, the real grid voltage and phase angle are not being measured, thus in the previous equation, these variables are also estimated. The observer error $\varepsilon = x - \hat{x}$ satisfies the equation:

$$\frac{d\varepsilon}{dt} = (A - LC)e + B_2(e^{j(\hat{\rho}_g)}v_g - \hat{v}_g) \tag{A.13}$$

where $\hat{v_g}$ and $\hat{\rho}$ corresponds to the estimated voltage amplitude and phase angle respectively. The linearisation of this error can be done by using the small-signal approach. To linearise, the relationship between the phase angle and the grid frequency is considered.

$$\frac{d}{dt}\begin{bmatrix}\tilde{\varepsilon}\\ \tilde{\varepsilon}_\rho\end{bmatrix} = \begin{bmatrix}A_o - L_oC_o & jB_2v_{g_o}\\ 0 & 0\end{bmatrix}\begin{bmatrix}\tilde{\varepsilon}\\ \tilde{\varepsilon}_\vartheta\end{bmatrix} + \begin{bmatrix}B_2\\ 0\end{bmatrix}\tilde{\varepsilon}_{v_g} + \begin{bmatrix}0\\ 1\end{bmatrix}\tilde{\varepsilon}_\omega \tag{A.14}$$

where; $\tilde{\varepsilon}_\rho = \tilde{\rho} - \tilde{\hat{\rho}}$, $\tilde{\varepsilon}_\omega = \tilde{\omega}_g - \tilde{\hat{\omega}}_g$, $\tilde{\varepsilon}_{v_g} = \tilde{v}_g - \tilde{\hat{v}}_g$

From this, the relationship between the current converter and the angular speed error can be determined as:

$$\frac{\tilde{\varepsilon}_{i(s)}}{\tilde{w}(s)} = \tilde{C}(sI - A_2)^{-1}B_\omega \tag{A.15}$$

where:

$$B_\omega = \begin{bmatrix}0 & 1\end{bmatrix} \tag{A.16}$$

$$A_2 = \begin{bmatrix}A_o - L_oC & jB_2v_{go}\\ 0 & 0\end{bmatrix} \tag{A.17}$$

$$\tilde{\varepsilon}_\mathbf{i}(s) = \hat{\mathbf{i}}_c - \tilde{\hat{\mathbf{i}}}_c \tag{A.18}$$

The selection of the full order observer gains is developed by the direct pole placement. This system has a third order dynamics that corresponds to the error dynamics.

$$\det(sI - A + LC) = (s + \alpha_o)(s^2 + 2\varepsilon_o\omega_o s + \omega_o^2) \tag{A.19}$$

Considering the gains, the current observer is constructed and the relationship between the current and the angular speed is determined. The imaginary component i_q^c is the one that presents a relationship with the angular speed perturbation each time the solar irradiance varies in large proportion. Due to this relationship, a PI adaptative controller is linked with the Luenberger observer. The objective of this is to reduce the error of the estimated i_q^c when perturbation occurs.

$$G_{\mathbf{i\omega(s)}} = \frac{\tilde{\mathbf{i}}(s)}{\tilde{\omega}(s)} = -\frac{jv_{go}}{s\dot{C}_f L_c L_g (s+\alpha_o)(s^2 + 2\varepsilon_o \omega_o s + \omega_o^2)} \tag{A.20}$$

From eq.A.20 a PI can be determined:

$$\hat{\omega}_g = k_p^{obs} \tilde{\varepsilon}_{i_q^c} + k_i^{obs} \int \tilde{\varepsilon}_{i_q^c} dt \tag{A.21}$$

The gains are calculated as follows:

$$k_{p_{obs}} = \frac{-2\varepsilon\omega . C_f . L_c . L_g \alpha\omega^2}{v_{g_o}} \tag{A.22}$$

$$k_{i_{obs}} = -\frac{\omega^2 . C_f . L_g . L_c \alpha\omega^2}{v_{g_o}} \tag{A.23}$$

Then, the phase angle and the frequency are estimated by:

$$\hat{\vartheta}_g = \int \hat{\omega}_g dt \tag{A.24}$$

$$\hat{f}_{obs} = 2\pi\hat{\omega}_g dt \tag{A.25}$$

The frequency estimator constructed is then tested in DigSilent PowerFactory together with the PV inverter control explained previously, the following section explains the study case and the results.

Simulations and Results

A PV generator of 0.6 MVA was simulated in DiGSILENT Power Factory as part of a LS-PVPP of 20 MVA. The PV generator's characteristics are summarized in Table A.1. The complete model and

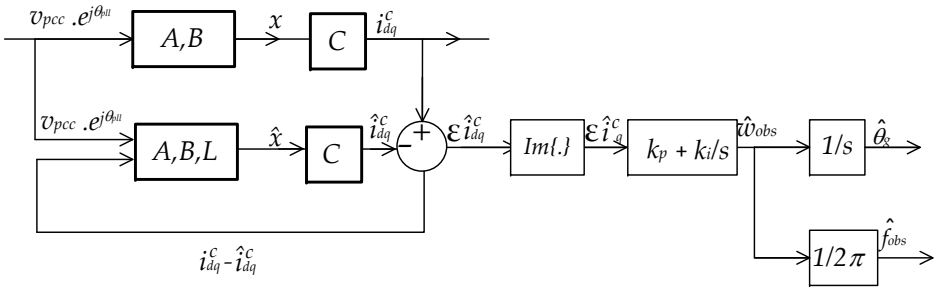

Figure A.6: Frequency estimator for grid tied PV inverter

Table A.1: PV panel and array characteristics

PV panel characteristics		**PV array characteristcs**	
V_{oc}	58.8 [V]	P_{array}	0.6 [MW]
I_{sc}	5.01 [A]	N_{ser}	15
I_{mpp}	4.68 [A]	N_{par}	175
V_{mpp}	47 [V]	T_{min}, T_{max}	0-70 [°C]
k_v	0.45 [1/°C]	G_{max}	1100 [W/m^2]
L_f	0.03 [p.u]	C_f	0.04[p.u]
L_g	0.05 [p.u]	ω_{go}	$2\pi \times 50$[rad/s]

control of the PV generator explained in the previous sections is implemented in DiGSILENT PowerFactory together with the designed frequency observer. For the analysis, the LS-PVPP is connected with a grid that has a short circuit ratio equal to five.

The PV generator together with the frequency observer is tested under two study cases scenarios:

- Study case A: Fast change of solar irradiance from 1000 to 0 W/m^2 and from 0 to 1000 W/m^2 (Fig.A.7 (a)).
- Study case B: One day of solar irradiance in Urcuquí-Ecuador (Fig. A.8 (a))

In each of these cases, the frequency calculated by the PLL and the observer is obtained. Additionally, two PLLs with different bandwidth are used. The first one is used for grid synchronization (PLL (A)) and the second one only to calculate the frequency grid (PLL(B)). For each PLL and the observer, the gains used are summarized in Table A.2. The results are illustrated in Fig. A.7(b) and Fig. A.8(b) for

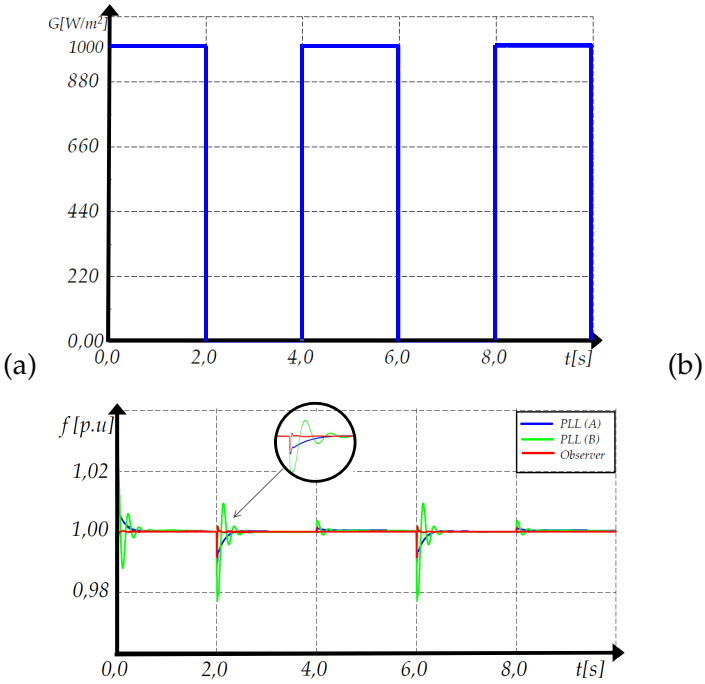

Figure A.7: Study case A . (a) Solar irradiance variation (b) Estimated and calculated frequency

study case A and B respectively.

For quick changes of solar irradiance (Study case A) from high irradiance to low, the frequency measured by the PLL (A), presents some perturbations due to its quick dynamics. The time that the PLL uses to stabilize is 0.6 s. After this time the frequency came back to be the same as the grid is imposing. With PLL (B), the perturbations have diminished but the time of stabilization is almost the same as PLL (A). The maximum perturbation has a value of 0.02 p.u. The observer, however, presents a frequency value with lower perturbations

Table A.2: Gain controllers

Controller	**kp**	**Unit**	**ki**	**Unit**
Observer	0.018	[H.rad/Vs^2]	0.01	[H.rad/Vs^2]
PLL (A)	10	[rad/Vs]	30	[rad/Vs^2]
PLL (B)	20	[rad/Vs]	30	[rad/Vs^2]

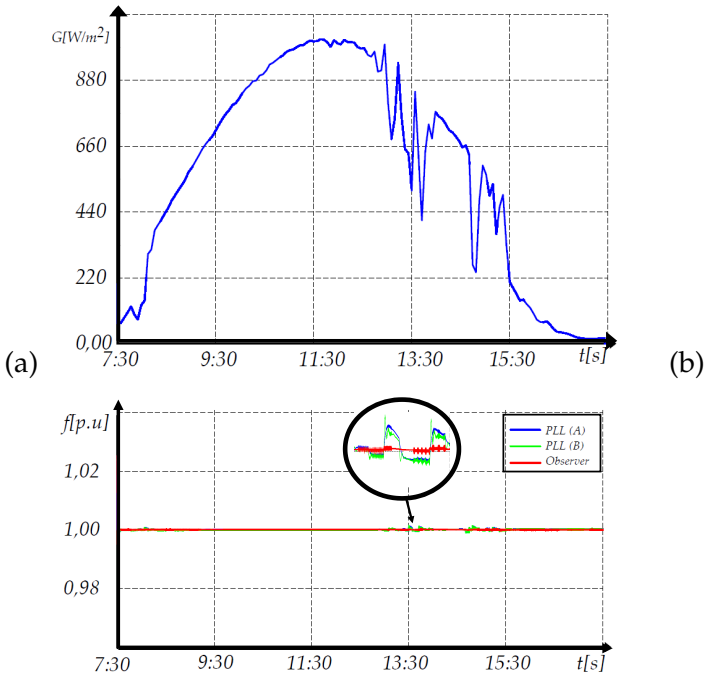

Figure A.8: Study case B . (a) Solar irradiance variation (b) Estimated and calculated frequency

(0.001p.u) and a time response of 0.072 s. But, when the irradiance goes from a low to a high value, the frequency calculated by any of the strategies is similar and the perturbations are close to 0 p.u. This behaviour is due to the MPPT that slows the dynamics of the PV generator when quick changes of solar irradiance occur. The power moves smoothly thanks to the dc voltage control. However, when solar irradiance goes from high to low, the MPPT by itself cannot control the quick change of power.

For study case (B), the frequency estimated or calculated by any of the strategies (PLL or observer) does not show high perturbations. The dynamics of the MPPT control permits that the variation of solar irradiance does not affect instantaneously the ac power supplied by the PV generator. However at 13:30 pm in Fig. A.8(b), a perturbation can be seen when the solar irradiance goes from 840 to 412 W/m^2, in ten minutes. Due to this change, the PV generator presents a ramp rate close to 2 MW/min. This change of power makes the ac voltage present some perturbations and thus the PLL (A or B) is

affected. The frequency calculated by these two PLLs presents some deviation from the real value. Meanwhile, the frequency estimated by the observer does not present these perturbations and is equal to the one imposed by the electrical system.

The observer presents fewer perturbations and faster response than the PLL when quick changes of solar irradiance occur. The perturbation and the settling time are both substantially diminished. However, this observer depends on the LCL filter and the grid inductance. For future work, an estimation of the L_g is going to be studied considering weak grids.

Appendix B

Publications

Journal Publications

a) A. Cabrera-Tobar, E. Bullich-Massagué, M. Aragüés-Peñalba, O. Gomis-Bellmunt, "Topologies for large scale photovoltaic power plants", *Renewable and Sustainable Energy Reviews.*, 59 (2016),pp. 309-309.

b) A. Cabrera-Tobar, E. Bullich-Massagué, M. Aragüés-Peñalba, O. Gomis-Bellmunt, "Review of advanced grid requirements for the integration of large scale photovoltaic power plants in the transmission system", *Renewable and Sustainable Energy Reviews.*, 62 (2016),pp. 971-987.

c) A. Cabrera-Tobar, E. Bullich-Massagué, M. Aragüés-Peñalba, O. Gomis-Bellmunt, "Capability curve analysis of photovoltaic generation systems", *Solar Energy*, 140 (2016),pp. 255-264.

d) A. Cabrera-Tobar, E. Bullich-Massagué, M. Aragüés-Peñalba, O. Gomis-Bellmunt, "Active and Reactive Power Control of a Photovoltaic generator for large scale application", *Submitted to Applied Energy*.

e) A. Cabrera-Tobar, E. Bullich-Massagué, M. Aragüés-Peñalba, O. Gomis-Bellmunt, "Dynamic response of a PV generator considering its capability curves", *Submitted to Solar Energy*.

Conference Publications

a) A. Cabrera-Tobar, E. Bullich-Massagué, M. Aragüés-Peñalba, O. Gomis-Bellmunt, "Dynamic response of a PV generator considering its capabilities curves", *Submitted to IET Renewable Power Generation*.

b) A. Cabrera-Tobar, O. Gomis-Bellmunt, "Dynamic study of a photovoltaic power plant interconnected with the grid", *PES Innovative Smart Grid Technologies Conference Europe (ISGT-Europe)*, Ljubljana, Slovenia. 9-12 Oct. 2016. pp. 1-6.

c) A. Cabrera-Tobar, O. Gomis-Bellmunt, "Performance of a small photovoltaic power plant under different meteorological conditions", *16th International conference on environmental and electrical engineering (EEIC)*, Florence, Italy. 7-10 June. 2016. pp. 1-6.

d) A. Cabrera-Tobar, E. Bullich-Massagué, M. Aragüés-Peñalba, O. Gomis-Bellmunt, "Reactive power capability analysis of a photovoltaic generator for large scale power plants", *5th IET International Conference on Renewable Power Generation (RPG)*, London, United Kingdom, 21-23 Sept. 2016, pp. 1-6.

e) A. Cabrera-Tobar, M. Aragüés-Peñalba, O. Gomis-Bellmunt, "Evaluation of a state observer for frequency estimation in a grid tied Photovoltaic inverter", *Submitted to IEEE 18th International Conference on Environment and Electrical Engineering*,Palermo, Italy, 12-15 June 2018, pp. 1-6.

f) A. Cabrera-Tobar, M. Aragüés-Peñalba, O. Gomis-Bellmunt, "Dynamic modelling and control of a PV generator for large scale applications", *IEEE International Conference on Industrial Technology (ICIT 2018)* ,Lyon, France, 20-22 February 2018, pp. 1-6.

g) A. Cabrera-Tobar, M. Aragüés-Peñalba, O. Gomis-Bellmunt, "Effect of variable solar irradiance on the reactive power response of photovoltaic generators", *Submitted to 5th IEEE International Energy Conference (ENERGYCON) 2018*,Limassol, Cyprus, 3-7 June 2018, pp. 1-6.